

## Article

# Biomass-Derived Carbon Materials for Advanced Metal-Ion Hybrid Supercapacitors: A Step Towards More Sustainable Energy

Syed Shaheen Shah 

Department of Material Chemistry, Graduate School of Engineering, Kyoto University, Nishikyo-ku, Kyoto 615-8520, Japan; shah.syedshaheen.78r@st.kyoto-u.ac.jp

**Abstract:** Modern research has made the search for high-performance, sustainable, and efficient energy storage technologies a main focus, especially in light of the growing environmental and energy-demanding issues. This review paper focuses on the pivotal role of biomass-derived carbon (BDC) materials in the development of high-performance metal-ion hybrid supercapacitors (MIHSCs), specifically targeting sodium (Na)-, potassium (K)-, aluminium (Al)-, and zinc (Zn)-ion-based systems. Due to their widespread availability, renewable nature, and exceptional physicochemical properties, BDC materials are ideal for supercapacitor electrodes, which perfectly balance environmental sustainability and technological advancement. This paper delves into the synthesis, functionalization, and structural engineering of advanced biomass-based carbon materials, highlighting the strategies to enhance their electrochemical performance. It elaborates on the unique characteristics of these carbons, such as high specific surface area, tuneable porosity, and heteroatom doping, which are pivotal in achieving superior capacitance, energy density, and cycling stability in Na-, K-, Al-, and Zn-ion hybrid supercapacitors. Furthermore, the compatibility of BDCs with metal-ion electrolytes and their role in facilitating ion transport and charge storage mechanisms are critically analysed. Novelty arises from a comprehensive comparison of these carbon materials across metal-ion systems, unveiling the synergistic effects of BDCs' structural attributes on the performance of each supercapacitor type. This review also casts light on the current challenges, such as scalability, cost-effectiveness, and performance consistency, offering insightful perspectives for future research. This review underscores the transformative potential of BDC materials in MIHSCs and paves the way for next-generation energy storage technologies that are both high-performing and ecologically friendly. It calls for continued innovation and interdisciplinary collaboration to explore these sustainable materials, thereby contributing to advancing green energy technologies.



**Citation:** Shah, S.S. Biomass-Derived Carbon Materials for Advanced Metal-Ion Hybrid Supercapacitors: A Step Towards More Sustainable Energy. *Batteries* **2024**, *10*, 168. <https://doi.org/10.3390/batteries10050168>

Academic Editors: Kangyu Zou, Tianjing Wu and Jiangmin Jiang

Received: 30 April 2024

Revised: 14 May 2024

Accepted: 17 May 2024

Published: 20 May 2024



**Copyright:** © 2024 by the author. Licensee MDPI, Basel, Switzerland. This article is an open access article distributed under the terms and conditions of the Creative Commons Attribution (CC BY) license (<https://creativecommons.org/licenses/by/4.0/>).

## 1. Introduction

The efficient utilization of renewable energy sources, such as solar and wind, relies heavily on sustainable energy storage. Hybrid supercapacitors (HSCs) have been created to store energy using electric double-layer capacitance and Faradaic pseudocapacitance modes [1]. Even though they are used in various applications, HSCs offer a larger specific capacitance, a longer service life, and a greater power density than general batteries and double-layer capacitors [2]. Hence, their exceptional performance makes them an outstanding choice for advanced energy storage devices in the next generation [3]. Supercapacitors, sustainable energy storage options, are gaining popularity in fulfilling energy requirements and decreasing dependence on traditional energy sources [4]. Electrochemical capacitors, also known as supercapacitors, are potential alternatives or additions to batteries because of their high specific power, durability, and rapid charging and discharging capabilities [5].

These devices have many applications, from portable electronics to hybrid electric cars and power plants. When combined with fuel cells or batteries in hybrid electric vehicles, HSCs can provide the necessary energy for rapid acceleration [6]. Over the years, supercapacitors have demonstrated an existence ranging from low-scale to high-power energy storage systems. Supercapacitors are heavily influenced by the elements incorporated in preparing HSCs due to their high capacitance values [7–9]. Overall, it is essential that sustainable energy storage technologies, such as HSCs, be used to produce renewable energy because they provide good proficiency and long durability.

Metal-ion HSCs (MIHSCs) are an unequalled venture in sustainable energy storage technologies. They incorporate two distinctive types of devices: supercapacitors and batteries. MIHSCs are a hybrid of supercapacitors and batteries, with both the high power density of supercapacitors and the high energy density of batteries. Li et al. [10] explained that by incorporating supercapacitor-type and battery-type electrodes, MIHSCs inherit two charge storage mechanisms, delivering a high level of power per unit volume from the supercapacitor and a high level of energy per unit volume from the battery. In other words, MIHSCs are vital in maintaining modern devices due to their acutely growing energy demands. Moreover, it could be inferred that the hybrid device type is already quite promising in energy storage technologies that can satiate the rapid increase in energy needs [11]. They are essential in maintaining energy storage because batteries and supercapacitors can be used in a hybrid configuration since MIHSCs combine supercapacitors' long-cycle stability with batteries' inherent disadvantages [12,13]. Furthermore, these devices are instrumental in refining energy storage. They pave the way for achieving equilibrium in energy utilization in density and power. Their use in energy storage allows for wide operating potential windows (OPWs), high energy, safer application, and high power density; thus, MIHSCs show promising potential as a leading contender for the future generation of storage devices [14,15].

MIHSCs, comprising zinc-, sodium-, potassium-, and aluminium-ion HSCs, are differentiated based on efficiency and performance. Zinc-ion HSCs (ZIHSCs) are a potential form of energy storage which possess both the large storage capacity of zinc-ion batteries and the high power of a supercapacitor; high energy/power density is suitable for effective and consistent energy storage. ZIHSCs were presented as having better initial and first-cycle capacity retention [16,17]. Sodium-ion HSCs (NIHSCs) are new alloying-based MIHSCs fabricated by overcoming sodium-ion and lithium-ion devices' explosive and toxic drawbacks. The NIHSCs are structurally proven to occupy the neutralizing position with the best energy and power density ratio. However, high-power alkalis have recently gained much attention since the breakthrough of ion batteries with sodium and potassium [18,19]. Potassium-ion HSCs (KIHSCs) exhibit a significant ability to maintain their capacity over multiple cycles. KIHSCs have the most reasonable energy density of 58.2 Wh/kg with exceptional cycling durability [19]. Aluminium-ion HSCs (AIHSCs) made entirely from nitrogen-doped carbon spheres with a hierarchical porous hollow structure exhibit much better performance [20]. AIHSCs were thus developed to have drastically superior energy and power densities and show great potential for electrochemical performance [21]. Therefore, these MIHSCs are optimal for energy storage systems fulfilling requirements.

Biomass-derived carbon (BDC) materials are essential for improving the efficiency and performance of MIHSCs. Carbon materials possess numerous benefits, such as cost-effectiveness, environmental friendliness, and sustainability, making them highly appealing for energy conversion and storage. BDC materials provide multiple characteristics that render them highly suitable for enhancing the electrochemical efficiency of supercapacitors [22–24]. The inherent characteristics of these carbon compounds encompass a substantial specific surface area (SSA), commendable electrical conductivity, and adjustable porosity. The efficiency of devices, especially MIHSCs, can be enhanced by utilizing BDC materials. Specifically, in a ZIHSC [25], BDC materials could function as high-performance electrode materials. Such materials offer a high SSA that ensures sufficient charge storage and an overall improvement in the capacitive behaviour of such devices. Utilizing BDC

materials in a NIHSC [24] could also realize high energy and power density. For KIHSCs, BDC materials could enhance capacity retention and cycling stability [26]. Lastly, these materials could improve ion adsorption and mobility in AIHSCs, increasing their energy and power density [27]. BDC materials, therefore, present a sustainable way of integrating high performance into MIHSCs. The unique natural properties of this type of carbon make it suitable for enhancing energy storage in these supercapacitors, which would, therefore, find an extensive range of applications in the current shift to sustainability.

This review study thoroughly examines using carbon materials produced from biomass to develop high-performance MIHSCs. The focus is primarily on sodium-, potassium-, aluminium-, and zinc-ion-based systems. BDC compounds are highlighted for their abundant availability, renewable nature, and exceptional physicochemical properties. These materials are considered excellent choices for supercapacitor electrodes, as they effectively combine environmental sustainability with technical progress. This paper explores creating, modifying, and designing the structure of these materials, focusing on their significant SSA, adjustable porosity, and the introduction of diverse elements, which are crucial for gaining excellent electrochemical performance in energy storage systems. An important innovation is the thorough comparison of these carbon materials in various metal-ion systems, revealing the combined effects of their structural characteristics on each type of supercapacitor. This review also discusses the difficulties of scalability and maintaining consistent performance and provides valuable insights for improving sustainable energy storage technologies. It highlights the potential of using BDC materials to develop advanced MIHSCs.

## 2. Basic Principles of MIHSCs

Capacitors, batteries, and HSCs are three energy storage technologies with unique attributes. Capacitors, specifically electrolytic capacitors, are efficient energy storage devices with notably high power capability and cyclic life [28]. They offer unprecedented ultrahigh power density and charge–discharge speed advantages, outperforming chemical batteries and electrochemical supercapacitors [29]. In contrast, batteries have notably high energy densities and are known for storing large amounts of energy. Various types of batteries are utilized in several industries, including portable electronic devices, electric cars, and large-scale electrical storage at power stations [30]. They use chemical reactions to store significantly more energy than capacitors, while their power capabilities are considerably lower than those of capacitance devices. Supercapacitors, alternatively called electrical double-layer capacitors [31], are rechargeable energy storage approaches with capacitors' and batteries' characteristics. Such power and energy delivery within traditional capacitors and batteries lend supercapacitors unique characteristics that make them promising energy storage device candidates [32]. Supercapacitors have a significantly greater power density than lithium-ion batteries but are behind these in energy density [12,33]. HSCs, specifically MIHSCs [16], combine the best of both worlds by providing energy and power density superior to capacitors or batteries. The devices consist of a battery-type electrode and a capacitive electrode, giving potential avenues for enhancing energy storage systems in the future [14]. Energy storage devices can be categorized based on the area in which they excel, with capacitors having superior power density and cyclic life, batteries having high energy density, supercapacitors offering power and many cycles, and hybrid capacitors having both exceptional power and energy density.

MIHSCs represent a significant advancement in energy storage technology since they effectively merge the advantages of batteries and supercapacitors for efficient energy storage applications. These devices are believed to enhance both unique power and energy densities [12]. MIHSCs leverage the advantageous features of both battery-type and capacitive electrodes. This allows them to achieve a high energy density similar to batteries and a high power density comparable to supercapacitors [16]. A diverse array of metal oxide/hydroxide materials can unite to undermine the integrity of the material, exhibiting a shift in valence at different potentials, which is incorporated to enhance

the efficiency of HSCs [34]. Different MIHSCs, including LIC and NHC, have distinct properties and performances [35]. Coating capacitor-type and active battery-type material for pseudocapacitive reactions is the standard format in which HSCs use more of what works well in the performance [36]. Batteries and supercapacitors are then integrated to achieve optimal performance in pseudocapacitive reactions, such as the features of battery-type material [37]. Bunker and his colleague's work on materials such as ZHSCs and PIHCS attempts to understand a battery that delivers optimal functionality [21,38]. Furthermore, researchers have created multivalent-ion HSCs to attain elevated energy and power densities [39]. MIHSCs constitute a significant advancement in energy storage technology that combines the benefits of batteries and supercapacitors. These devices utilize a range of metal ions and electrode materials to enhance power and energy density, making them a promising alternative for the future of energy storage.

MIHSCs integrate battery-type and capacitive electrodes to achieve high energy density, fast energy discharge, and extended lifespan [40]. The process of charging and discharging between the two electrodes exhibits significant differences. During the charging process, ions are stored in the electrolyte on the electrode's surface, forming an electric double layer in electrodes similar to supercapacitors [41]. For a battery-type electrode, ions are propelled into an electrode material via a redox process. The charging process of MIHSCs commences by applying a voltage to the device, enabling the ions in the electrolyte to propel themselves towards the electrode's surface through different methods. Electrons are generated via intermediary electrodes [42] or redox reactions [43]. Charging refers to the input of electric current retained within the device and availed during discharge. In this regard, discharging involves the removal of stored charge as the ions migrate back into the composition from the negatrod and positrode.

Consequently, a current is produced and can drive electrically driven devices [44]. The working principles of MIHSCs are the primary determinants of efficiency when measuring their performance. The device can produce a high power output and store a significant amount of charge throughout multiple life cycles due to the integration of supercapacitors and battery technologies [45]. The choice of electrodes, the electrolyte composition, and the charging approach determine the overall efficiency [12]. Highly appropriate charge-discharge operations are crucial to fully realizing sophisticated energy storage devices' energy storage and distribution functionalities. MIHSCs exploit capacitive and battery-type securities as electrodes; hence, they avail the merged properties of supercapacitors and batteries. Battery-type securities undertake redox responses, with capacitive securities acting as an electrochemical double layer or pseudocapacitors during charging and discharging, as demonstrated in Figure 1a,b. Therefore, when designing MIHSCs, ensuring security, including the battery, is essential [46,47].

Carbon-based zinc HSCs' energy storage and release mechanism involves multiple processes. The charge and discharge processes are enabled by the reversible deposition and removal of  $Zn/Zn^{2+}$  on the zinc metal electrode during charge and discharge, respectively (Equation (1)). However, the mechanism of the carbon negatrod is more complex. Some researchers believe that the  $Zn^{2+}$  ions' adsorption/desorption on the carbon surface is a critical component of the capacity (Equation (2)) [48,49]. In contrast, others propose that anions, such as sulfate ( $SO_4^{2-}$ ), also play a substantial role in the energy storage process (Equation (3)) [50]. The behaviour of these negatively charged ions in the electric double layer is contingent upon the carbon material's operating voltage and zero charge potential. In addition to physical adsorption/desorption, chemical adsorption/desorption can occur, especially in carbon materials doped with heteroatoms such as oxygen and nitrogen. This leads to the generation of extra pseudocapacitance (Equations (4) and (5)) [51].

Zn positrode:



Carbon-based negatrod:

i. Process of physical adsorption or desorption



Here, C stands for the carbon, while  $X^-$  symbolizes the electrolyte anion.

ii. Process of chemical adsorption or desorption



Here,  $C \cdots O$  represents oxygen-containing functional groups on the carbon material, while  $N \cdots O$  denotes nitrogen-containing functional groups. These groups play roles in the chemical processes occurring on carbon-based electrodes.

Carbon-based MIHSCs have demonstrated exceptional performance, which promises to transform future energy storage. This technology exhibits a strong combination of high energy density, rapid charge–discharge rate, and excellent cycle life. It is a significant competitor in multiple industries, such as portable devices, electric cars, and renewable energy systems.

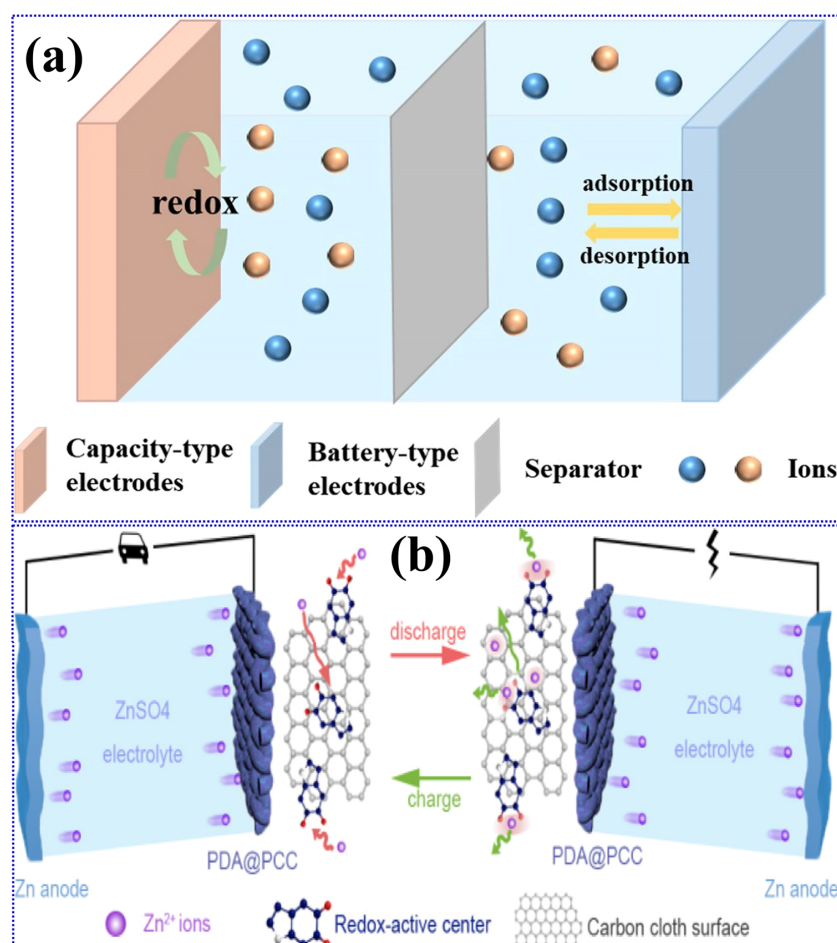


**Figure 1.** (a) A schematic representation for an MIHSC consisting of battery-type and capacitor-type electrodes. Reproduced with permission from Ref. [46]. Reproduced under the term CC BY 4.0. Copyright 2024, Fan et al., Springer Nature. (b) A specific charge–discharge demonstration of a ZIHSC using a carbon-based negatrod. Reproduced with permission from Ref. [47]. Copyright 2020, American Chemical Society.

### 3. Synthesis of BDC Materials for MIHSCs

Several essential techniques and aspects are involved in synthesizing BDC materials for MIHSCs to improve their electrochemical performance. Pyrolysis is the most commonly used technique for converting biomass into carbon materials at high temperatures without oxygen to produce porous carbon structures suitable for energy storage applications [52]. Hydrothermal carbonization is another critical technique for converting biomass into carbon at high temperatures and pressure in water, resulting in unique properties of carbon materials [53]. Template methods are also used to control the morphology and porosity of BDC materials, which involves sacrificing templates to form specific structuring in the synthesized materials [54]. Activation techniques, such as chemical or physical methods, are mainly used to increase the SSA and porosity of carbon compounds derived from biomass sources. While these alterations directly enhance the SSA and porosity, they also indirectly improve the electrochemical performance. This is because a larger surface area and enhanced porosity enable more efficient movement of ions and easier access to the electroactive sites. This can result in a noticeable improvement in conductivity during operation [55]. Alloying or doping bio-based carbons with heteroatoms such as nitrogen or phosphorus enhances conductivity and produces the appropriate materials for supercapacitors [56]. The porosity development of BDC materials is critical to maximizing energy storage capacity. Surface functionalization methods include surface chemistry modification for improved interaction with various electrolytes that contribute generously to the supercapacitors' electrochemical performance [57]. The performance qualities of bio-based carbons are influenced by their electrochemical properties, including capacitance and cyclic stability. These features are considered while choosing appropriate synthesis methods [58]. Figure 2a depicts the essential electrode materials for MIHSCs, with the electrolyte playing a critical role in charging the contact between the electrode and the electrolyte [59]. Research on electrode materials aims to enhance long-term charge propagation and stability in MIHSCs by optimizing pore size and distribution. Similarly, Figure 2b showcases a range of carbon-based materials employed in supercapacitive storage systems, highlighting their distinct attributes [60]. The synthesis of BDC materials for MIHSCs involves critical techniques, pyrolysis, hydrothermal carbonization, template methods, activation techniques, heteroatom doping, porosity development, surface functionalization, and other processes to ensure proper suitability for supercapacitors.

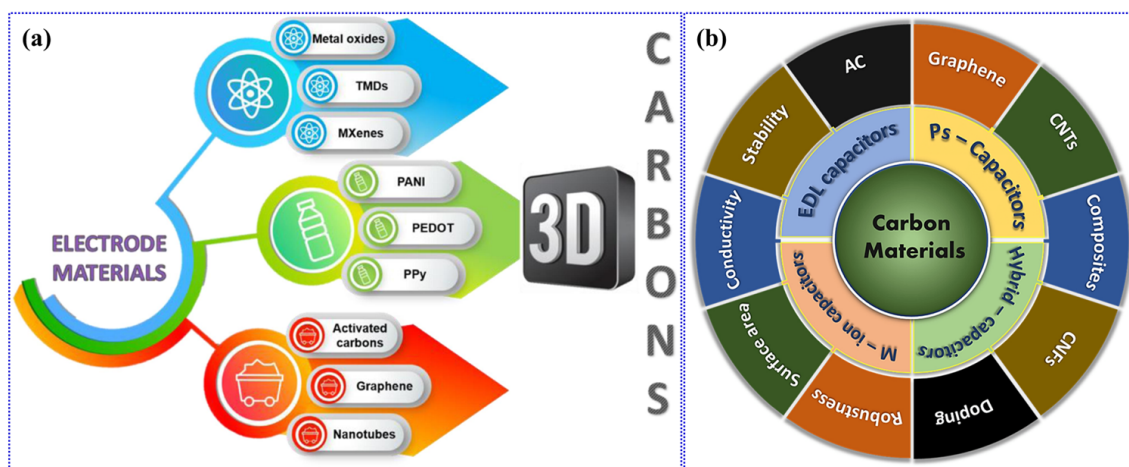


**Figure 2.** (a) Segmentation of electrode materials for MIHSCs. Reproduced with permission from Ref. [59]. Reproduced under the term CC BY 4.0. Copyright 2020, Galek et al., Frontiers. (b) Schematic representation for various carbon-based materials used as electrodes in different supercapacitive storage systems. Reproduced with permission from Ref. [60]. Reproduced under the term CC BY 4.0. Copyright 2022, Olabi et al., MDPI.

### 3.1. Synthesis of BDC Materials for ZIHSCs

BDC materials have attracted considerable interest because of their varied structural characteristics and possible uses in energy storage systems, particularly in synthesizing ZIHSCs. These materials offer renewability, sustainability, and cost-effectiveness advantages, making them attractive for various electrochemical applications [58,61]. BDC materials' structural diversity, porosity, and surface heteroatom doping have significantly impacted their performance in supercapacitors and other energy storage systems [61]. Additionally, synthesizing activated carbon (AC) from lignocellulosic biomass via chemical activation is promising for obtaining suitable precursors for energy storage applications [62]. Furthermore, incorporating self-doped heteroatoms in biomass-derived ACs has enhanced their electrochemical performance, laying a foundation for their supercapacitor application [63]. The potential of BDC materials in synthesizing ZIHSCs has been further supported by developing novel electrode materials and electrolytes. For instance, combining a zinc-activated positrode and a BDC negatrobe has been explored, leading to the assembly of an aqueous ZIHSC with promising performance [16,64,65].

Moreover, using hydrogel electrolytes based on naturally abundant cellulose has been identified as an ideal approach for constructing flexible solid-state ZIHSCs, aligning with the principles of resource renewability and environmental sustainability [66]. Furthermore, the study of hollow mesoporous carbon spheres as electrode materials for symmetrical and aqueous ZIHSCs has shown promise for developing high-performance energy storage devices [67]. BDC materials provide a flexible foundation for creating electrode materials and electrolytes, which allows for the advancement of high-performance ZIHSCs. Due to their varied structure, ability to hold substances, the introduction of different elements on their surface, ability to be replenished, and ability to be maintained over time, these materials are appealing options for meeting the increasing need for effective energy storage solutions [68,69].

Samage et al. [70] explored the transformation of *Solanum melongena* (SM), an agro-waste, into a self-doped carbon material suitable for symmetric supercapacitors and ZIHSCs through a one-step pyrolysis process. Initially, the SM was washed to remove impurities, chopped into small pieces, and sun-dried before being crushed into a fine powder, as shown in Figure 3a. The pyrolysis process was carried out in a nitrogen atmosphere that does not react with the materials. The temperature was increased gradually at a rate of 5 °C per minute, reaching 700 °C, 800 °C, and 900 °C successively. The pyrolysis process lasted for a total of 3 h. After the pyrolysis process, the carbonized samples were subjected to a washing step using 0.5 M HCl. They were then rinsed with distilled water until the pH became neutral and dried at 80 °C for 12 h. The resulting SM-derived carbon (SMC) exhibited a three-dimensional porous structure with uneven flake-like shapes, with SMC-700 showing a more hydrophilic nature than SMC-800 and SMC-900. Surface morphology examined through FESEM revealed the formation of porous structures at 700 °C and 800 °C, while 900 °C samples showed pore structure collapsing due to aggregated carbon, which undergoes a process where it transforms into thick layers resembling flakes. The nitrogen sorption isotherms revealed that SMC-800 had a significant SSA of 686.29 m<sup>2</sup>/g, mainly attributed to micropores and mesopores, resulting in a high porosity. The iron content in the precursor was used strategically for graphitization, converting amorphous carbon into graphitic nanostructures during pyrolysis.

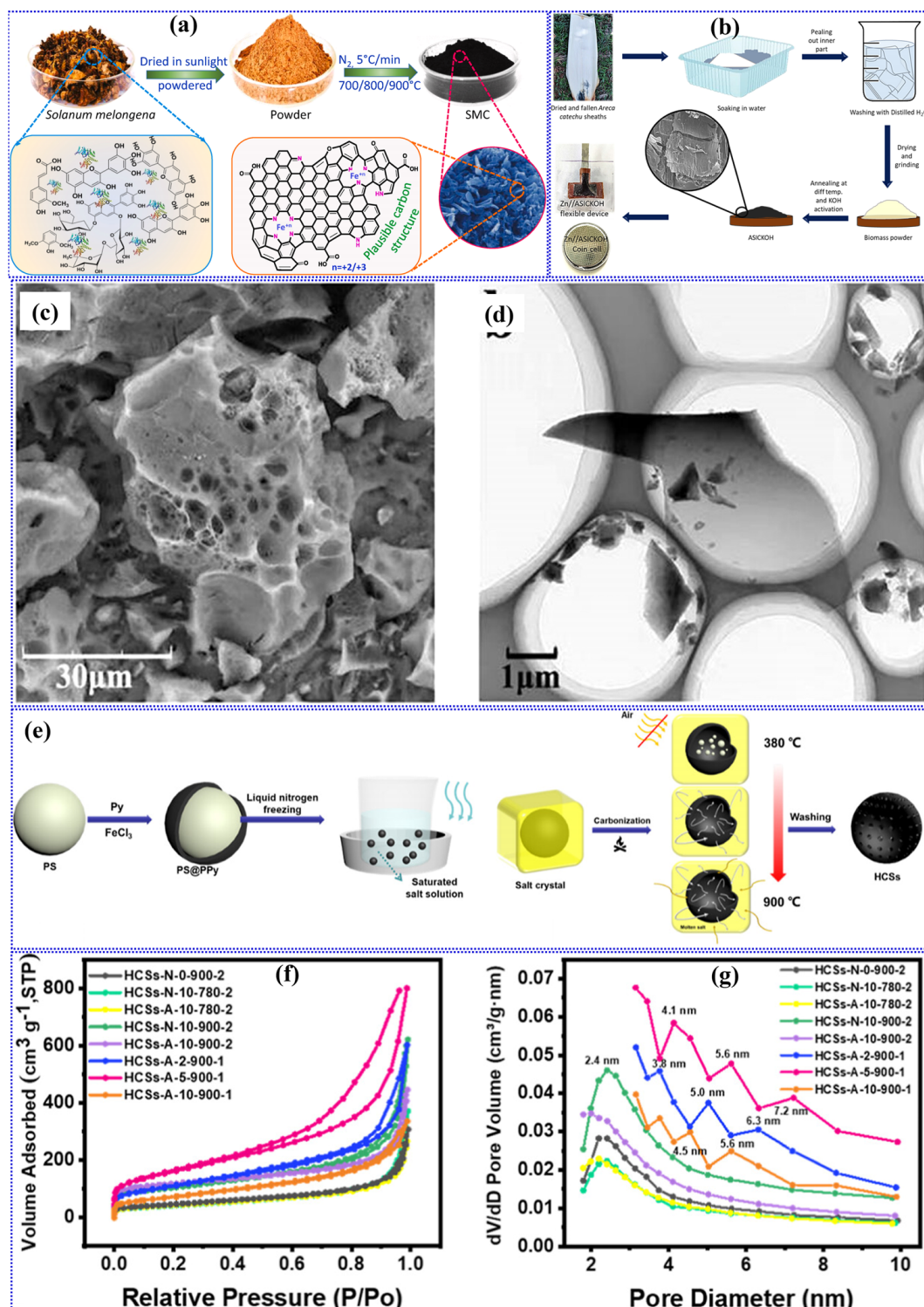


**Figure 3.** (a) A diagram illustrating the process of preparing the self-doped SMC. Reproduced with permission from Ref. [70]. Copyright 2024, Elsevier. (b) Diagram showing the process for synthesizing an AC from Areca Catechu sheaths, along with its application in ZIHSCs in coin and pouch cell formats. Reproduced with permission from Ref. [71]. Copyright 2022, American Chemical Society. (c) FESEM and (d) TEM micrographs of the N/S-AC. Reproduced with permission from Ref. [72]. Copyright 2023, American Chemical Society. (e) Diagram illustrating the process of preparing HCSs. (f) Nitrogen adsorption/desorption isotherms and (g) pore size distribution of the HCSs under different circumstances. Reproduced with permission from Ref. [73]. Copyright 2024, American Chemical Society.

Naik et al. [71] investigated the production of high-performance flexible ZIHSCs using carbon sheets produced from agricultural waste. The carbon material is derived from *Areca Catechu sheaths*, an abundant agricultural waste, through a multi-step process. As demonstrated in Figure 3b, the synthesis begins with collecting dried sheaths from a local farm, washing them, and soaking them in water to remove the inner part. After peeling, the inner section is dehydrated, pulverized into a fine powder, and subjected to annealing in a tubular furnace at temperatures between 700 and 900 °C for 3 h while exposed to a nitrogen flow. Post-carbonization, the carbon materials undergo a washing procedure using a solution of 1 M HCl and a mixture of ethanol and water. Subsequently, they are dried at 80 °C for one night. The carbon obtained at a temperature of 900 °C exhibited superior performance and was subsequently subjected to KOH activation, leading to KOH-AC formation. The carbon compounds demonstrate a significant SSA, with KOH-AC boasting a value of 2760 m<sup>2</sup>/g. The enhanced SSA and reduced pore diameter in KOH-AC contribute to its improved electrochemical performance.

Lignin, a significant biomass constituent, produces nitrogen and sulfur co-doped hierarchical porous carbon (N/S-AC) materials for high-performance ZIHSCs [72]. The preparation entails a dual-phase procedure: charring and activation using co-doping. The process involves combining lignin with urea and thiourea to provide nitrogen and sulfur, subjecting the mixture to carbonization at a temperature of 750 °C. As a result, nitrogen and sulfur co-doped activated carbon is formed. The materials possess a hierarchical pore structure, which is essential for offering active sites with a high SSA and an appropriate distribution of pore sizes. The FESEM image (Figure 3c) reveals that the N/S-AC has micrometre-sized particles with a porous structure, while TEM analysis (Figure 3d) confirms an interconnected porous nature. The BET SSA for the N/S-AC material is estimated at 2773.02 m<sup>2</sup>/g, demonstrating significant porosity. Additionally, the doped heteroatoms contribute to adjusting the pore structure and increasing surface wettability, providing enhanced conductivity and pseudocapacitance, making them ideal for high-performance ZIHSCs.

Zhao et al. [73] proposed a sustainable technique for producing hierarchically porous hollow carbon spheres (HCSs) as negatrodne materials in ZIHSCs. The procedure entails the pyrolysis of polystyrene–polypyrrole nanoparticles within a sodium chloride confinement, as shown in Figure 3e. This synthesis is performed in a single vessel, in the presence of air, eliminating the requirement to use inert gas to protect the reaction. The HCSs obtained display a hierarchical pore structure with a significant SSA of 578.2 m<sup>2</sup>/g. They are also doped with 2.6 at.% oxygen and 5.6 at.% of nitrogen. Figure 3f,g display the N<sub>2</sub> adsorption/desorption isotherms and the related pore size distribution of the HCSs under different circumstances. The carbon spheres' form and structure remain intact throughout the pyrolysis process, and their porous nature enhances their electrochemical properties. Du et al. [74] proposed a technique for creating a two-dimensional (2D) porous carbon matrix co-doped with nitrogen and oxygen. This matrix is synthesized using biomass generated from yeast cell walls. The synthesis involves a molten salt method, where yeast cell walls are mixed with a urea solution, freeze-dried to form precursors, and heated at 800 °C in an air atmosphere with NaCl and KCl. The resulting material exhibits a 2D lamellar structure, with its porous nature further enhanced by the urea decomposition, which introduces micro- and mesopores into the carbon matrix. The material, known as NAC-20, possesses a significant SSA of 368.63 m<sup>2</sup>/g. It is composed of a carbon structure that has been co-doped with nitrogen (6.03%) and oxygen (9.96%). This co-doping enhances the material's electrical conductivity and wettability. Several BDCs have been synthesized and utilized in ZIHSC configurations. Biomass-based nitrogen–oxygen co-doped carbons have exhibited high SSAs, heteroatom doping, and porous morphologies contributing to the performance of these electrodes. Their characteristic properties and performance capabilities, including morphology and SSA, are listed in Table 1. Thus, it is clear from the literature that biomass-based carbons with improved morphologies, porous structures, and enhanced SSAs were addressed to permit effective ZIHSCs. The hierarchical pores and

substantial heteroatom doping of catalytic zinc ions may improve these devices' specific capacitance, energy, cyclability, and power.

### 3.2. Synthesis of BDC Materials for NIHSCs

BDC materials have attracted considerable interest for their possible use in NIHSCs due to their capacity to be renewed, their sustainability, and their cost-effectiveness [23,75,76]. These materials have been investigated as potential electrode materials for high-energy NIHSCs, showing promising electrochemical performance [23]. BDC materials' inherent structural benefits, cost-effectiveness, and renewability make them highly appealing for sodium-ion energy storage systems [76]. Moreover, introducing heteroatoms into BDC materials increases the interlayer distance, enhancing the efficiency of transporting and storing sodium ions. As a result, sodium-ion batteries exhibit exceptional performance at high rates [61]. The synthesis of BDC materials has been a subject of interest, with research focusing on tailoring their structure to enhance their performance in NIHSCs. For instance, hierarchically porous carbon derived from shiitake mushrooms has been investigated for capacitive energy storage, demonstrating the potential for BDC materials in energy storage applications [77].

Furthermore, the favourable tubular composition of BDC has been identified as a possible positive option for sodium-ion batteries, thanks to its abundant availability, affordable price, and sustainable nature [78]. In addition, there have been new developments in energy storage using NIHSCs and ZIHSCs, revealing the potential of biomass-derived materials to meet energy storage requirements [18]. BDC materials show significant potential for NIHSCs, providing a viable and economical option for energy storage applications. These materials' diverse structure and electrochemical activity, combined with continuing research on their synthesis and performance improvement, make them viable contenders for meeting the increasing need for effective sodium-ion energy storage solutions.

The research works by Niu et al. [79] mainly focused on synthesizing two types of BDC materials using gelatine and phytic acid as precursors, as demonstrated in Figure 4a. The synthesis was carried out using sustainable concepts, including non-toxic precursors, which are readily available, low in cost, and ecologically friendly processes. The synthesis also included the utilization of physisorption, nanostructure engineering, and heteroatom doping, particularly phosphorus and nitrogen, to enhance the efficiency of carbon materials. P- and N-doped networked carbon nanosheets with hierarchical porosity were formed. They exhibited porous nanosheet networks synthesized directly by KCl/ice as a dual template or KOH for microporosity. The materials illustrated several morphologic features, such as nanosheet networks and a high SSA, essential for their application as electrodes in NIHSCs. Guo et al. [80] investigated the sustainable fabrication of dual (N, O)-doped biocarbon nanosheets from marine biomass. As described in Figure 4b, the direct pyrolysis of cuttlebones, along with the air oxidation activation approach, allows for a precise decrease in the thickness of carbon sheets from 35 to 5 nm. Consequently, this leads to the formation of a distinct hierarchical porous structure characterized by enhanced SSA and porosity and an increase in N-doping content from 7.5% to 13.9% at the atomic level. The controlled N-doping content of the nanosheets was independently monitored by the new role of air oxidation activation in regulating heteroatom content in the carbon matrix, ensuring novel biocarbon nanosheets with significant nitrogen and oxygen doping in the carbon matrix. The dual-doped structure provides improved conductivity and additional charge storage.

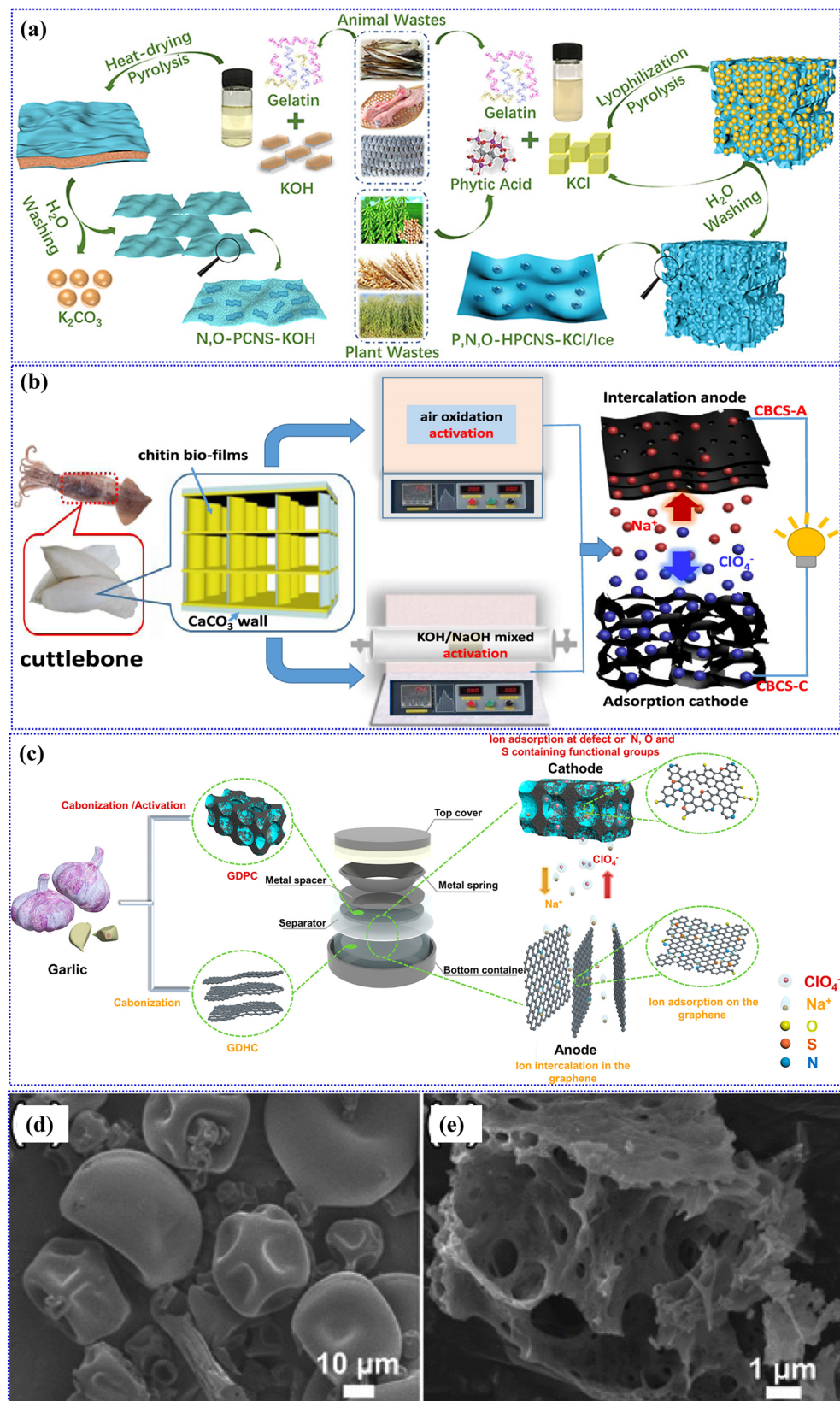


**Figure 4.** (a) A diagram illustrating the synthesis of interconnected carbon nanosheets with hierarchical porosity, incorporating phosphorus (P) and nitrogen (N) dopants. This synthesis involves dual KCl templates and ice (P, N-HPCNS-KCl/Ice). Reproduced with permission from Ref. [79]. Copyright 2020, American Chemical Society. (b) The diagram illustrates the synthesis process of the material and the corresponding charge storage processes at the positrode and negatroe in a NIHSC. Reproduced

with permission from Ref. [80]. Copyright 2018, American Chemical Society. (c) A scheme outlining the GDHC and GDPC preparation process and the mechanisms underlying sodium-ion storage in NIHSCs. Reproduced with permission from Ref. [81]. Copyright 2019, American Chemical Society. (d,e) FESEM micrographs of the PCNS at different magnifications. Reproduced with permission from Ref. [82]. Copyright 2020, Elsevier.

Liu et al. [81] examined a NIHSC made from carbon compounds obtained from garlic. The synthesis (Figure 4c) involves two methods: high-temperature pyrolysis at 1100 °C to create a durable carbon positrode, referred to as GDHC, and carbonization tailored by KOH activation to generate a porous carbon negatrode, referred to as GDPC. The GDHC positrode demonstrates a pseudo-graphitic arrangement characterized by an interlayer distance ranging from 0.365 to 0.376 nm. Conversely, GDPC possesses a highly permeable structure, with an SSA measuring 1682 m<sup>2</sup>/g. The carbon material structure is assessed using scanning electron microscopy, which identifies the block-like morphology of GDHC and the porous structure of GDPC. In addition, XRD and Raman spectra provide evidence of a well-organized structure and the presence of graphite. Zhang et al. [82] studied fabricating a three-dimensional porous carbon nanosheet (PCNS) utilizing soy protein and zinc nitrate. The synthesis involves using a chemical gas expansion approach followed by calcination to produce a three-dimensional PCNS material doped with nitrogen and sulfur. The resulting PCNS has a hierarchical porous structure characterized by a significant abundance of micropores and mesopores, as revealed in Figure 4d,e. The PCNS exhibits an SSA of ~516.6 m<sup>2</sup>/g. The carbon compounds exhibit an interlayer spacing of 0.385 nm, surpassing that of graphite. This higher spacing aids in the process of Na<sup>+</sup> intercalation and deintercalation. The result showcases a distinctive linked structure of carbon nanosheets, which offer abundant pathways for ion transport and improve its ability to store salt. Zhang et al. [83] examined the production of rigid carbon material from lotus stems. The synthesis entails subjecting the lotus stems to carbonization at several temperatures, namely 1200, 1400, and 1600 °C. The resultant materials, LS1200, LS1400, and LS1600, maintain a porous structure with a hierarchical channel array inherited from the lotus stems. FESEM and TEM investigations demonstrate that greater carbonization temperatures result in an elevated graphitization degree and a decreased tube wall thickness. The materials exhibit  $d_{002}$  spacings of 3.69 Å, 3.68 Å, and 3.61 Å, corresponding to LS1200, LS1400, and LS1600, respectively. These values indicate different levels of graphitic ordering. The carbons have a relatively low SSA ranging from 23.73 to 25.81 m<sup>2</sup>/g. This SSA gradually decreases as the carbonization temperature increases. Several more carbon materials generated from biomass, characterized by their unique shapes, porous architectures, and large SSA, have greatly improved the efficiency of NIHSCs. The presence of a distinct microstructure, which includes both hierarchical porosity and doped structures, enables enhanced ion transport and charge storage capabilities. These supercapacitors have remarkable electrochemical properties, including a high capacitance, energy density, power density, and great cycle stability. All of these factors are thoroughly presented in Table 1.

### 3.3. Synthesis of BDC Materials for AIHSCs

BDC materials are considered promising options for developing AIHSCs because of their capacity to be renewed, their sustainability, and their environmentally beneficial characteristics [61,84]. These materials provide a viable and long-lasting option for storing energy, in line with the ideals of using renewable resources and promoting environmental sustainability. BDC materials' structural diversities and synthesis methods have been demonstrated to significantly enhance their performance in supercapacitors [61,84]. An example is using a nitrogen-doped carbon nanofiber network obtained from biomass as a template to decorate ultrathin nickel–cobalt-layered double hydroxide nanosheets [52]. This demonstrates the high performance of the nanosheets as an electrode for an asymmetric supercapacitor [25]. Furthermore, using biomass straw-derived porous carbon to produce

supercapacitors through ball milling has attracted interest because of its renewable nature, abundant availability, affordability, and positive environmental impact [85]. Moreover, researchers have investigated the various structural variations in BDC materials for their potential uses in energy storage, focusing on the significance of their porous nature and the introduction of heteroatoms on their surfaces [61]. The synthesis methods of BDC materials are a subject of interest, with research focusing on tailoring their structure to enhance their performance in AIHSCs. These materials' renewable and eco-friendly characteristics and their wide range of structures make them appealing for meeting energy storage requirements, especially in AIHSCs. Using BDC materials in AIHSCs has significant potential for creating long-lasting and effective energy storage solutions. BDC materials provide a sustainable and cost-effective framework for creating AIHSCs. Their structural diversity and capacity to be renewed make them excellent options for meeting the increasing need for efficient energy storage solutions.

The research reported by Feng et al. [86] presents a sustainable and solvent-free technique for producing polymer spheres using m-phenylenediamine and hexamethylenetetramine (HMTA), with Pluronic F127 serving as a guiding agent for the structure, as demonstrated in Figure 5a. The combination is subjected to a temperature of 160 °C, initiating the polymerization process of MPF resin spheres. Subsequently, these spheres are subjected to a temperature of 600 °C, converting them into porous carbon spheres (PCSs). The PCSs possess a significant SSA of 3115 m<sup>2</sup>/g and a 3.05 cm<sup>3</sup>/g pore volume. The FESEM study (Figure 5b,c) reveals that the resin spheres maintain a spherical shape throughout the activation and carbonization techniques. Figure 5d displays the solid-state <sup>13</sup>C NMR spectrum, which reveals a peak at 18 ppm for methyl and methylene. The 70, 73, and 75 ppm peaks show bonding between carbon and oxygen. A series of distinct peaks (104, 113, 129, and 147 ppm) associated with different carbon environments in the benzene ring are produced by the chemical shift over 100 ppm. Figure 5e displays the FTIR spectra of MPF resin spheres, revealing aromatic, methylene, amino, and hydroxyl functional groups. The FTIR data corroborate the atomic structure of the MPF resin. According to NMR and FTIR investigations, the m-phenylenediamine and formaldehyde derived from the breakdown of HMTA polymerize almost entirely; full polymerization results in volumetric productivity and ultrahigh yield. The carbon material obtained has a hierarchical structure containing micropores and mesopores, making it well suited for energy storage.

Seon et al. [87] examined the production of AIHSCs that incorporate a battery-like aluminium positrode with a capacitor-like graphene negatrode. They employed an ionic liquid, namely 1-ethyl-3-methylimidazolium chloride (EMIImCl), and aluminium chloride (AlCl<sub>3</sub>) as the electrolyte. The investigation is focused on two surface treatment approaches, electropolishing and electrodeposition, to improve the electrochemical performance of the aluminium positrode. The aluminium positrode, formed by electrodeposition on a molybdenum foil substrate, has a dendritic structure and a significant SSA. The presence of roughness and dendritic development improves the electrochemical activity of the material, resulting in higher efficiency in storing Al<sup>3+</sup> ions. The XPS and GIXRD analysis reveals a reduction in the thickness of oxide layers and the presence of Al-OH species, which contribute to the formation of redox-active sites.

Lei et al. [88] reported the development and production of AIHSCs with a nitrogen-doped graphene negatrode, aluminium positrode, and [EMIIm]Cl and AlCl<sub>3</sub> electrolyte with high capacitance. A layer of nitrogen-doped graphene was applied to a tantalum foil, creating a flexible negatrode with a nitrogen concentration of 3–5% by weight. Doping alters the arrangement of energy levels in the band structure, amplifies the ability of graphene to conduct electricity, and boosts its ability to store electrical charge. The FESEM study revealed crumpled graphene layers stacked on each other, resulting in a large SSA that facilitates electrochemical reactions. Sun et al. [89] presented using a nitrogen-doped micro-mesoporous carbon sphere (NCS) as a negatrode material in aluminium-based HSCs. The NCS was produced by combining phenolic resin with melamine in a 1:1 mass ratio,

followed by carbonization at 600 °C in nitrogen. Subsequently, the carbon precursor was mixed with KOH and heated at 800 °C, forming a porous configuration. The SESEM study indicated the presence of round particles with sizes ranging from 0.1 to 1 μm. TEM demonstrated that these particles have an amorphous structure. The NCS has a BET SSA of 3078 m<sup>2</sup>/g, considerably greater than the 506 m<sup>2</sup>/g of the NC precursor containing nitrogen. This difference allows for more adsorption sites and facilitates more efficient ion diffusion.

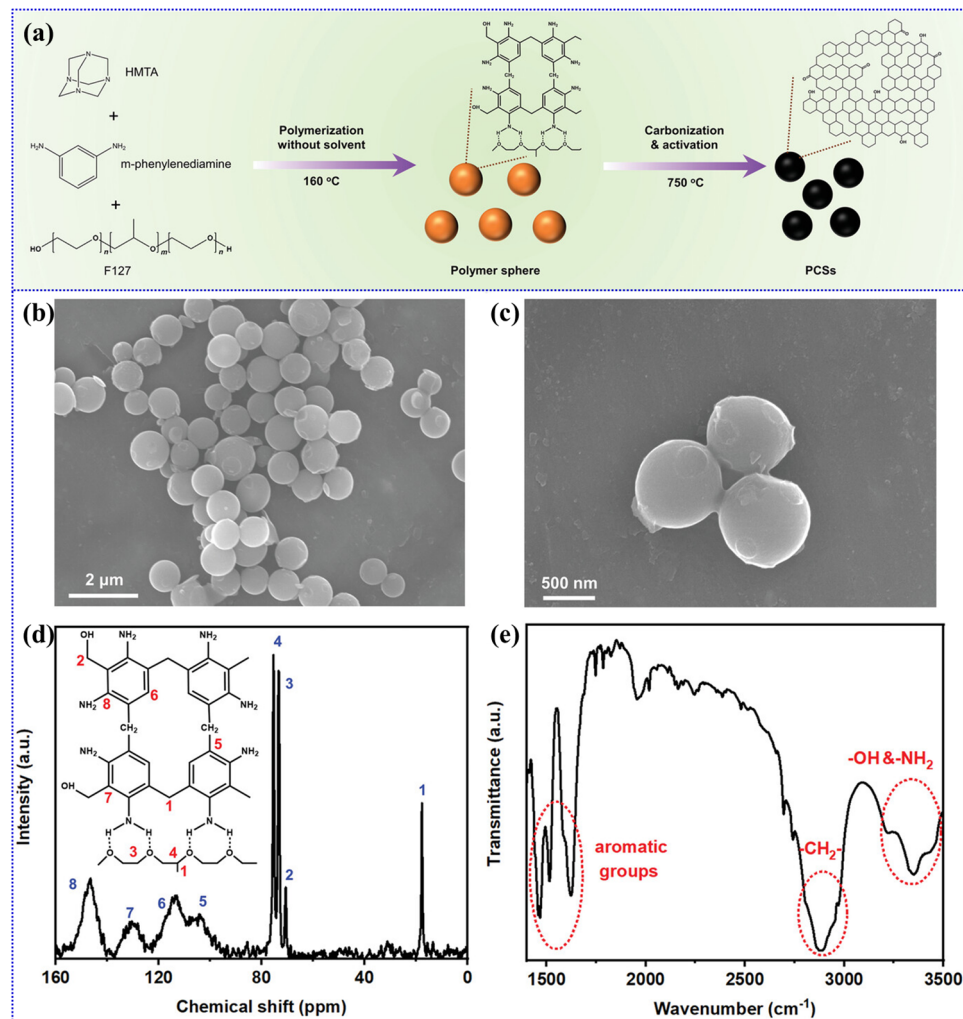


**Figure 5.** (a) The solvent-free synthesis method for MPF polymer spheres and PCSs is illustrated schematically. Morphological and structural characterization of MPF resin spheres; (b) low- and (c) high-magnification FESEM micrographs; (d) solid-state <sup>13</sup>C NMR spectrum; and (e) FTIR spectrum. Reproduced with permission from Ref. [86]. Copyright 2023, Wiley.

Optimizing the synthesis parameters during the carbon generation from biomass is essential for improving the efficiency of AIHSCs. BDC materials provide a sustainable and environmentally friendly option for producing electrodes, including distinctive structures that may be fine-tuned to achieve exceptional electrochemical capabilities. Research emphasizes the importance of various parameters, including SSA, porosity, nitrogen doping, and the existence of electrochemically active metals in carbons generated from biomass [90–92]. These properties can all be affected by the procedure used for synthesis. Researchers may customize the characteristics of BDCs for supercapacitor applications by precisely controlling culture conditions, nutrient concentrations, and activation methods. This enables them to attain a high specific capacitance, exceptional cycle stability, and enhanced

energy storage capacities. Various essential parameters for producing BDCs for AIHSCs are tabulated in Table 1.

### 3.4. Synthesis of BDC Materials for KIHSCs

BDC materials have garnered considerable attention in the field of KIHSCs due to their renewable nature, sustainability, and promise for efficient energy storage applications [93,94]. These materials offer a sustainable and cost-effective energy storage alternative, aligning with resource renewability and environmental sustainability principles. BDC materials' synthesis processes and structural design have been demonstrated to be significantly improved [93–95]. An example is the deliberate arrangement of well-distributed, extremely thin MoS<sub>2</sub> nanosheets within a hollow carbon structure, showing rapid potassium storage. This emphasizes the promise of BDC materials in KIHSCs [96]. Furthermore, the recent advancements and prospects of biomass-derived hierarchically porous carbon have been examined, focusing on the significance of developing and fabricating these materials for supercapacitor applications, specifically KIHSCs [94]. Using BDC materials in KIHSCs has significant potential for creating sustainable and highly effective energy storage solutions. The SSA, distribution of pore sizes, and ultimate electrochemical performance of the carbon materials are determined by the type of biomass precursor used and the activation processes employed. This emphasizes the significance of synthesis methods in customizing the properties of these materials for KIHSCs. Moreover, the recent advancements in creating and using hybrid electrodes made from biomass have given us valuable knowledge about the electrochemical properties of these materials and the ways they store ions in various types of batteries, such as potassium-ion batteries. This highlights the potential of BDC materials in KIHSCs [97]. BDC materials offer a sustainable and cost-effective platform for developing KIHSCs, with their structural diversity and renewability positioning them as valuable candidates for addressing the increasing need for effective energy storage technologies.

Graphene-like AC nanosheets and hard carbon (HC), two different carbon compounds made from almond shells, were synthesized according to Pham et al. [98]. The production of the HC involves a straightforward carbonization procedure at various temperatures, whereas the AC is generated by chemically activating it with KOH as the activating agent. An analysis of the structural properties of the materials shows that the hard carbon has a notable distance between its layers, which is advantageous for the process of potassium-ion (de)intercalation. The AC nanosheets possess a high SSA and an intricate porous structure. These observations, along with the analysis of the structure and chemistry, suggest that both HC and AC possess qualities that make them appropriate for storing potassium ions. A schematic representation for the dual-carbon KIHSCs using carbon nanosheet negatrodes derived from biomass and similar to graphene is shown in Figure 6a. Chen et al. [99] presented an innovative “plains–hills” model of carbon structure for producing electrode materials inspired by a lotus leaf’s surface structure. This design comprises ultrathin carbon nanosheets, also known as “plains”, which are formed with multiple lumps, referred to as “hills”, (Figure 6b) using a one-step pyrolysis method. The synthesis entails utilizing CaCl<sub>2</sub> as a dual-purpose compound, complexing agent, and oxygen scavenger in a Ca<sup>2+</sup>-bio gel, as demonstrated in Figure 6c. This structure integrates an unstacked nanosheet with different levels of imperfections, achieving a harmonious balance between pseudocapacitance and conductivity. The carbon materials obtained exhibit a balanced combination of high pseudocapacitance and conductivity. They have an SSA of 581 m<sup>2</sup>/g and a drop in oxygen doping from 24.9% to 12.3%. This reduction contributes to the presence of both ordered and amorphous carbon structures.

Huang et al. [100] outlined a single-step calcination technique for converting mango seed husk into BDC doped with nitrogen and oxygen (NOHC). This material is intended to be a positrode KIHSC. The NOHC materials that have been synthesized exhibit a significant level of graphitization, with interlayer spacings that vary between 0.39 and 0.38 nm in correlation with increasing temperature. The materials demonstrate a BET SSA of up to

489.4 m<sup>2</sup>/g, suggesting a porous structure advantageous for capacitive charge storage. A combination of rod- and sheet-like structures characterizes the shape of the NOHC. Doped nitrogen and oxygen are included to enhance the electronic conductivity and create active spots.

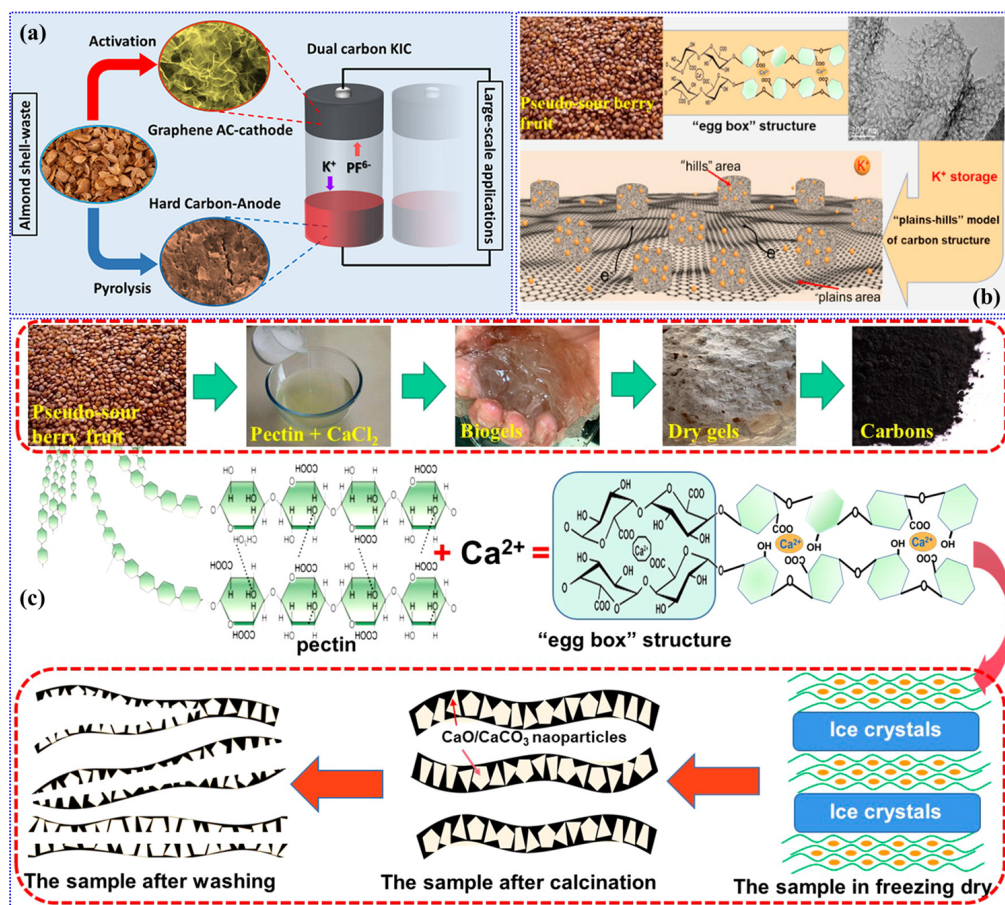


**Figure 6.** (a) Dual-carbon KIHSCs using carbon nanosheet negatodes derived from biomass and similar to graphene. Reproduced with permission from Ref. [98]. Copyright 2020, American Chemical Society. (b) A graphical representation for the K<sup>+</sup>-ion storage in BDC materials. (c) A graphical depiction of the CACF samples' synthesis protocol. Reproduced with permission from Ref. [99]. Copyright 2021, American Chemical Society.

Developing efficient synthesis techniques for carbon produced from biomass is crucial in determining the optimal performance of HSCs that use potassium ions. Supercapacitors have attracted significant attention because of their remarkable power density, long cycle life, and ecologically sustainable characteristics. However, the properties of the carbon compounds used as the electrode material significantly impact the device's performance. BDC is an ideal substitute for carbon since it is naturally abundant, inexpensive, and environmentally friendly. The synthesis techniques used to produce carbon, such as carbonization and activation processes, significantly impact its structure and other properties, thus affecting the performance of supercapacitors. The optimization of KIHSCs can be influenced by various parameters, as indicated in Table 1. The criteria encompass SSA, pore size distribution, surface functional groups, electrical conductivity, and other aspects, such as element content, which will be elaborated on later. Scientists can customize the carbon material by optimizing the synthesis technique to improve its capacitive behaviour, ion transport kinetics, and other energy-related characteristics. Thus, to enhance the above procedures, researchers can utilize several precursors and employ varied carbonization temperatures, activation methods, and post-treatment strategies.

**Table 1.** Synthetic protocols for preparing BDC materials in high-performance MIHSCs.

Biomass Source	Carbon Preparation Protocols	Morphology	SSA ( $\text{m}^2/\text{g}$ )	Ref.
Solanum melongena	Pyrolysis; 700, 800, and 900 °C; $\text{N}_2$ gas	Irregular flake-like 3D porous structure	574.34, 686.29, and 239.16	[70]
Areca Catechu sheaths	Pyrolysis; KOH activation; 900 °C; $\text{N}_2$ gas	Porous nanosheet	2760	[71]
Lignin	Pyrolysis; KOH activation; 750 °C; $\text{N}_2$ gas	Particles with a porous structure	2773.02	[72]
Salt crystals	Carbonization; $\text{FeCl}_3$ activation; 900 °C; $\text{N}_2$ gas	Hierarchically porous hollow spheres	578.2	[73]
Recycled yeast cell wall	Carbonization, $\text{NaCl}/\text{KCl}$ activation, 800 °C; air	2D lamellar structure	368.63	[74]
Ipomoea carnea leaves	Carbonized; KOH activation; 900 °C; $\text{N}_2$ gas	Transparent spheres	736.7	[101]
Resorcinol-furfural resin	Carbonization, KOH activation, 900 °C, $\text{N}_2$ gas	3D hierarchical porous structure	1350	[102]
Anhydrous glucose	Pyrolysis; magnesium oxide and potassium bicarbonate activation; 750 °C; Ar gas	3D honeycomb-like structure with interconnected pores	2265	[103]
Sodium lignosulfonate	Carbonization; KOH activation; 900 °C; $\text{N}_2$ gas	Hierarchical porous structure	2460	[104]
Tannin	Pyrolysis; 800 °C; $\text{N}_2$ gas	Hierarchical micro- and mesoporous structure	967	[105]
Pine needles	Carbonization; KOH activation; 800 °C; Ar gas	Microporous structures with interconnected pores and channels	2493.4	[106]
Zeolitic imidazolate framework	Carbonization; thiourea mixing; 800 °C; Ar gas	Cubic porous structure	677.2	[107]
Fallen autumn leaves	Carbonization; KOH activation; 950 °C; $\text{N}_2$ gas	Amorphous and porous structures, with minor graphitic flakes	2114	[108]
Osmanthus flowers	Freeze drying; carbonization; 800 °C; Ar gas	Foamy-like structure with hierarchical pores	690.3	[109]
Aerial roots of Ficus macrocarpa	Pyrolysis; $\text{KHCO}_3$ activation; 900 °C; $\text{N}_2$ gas	Hierarchical porous nanosheet structure	1454.7	[110]
Gelatine/phytic acid	Pyrolysis; KOH/ $\text{KHCO}_3$ activation; 900 °C; $\text{N}_2$ gas	Ultrathin and small nanosheets	1911	[79]
Marine biomass	Carbonization; 600 °C; $\text{N}_2$ gas	Porous nanosheets	1489	[80]
Garlic	Pyrolysis; KOH activation; 1100 °C; $\text{N}_2$ gas	Blocky morphology	1682	[81]
Soy protein	Pyrolysis; zinc nitrate activation; 700 °C; Ar gas	Hierarchical porous structure with abundant micropores and mesopores	516.6	[82]
Lotus stems	Carbonization; 1200, 1400, and 1600 °C; Ar gas	Turbostratic graphitic structure	25.81, 24.37, and 23.73	[83]
Apricot shell	Pyrolysis; 900, 1100, 1300, and 1500 °C; $\text{H}_2/\text{Ar}$ atmosphere	Porous structure with well-connected porous network	2.7 to 56.7	[111]
Mango peels	Carbonization; sulfur and hexamethylenetetramine mixing; 1000 °C/800 °C; Ar gas	Porous flake-like morphology	1079.88	[112]

**Table 1.** Cont.

Biomass Source	Carbon Preparation Protocols	Morphology	SSA ( $\text{m}^2/\text{g}$ )	Ref.
Agricultural wastes, specifically peanut shell, wheat straw, rice straw, corn stalk, cotton stalk, and soybean stalk	Hydrothermal reaction with $\text{H}_2\text{SO}_4$ aqueous solution and subsequent chemical activation with KOH at 800 °C; Ar atmosphere	Porous sheet structure with interconnected macropores, mesopores, and micropores	534.3 to 1994.2	[113]
Cassava peel	Pre-carbonization 350 °C; KOH activation at 600 °C; Ar atmosphere	Slit-type pores and a highly disordered structure	1032	[114]
Corn silk	Pre-carbonization at 350 °C; KOH activation; carbonization at 800 °C; Ar atmosphere	Microporous nanosheets	2550	[115]
Sugarcane bagasse	$\text{NaH}_2\text{PO}_2 \cdot 2\text{H}_2\text{O}$ and melamine dispersion; hydrothermal reaction at 180 °C for 24 h; KOH activation; carbonization; 700 °C; Ar atmosphere	3D interconnected hierarchical porous structure	2803.2	[116]
m-phenylenediamine-formaldehyde resin	Carbonization; KOH activation; 750 °C; Ar atmosphere	Spherical morphology	3115	[86]
Graphene	...	Nanosheets	2675	[87]
Nitrogen-doped graphene derived from a synthetic approach	...	Wrinkled and overlapping morphology with a few layers	...	[88]
Phenol resin and melamine	Pre-carbonized at 600 °C; KOH activation at 800 °C; $\text{N}_2$ environment	Spherical particles	3078	[89]
Almond shells	Carbonization; KOH activation; 1100 °C; $\text{N}_2$ environment	Sheetlike nanostructures	127	[98]
Sour berry fruits	Freeze drying, $\text{CaCl}_2$ curing; bio gel and dry gel production; acid treatment	Nanoflakes	581	[99]
Mango seed shuck	Carbonization; 900, 1100, and 1300 °C; Ar atmosphere	Rod- or sheet-shaped feature	489.4, 383.2, and 319.1	[100]
Petroleum pitch	Pyrolysis; $\text{KHCO}_3$ activation; 800 °C; inert atmosphere	Cross-linked nanosheets	48.8	[117]
Gpositroderma lucidum spores	Carbonization at 850 °C; mixing with diethylene triamine and ammonium molybdate tetrahydrate; hydrothermal reaction at 200 °C; pyrolysis at 850 °C; $\text{N}_2$ atmosphere	Porous cage-like structure with double walls and a 3D network of interconnected carbon structures	217	[118]
Potato	Two-step carbonization; pre-pyrolysed at 500 °C; carbonization at various temperatures (900 °C, 1000 °C, and 1100 °C); Ar atmosphere	Mesoporous	620.77, 531.67, and 325.73	[119]
Hemp stalk core	Carbonization; 800 °C; $\text{N}_2$ atmosphere	Honeycomb-like structure	1185.3	[120]
Walnut septum	Pyrolysis; urea activation, 800 °C; $\text{N}_2$ atmosphere	Tubular cellular structure	176.9	[121]

#### 4. Application of BDCs in MIHSCs

Carbon materials derived from biomass have emerged as potential candidates for MIHSCs, especially in the case of zinc and other moieties, namely sodium, potassium, and AIHSCs. This approach is attractive, as using such precursors would be sustainable and relatively cheaper than other biomass-based energy storage materials. Carbon materials can be prepared from biomass using pyrolysis, hydrothermal carbonization, or activation methods to obtain porous carbons with desired properties as a supercapacitor electrode [105,122,123]. Since the initiation of research on MIHSCs, scientists have investigated many types of electrode materials [124]. Figure 7a illustrates the configuration of these capacitors, emphasizing the primary materials employed for electrodes. The positrode materials are classified into various groups, including carbon-based materials, titanium-based compounds, niobium pentoxide ( $\text{Nb}_2\text{O}_5$ ), and other transition metal compounds such as molybdenum, tungsten, and vanadium. Scientists have also employed various methods to customize and optimize the active substances to improve the rate capability, prolong the lifespan, and increase the capacity of the capacitors, as shown in Figure 7b. The

following discussion will explore the progress in developing practical positrode materials, organized by their respective types. Among various MIHSCs, biomass-based carbon materials are most commonly used in ZIHSCs. Prior research has demonstrated that using carbon derived from biomass can enhance the energy storage capacity of ZIHSCs, resulting in improved gravimetric and volumetric energy density [21,76,125]. Hierarchical carbon structures prepared from biomass have mainly been effective in increasing the energy storage of ZIHSCs. Moreover, the nitrogen doping of biomass-originated carbon can facilitate the performance of potassium supercapacitors, thus suggesting new possibilities for the applications of advanced energy storage solutions. Additionally, sodium and AIHSC applications have been investigated using BDC materials. These materials enabled relatively high energy storage for the sodium battery to develop a sustainable energy storage solution. Biomass-originated carbons are still being studied in AIHSCs to improve energy retention performance and energy density without volume expansion, as previously reported in the field. The possible designs and study suggest a sustainable and flexible approach to MIHSCs using biomass-based carbon material.

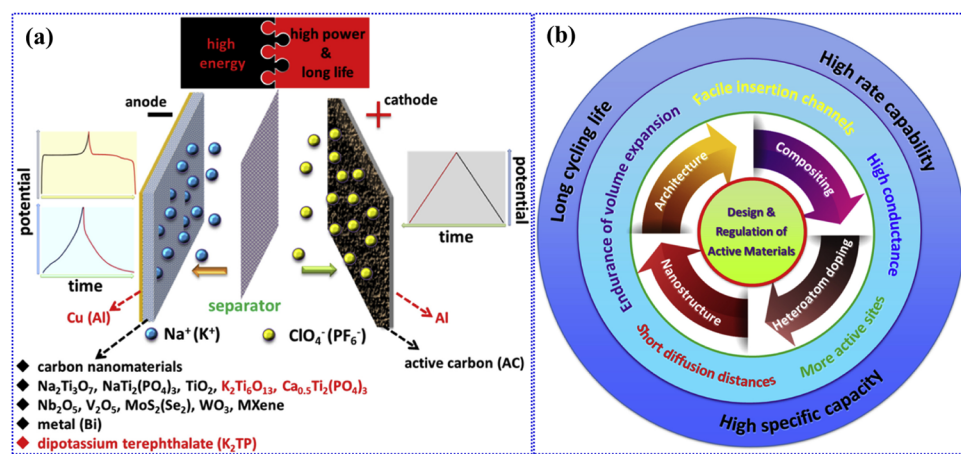


**Figure 7.** (a) Structural diagram of an MIHSC, illustrating the key components and materials. (b) Illustration of various strategies employed in designing and optimizing electrode materials for enhanced performance. Reproduced with permission from Ref. [124]. Copyright 2019, Elsevier.

The overall performance of MIHSCs is substantially influenced by the interaction of electrolyte volume, electrode mass, and surface area, which are essential considerations. The electrolyte volume impacts the quantity of charge that may be stored, where a smaller volume may result in a greater energy density [126]. MIHSCs can increase the device's energy density by reducing the electrolyte's total volume. In addition, selecting electrolytes such as water-in-salt electrolytes can significantly impact the performance of these supercapacitors [127]. The mass of the electrode is a crucial factor affecting MIHSCs' performance. High capacitance, cycle life, and operating voltage require optimal electrode mass ratios [128]. The electrode material's mass directly impacts the MIHSCs' charge storage capacity, affecting energy density [128]. In addition, the electrode material should possess a high surface area relative to its volume or mass to improve its performance [129]. The electrochemical performance of MIHSCs is significantly influenced by surface area. Maximizing the electrochemical double-layer capacitance and pseudocapacitance requires a large surface area for the electrodes, which leads to enhanced performance [130]. BDCs with mesopores are preferred for MIHSCs because of their expansive specific surface area and appropriate distribution of pore sizes, which enhance their overall performance. Additionally, it is essential to develop electrode materials that possess significant active surface areas and facilitate rapid ion transfer to attain superior energy density and rate capability in supercapacitors. Overall, the performance of MIHSCs is influenced by the synergistic interaction of electrolyte volume, electrode mass, and surface area. By optimizing these

characteristics, it is possible to improve the energy density, power density, and cycling stability of these sophisticated energy storage devices.

#### 4.1. ZIHSCs

BDC materials are considered suitable candidates for optimizing the performance of ZIHSCs. BDC materials are recognized for their ability to have a regulated microstructure with a large SSA. Due to their environmentally benign nature, they are considered a desirable choice for creating energy storage systems [131]. In this case, the application of BDC materials in ZIHSCs is addressed to assess the opportunity to improve the power capability of these supercapacitors. Porous carbon compounds derived from biomass are commonly recognized as superior electrodes for charge storage devices, such as supercapacitors, owing to their affordability and resilience. These materials have proven to be highly efficient in tackling energy storage and conversion challenges [23,132].

Consequently, implementing BDC materials in ZHSCs is aligned with the sustainable strategy. It provides a direction for one of the various commercial implementations to develop high-efficiency energy storage systems. Additionally, the negatrod material for ZIHSCs is critical to the carbon-based material's structural characteristics and electrochemical performance. Recent research analysed the influence of carbon materials, including AC, N-doped AC, graphene oxide, and carbon nanotube, on the development of ZIHSCs, focusing on the role of carbon materials in high-efficiency and -power functionality [133,134]. By incorporating the unique qualities offered by BDC materials, particularly the large SSA and regulated porosity, enhancing the energy density and power density of ZIHSCs is necessary to assure the practicality of high-power applications. This type of development collaborates with high-performance ZIHSCs for the marketable implementation of zinc-ion batteries due to the opportunity to provide high-efficiency, sustainable energy storage systems.

The ZIHSCs were created using the SMC as the negatrod, commercial zinc foil as the positrode, and a 2 M  $\text{ZnSO}_4 \cdot 7\text{H}_2\text{O}$  solution as the electrolyte, with a Whatman filter paper as the separator, as shown in Figure 8a [70]. The electrochemical studies indicated the potential for energy storage applications. The specific capacitance, energy, and power for SMC-800-based ZIHSCs were 313.08 F/g, 141.35 Wh/kg, and 6935.38 W/kg, respectively. The ZIHSC devices exhibited excellent cyclic stability, losing only 1.92% over 20,000 GCD cycles at 4 A/g. The symmetric supercapacitors fabricated using produced carbon samples with 6 M KOH delivered high specific capacitance, with SMC-800 achieving the best performance. The symmetric supercapacitor with SMC-800 demonstrated a high specific capacitance of 154.64 F/g at 0.1 A/g and excellent stability with over 99% retention after 50,000 GCD cycles at 10 A/g. These results suggest that the developed BDC materials suit high-performance energy storage applications in ZIHSCs. The flexible ZIHSC was fabricated with KOH-AC as the positrode electrode and metallic zinc as the negatrod [71]. The positrode in the coin cell format was formed by depositing the active material slurry onto a pre-cut titanium foil using drop-casting, followed by drying in an oven. The electrolyte employed was a zinc sulfate solution with a concentration of 1 Molar. The ZIHSC with the KOH-AC positrode exhibited a notable specific capacitance, reaching 208 F/g at a current density of 0.1 A/g. Additionally, it demonstrated exceptional rate capability, maintaining 84.5% of its capacitance after undergoing 10,000 cycles at a 5 A/g current density. Figure 8b displays the CV curves of ZIHSC utilizing Areca catechu sheath-derived AC, together with the background information, which includes a digital image of the sandwich-type pouch cell architecture. A laser-scribed carbon pattern on a polyimide sheet was used as the current collector for both the positrode and negatrod in order to create a flexible pouch cell. This design showcased excellent flexibility and stability when subjected to mechanical stress. Under bending conditions, the flexible device exhibits an energy density of 32.6  $\mu\text{Wh}/\text{cm}^2$  and a high power density of  $\sim 2 \text{ W}/\text{cm}^2$ . The electrochemical tests suggest that BDC sheets derived from agricultural waste show great potential for high-performance ZIHSCs, providing both sustainability and cost-effectiveness in energy storage applications.

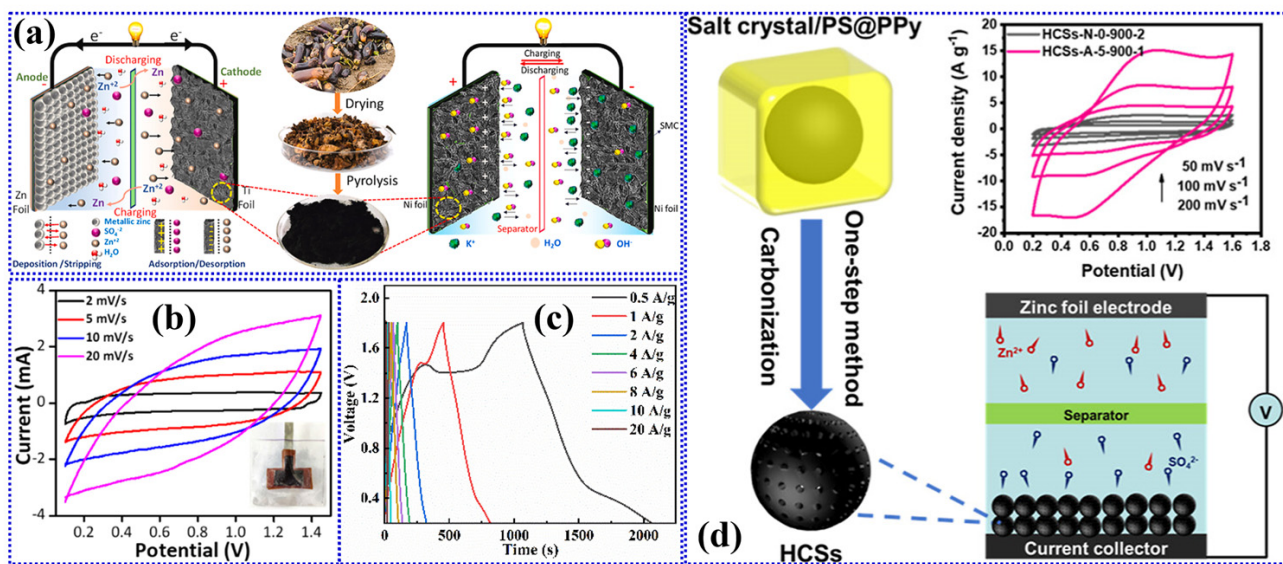


**Figure 8.** (a) The diagram illustrates the process of creating a ZIHSC utilizing SMC as the positrode. Reproduced with permission from Ref. [70]. Copyright 2024, Elsevier. (b) CV curves of ZIHSC using Areca catechu sheath-derived AC; the background includes a digital image of the sandwich-type pouch cell configuration. Reproduced with permission from Ref. [71]. Copyright 2022, American Chemical Society. (c) The GCD profiles of the N/S-AC-based ZIHSC at various current densities. Reproduced with permission from Ref. [72]. Copyright 2023, American Chemical Society. (d) Schematic representation of the HCSs' synthesis and their electrochemical performance in ZIHSCs. Reproduced with permission from Ref. [73]. Copyright 2024, American Chemical Society.

The synthesized N/S-AC materials were used to fabricate the ZIHSC with a carbon negatrode and zinc foil positrode, employing 2 M  $\text{ZnSO}_4$  aqueous electrolyte [72]. The electrochemical results (Figure 8c) designate that the specific capacitance for the N/S-AC-based ZIHSCs reached 307 F/g at 0.5 A/g, demonstrating an excellent capacity retention of 99.72% after 20,000 cycles at 10 A/g. The achieved energy density was 108.8 Wh/kg, whereas the achieved power density was 115,200 W/kg. The exceptional electrochemical capabilities of this material can be attributed to the combined effects of nitrogen and sulfur doping, as well as the hierarchical porous structure. Moreover, the manufacturing procedure enables the creation of a significant quantity of BDC materials, demonstrating the capacity of these materials for creating high-performance ZIHSCs on a wide scale.

Zhao et al. [73] created ZIHSCs by using the manufactured HCSs as negative electrodes, zinc foil as the positrode, and a 2 M  $\text{ZnSO}_4$  electrolyte, as shown in Figure 8d. The ZISCs based on HCSs-A-5-900-1 had a specific capacitance of 108 F/g at a current density of 0.2 A/g. They also had an energy density of 26.2 Wh/kg and a power density of 140.1 W/kg. In addition, the supercapacitors demonstrated remarkable cycling stability, maintaining 65% of their capacity after undergoing 5000 cycles. The ZIHSCs exhibited a significant capacitive-controlled storage level, contributing to their exceptional electrochemical performance. The hierarchical porosity and doping levels of the HCSs are essential factors that significantly contribute to their performance, rendering these carbon materials highly favourable for energy storage applications. Du et al. [74] demonstrated the electrochemical performance of the synthesized carbon matrix by constructing ZIHSCs using NAC-20 as the negatrode, zinc flakes as the positrode, and a 2 M  $\text{ZnSO}_4$  electrolyte. The ZIHSCs showed a capacitance of 191.1 F/g at 0.5 A/g, a stable cycle life of over 10,000 cycles, and a 103% capacity retention. Additionally, these supercapacitors achieved an energy density of 37 Wh/kg at a power density of 91 W/kg. Combining a high SSA, porous structure, and heteroatom doping contributes to this remarkable performance, allowing ZIHSCs assembled with NAC-20 to store energy effectively and light up a red LED for nearly 5 min, demonstrating their practical application. Several different BDCs have

been used as electrodes in ZIHSCs, significantly increasing their performance. Nitrogen–oxygen co-doped carbon obtained from yeast cell walls and other feedstock demonstrated exceptional electrochemical characteristics. There has been a notable increase in interest in electrochemical energy storage in recent years, with a specific emphasis on ZIHSCs. These investigations have been conducted to explore the use of BDC materials. These materials are valued for their sustainability, cost-effectiveness, and ecologically favourable properties. These materials have shown great potential in improving the electrochemical performance of ZIHSCs through several methods, such as maximizing surface area, porosity, and electrical conductivity [134–141]. Various studies have examined ZIHSCs using BDCs derived from hemp biomass [142], glutinous rice [143], platanus achene fruits [144], pyrolytic carbon black and critical PANI [145], metal organic frameworks (MOFs) [146,147], carp scales [148], green cokes [149], bamboo [150,151], rice husk [152], heavy fraction of bio-oil [153], yeast [154], by-product of traditional Chinese medicine [155], wood [156], lignin [157,158], corncob cellulose [159], heavy bio-oil [160], and sugarcane [161]. The wide variety of BDCs, each with their own unique structure and electrochemical properties, has played a significant role in the progress of ZIHSCs. Their utilization has resulted in significant enhancements in performance indicators, including specific capacitance, energy density, power density, and cycling stability, establishing their position in the future of sustainable energy storage technologies. Several important performance metrics from the experimental results of these carbonaceous materials are presented in Table 2, revealing their ability to drive ZIHSCs to the next level.

#### 4.2. NIHSCs

BDC materials have emerged as potential materials for enhancing the efficiency of NIHSCs in recent years. BDC materials are affordable and eco-friendly alternatives that are extensively used to improve the efficiency of SIHSCs. Moreover, these materials possess other distinctive characteristics compared to conventional carbon, such as large interlayer spaces, disorderly carbon structures, and more active functional groups that ensure better charge storage than conventional carbon [94,162]. The commercial potential of BDC materials in supercapacitors arises from the diverse structure and superior properties of these materials. They fit the supercapacitor performance property and tailored structure. It is feasible to enhance the energy density, power density, and cycling stability of BDC materials used in supercapacitors. Therefore, their commercial potential in the commercial sector plays a natural role in producing sodium-ion batteries for industrial applications. Their eco-friendly nature and sources, coupled with their versatile high-performance structure moulded by nature, make BDCs promising candidates for sustainable energy storage in the sodium-ion battery industry [76]. The progress in research on BDC materials for sodium-ion energy storage devices indicates their potential for innovation and collaborative development in supercapacitors.

**Table 2.** A summary of electrochemical performance for the BDC materials in high-performance MIHSCs.

Positrode	Negatrod	Electrolyte	HSC Type	Specific Capacitance (F/g) @ Current Density (A/g)	Energy Density (Wh/kg) @ Power Density (W/kg)	Capacitance Retention (% @ No. of Cycles)	Ref.
SMC	Zn foil	2 M ZnSO <sub>4</sub> ·7H <sub>2</sub> O	ZIHSC	313.08 @ 0.1	141.35 @ 6935.38	99 @ 50,000	[70]
KOH-AC	Zn foil	1 M ZnSO <sub>4</sub>	ZIHSC	208 @ 0.1	52 @ 1906.4	84.5 @ 10,000	[71]
N/S-AC	Zn foil	2 M ZnSO <sub>4</sub>	ZIHSC	307 @ 0.5	108.8 @ 115,200	99.72 @ 20,000	[72]
HCSs	Zn foil	2 M ZnSO <sub>4</sub>	ZIHSC	108.7 @ 0.2	26.2 @ 140.1	65 @ 5000	[73]
NAC	Zin sheet	2 M ZnSO <sub>4</sub>	ZIHSC	191.1 @ 0.5	37 @ 91	103 @ 10,000	[74]
ICF	Zn foil	1 M ZnSO <sub>4</sub> /MnSO <sub>4</sub>	ZIHSC	168 @ 1	39.7 @ 9000	79.5 @ 5000	[101]
Porous carbon	Zn foil	2 M ZnSO <sub>4</sub>	ZIHSC	291 @ 0.1	79 @ 391	96 @ 50,000	[102]
HHPC	Zn foil	2 M ZnSO <sub>4</sub>	ZIHSC	147 mAh/g @ 0.2	117.6 @ 160	88 @ 20,000	[103]
LHPC	Zinc metal	1 M ZnSO <sub>4</sub>	ZIHSC	298 @ 0.1	135 @ 101	97 @ 8000	[104]
TOMC	Zn foil	2 M ZnSO <sub>4</sub>	ZIHSC	331.2 @ 0.2	148.9 @ 180	85.7 @ 10,000	[105]
PNMNC	Zn foil	1 M ZnSO <sub>4</sub>	ZIHSC	472.5 @ 0.1	39.7 @ 9000	97.1 @ 10,000	[106]
S, N-CNC	Zn foil	2 M ZnSO <sub>4</sub>	ZIHSC	331 @ 1	148.9 @ 900	70 @ 10,000	[107]
AC650	Zn foil	2 M ZnSO <sub>4</sub>	ZIHSC	95 @ 0.1	86 @ 210	73 @ 10,000	[108]
NPFC700	Zn foil	1 M Zn(CF <sub>3</sub> SO <sub>3</sub> ) <sub>2</sub>	ZIHSC	207.9 @ 0.1	85.7 @ 15.4	97.4 @ 20,000	[109]
FHPCNSs-800	Zn foil	2 M ZnSO <sub>4</sub>	ZIHSC	220.1 mAh/g @ 0.2	181.6 @ 165	100 @ 30,000	[110]
P,N-HPCNS-KCl/Ice	HPCB-KOH	1 M NaClO <sub>4</sub>	NIHSC	119 mAh/g @ 0.035	135.3 @ 30	88.6 @ 8000	[79]
CBCS-A3	CBCS-C	1 M NaClO <sub>4</sub>	NIHSC	640 mAh/g @ 0.1	36,000 @ 53,000	90.5 @ 8000	[80]
GDHC	GDPC	1 M NaClO <sub>4</sub>	NIHSC	260 mAh/g @ 0.05	156 @ 355	73 @ 10,000	[81]
PCN	HPC	1 M NaClO <sub>4</sub>	NIHSC	205 mAh/g @ 0.5	119 @ 200	82 @ 8000	[82]
LS1400	Sodium foil	1 M NaClO <sub>4</sub>	NIHSC	350 mAh/g @ 0.1	...	94 @ 450	[83]
HASH	HASH	1 M NaClO <sub>4</sub>	NIHSC	400 mAh/g @ 0.1	...	91.7, 500	[111]
NS-MPC	Na-metal foil	1 M NaClO <sub>4</sub>	NIHSC	765 mAh/g @ 0.1	...	52 @ 2500	[112]
BDC	Na <sub>2</sub> Ti <sub>2.97</sub> Nb <sub>0.03</sub> O <sub>7</sub>	1 M NaClO <sub>4</sub>	NIHSC	60.5 @ 0.2	169.4 @ 120.5	83.8 @ 500	[113]
CAC	CAC	1 M NaClO <sub>4</sub>	NIHSC	247 @ 0.5	160 @ 425	100 @ 10,000	[114]
CSC	CSC	1 M NaClO <sub>4</sub>	NIHSC	126 @ 0.3	116 @ 1560	68 @ 300	[115]
SBNPK	SBNPK	1 M NaClO <sub>4</sub>	NIHSC	356.4 @ 1	6.5 @ 251.9	96.5 @ 20,000	[116]
EMIMAICl <sub>4</sub>							
PCSs	Al foil	(1-ethyl-3-methylimidazolium tetrachloroaluminate)	AIHSC	200 mAh/g @ 0.100	220 @ 900	80 @ 1500	[86]
Graphene	Al foil	EMImCl and AlCl <sub>3</sub>	AIHSC	211 @ 3	51 @ 3390	87 @ 5000	[87]
Nitrogen-doped graphene	Al foil	EMImCl and AlCl <sub>3</sub>	AIHSC	240 @ 0.1	...	90 @ 2000	[88]
NCS	Al foil	EMImCl and AlCl <sub>3</sub>	AIHSC	224 mAh/g @ 0.3	...	100 @ 35,000	[89]
AS-AC	AS-HC	1 M KPF <sub>6</sub>	KIHSC	88 @ 0.053	105 @ 250	96 @ 10,000	[98]
CACF	CACF	1 M potassium bis(fluorosulfonyl)imide (KFSI)	KIHSC	350 mAh/g @ 0.1	178.4 @ 1115	75.2 @ 10,000	[99]
NOHC	Hard carbon	0.8 M KPF <sub>6</sub>	KIHSC	186.3 mAh/g @ 0.1	68 @ 2000	80 @ 1000	[100]
ACNs	SCNs	0.8 M KPF <sub>6</sub>	KIHSC	89.1 @ 0.1	124.0 @ 198.9	89.4 2 @ 9000	[117]
NOBC	Potassium disk	1 M KPF <sub>6</sub>	KIHSC	251.2 mAh/g @ 0.5	...	77.74 @ 2000	[118]
PBPC	Potassium metal	3 M potassium bis(fluoro-sulfonyl)imide (KFSI)	KIHSC	248 mAh/g @ 0.1	...	87.5 @ 400	[119]
N-CHC	N-CHC	1 M KPF <sub>6</sub>	KIHSC	42.4 mAh/g @ 0.3	27.36 @ 203.4	91 @ 600	[120]
NHPC	NHPC	0.8 M KPF <sub>6</sub>	KIHSC	263.6 mAh/g @ 0.1	...	84 @ 1000	[121]

Marine-biomass-derived porous carbon nanosheets (CBCS-A3) served as the positrodes in NIHSCs [80]. As demonstrated in Figure 9a, the CBCS-A3 positrode showed an outstanding capacity of 640 mAh/g at 0.1 A/g, and it showed state-of-the-art Na<sup>+</sup> storage performance, which is very close to the same performance of lithium-ion storage in similar materials. Furthermore, devices showed high cycling retention, retaining 270 mAh/g and 138 mAh/g after ten thousand cycles at 2 A/g and 10 A/g, respectively. The NIHSCs which used a CBCS-A3 positrode and a CBC-C negatrodne displayed an excellent combination of energy–power densities at 5 A/g, 36 Wh/kg at 53,000 W/kg, and retained 90.5% capacitance retention after 8000 cycles. This research demonstrates the applicability of BDC materials for enhanced Na-ion storage and extensive energy. Niu et al. [79] obtained carbon materials from biomass and implemented them as electrode materials in NIHSCs. Specifically, the P- and N-doped and N-doped BDCs acted as the negatrodne and positrode, respectively. The supercapacitors demonstrated excellent electrochemical performance, as demonstrated by the GCD profiles in Figure 9b,c, combining a high energy density (135.3 Wh/kg) with high power density (16.1 kW/kg), and outstanding long-term stability, retaining 88.6% of the initial capacity even after 8000 cycles. These results can be explained by the unique structural features of carbon materials, comprising hierarchical porosity and heteroatom doping. These features enabled the supercapacitors to maintain excellent kinetic compatibility between the negatrodne and positrode. Therefore, utilizing carbon materials obtained from renewable biomass sources in sophisticated energy systems is extremely advantageous because of their sustainable production and exceptional electrochemical capabilities. A NIHSC was made using a GDHC positrode and a GDPC negatrodne, with the electrodes having a 1:1 mass ratio [81]. The developed NIHSC performed excellently in a wide (4 V) operating potential window, as shown in Figure 9d. The capacitor has an energy density range of 31 to 156 Wh/kg and a power density range of 355 to 38,910 W/kg. In addition, the capacitor exhibits remarkable cycling stability (Figure 9e), maintaining 73% of its original capacity after undergoing 10,000 cycles at a 30 A/g current density. The capacitance decline shown in Figure 9e is mainly ascribed to the interconnected phenomena that affect the electrochemical performance and durability of the electrode materials in NIHSCs. One of the most important factors is the creation and continuous development of the Solid Electrolyte Interface (SEI). Although initially advantageous in stabilizing electrochemical reactions at the interface, the passivating layer can gradually thicken and lose conductivity, hindering ion movement and causing capacity degradation. Simultaneously, the electrode material undergoes mechanical degradation due to the stress caused by volumetric changes during ion insertion and extraction. This degradation leads to the loss of electrical contact and active material from the structure of the electrode. In addition, the frequent insertion of ions can lead to the blockage of pores and the formation of a protective layer on the electrodes, resulting in a significant decrease in the accessible surface area for ion storage and a reduction in the overall capacitance. The decline is worsened by the decomposition of electrolytes, which results in the creation of non-conductive deposits on the surfaces of electrodes, further impeding the movement of ions. The combined impacts lead to a gradual decrease in the capacitor's capacity to hold charge. This requires sophisticated material designs and engineering techniques to improve the strength of the structure, optimize the interaction between the electrolyte and electrode, and maintain consistent electrochemical performance over long periods of use. It is essential to tackle these problems to enhance the longevity and effectiveness of sodium-ion capacitors in real-world use. The electrochemical performance of the NIHSC showcases the potential of carbon materials derived from biomass in the advancement of sustainable and high-performance energy storage systems. This study focuses on the synthesis technique of carbon materials and their efficient utilization in developing high-performance NIHSCs.

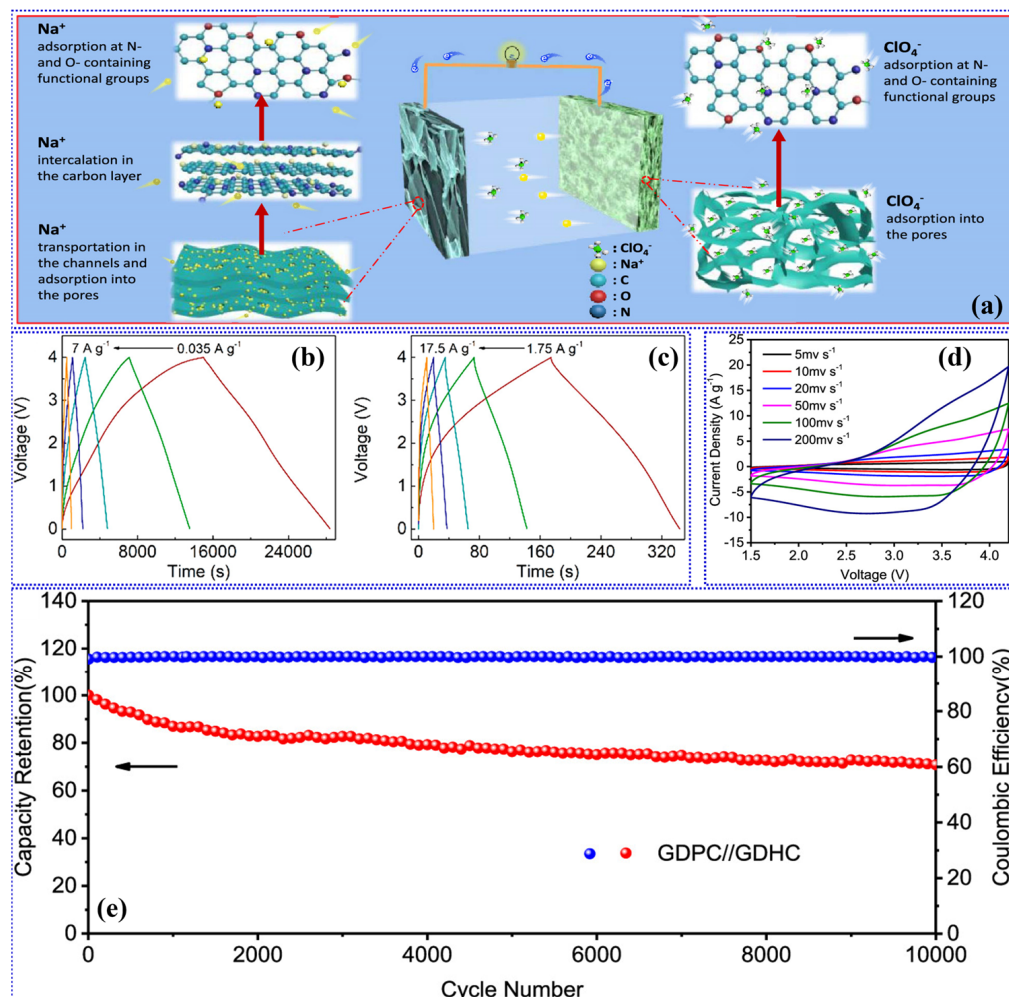


**Figure 9.** (a) Schematic depiction of the charge storage techniques employed in the NIHSC. Reproduced with permission from Ref. [80]. Copyright 2018, American Chemical Society. (b,c) GCD profiles at different current densities for the BDC-based NIHSC. Reproduced with permission from Ref. [79]. Copyright 2020, American Chemical Society. (d) CV curves at various scan rates and (e) cyclic stability and Coulombic efficiency for 10,000 GCD cycles of the GDPC//GDHC NIHSC. Reproduced with permission from Ref. [81]. Copyright 2019, American Chemical Society.

The PCNS functions as the positrode in NIHSCs in conjunction with a negatrode made of hierarchically porous carbon with capacitive properties [82]. The supercapacitor exhibits an energy density of 119 Wh/kg when subjected to a power density of 200 W/kg and a lower energy density of 53 Wh/kg when subjected to a higher power density of 20 kW/kg. Furthermore, it maintains 82% of its capacity after undergoing 8000 cycles at a current density of 5 A/g, demonstrating exceptional cycling stability. The outstanding performance of these devices may be due to the synergistic coupling of a battery-type positrode and a capacitive-type negatrode, which leads to a device with high energy and power density. This work highlights the capacity of carbon materials obtained from biomass to be used in sodium-ion storage systems that are both sustainable and high-performing. The created carbon compounds were evaluated as positrodes in NIHSCs [83]. When exposed to a current density of 100 mA/g, the LS1400 material exhibits a substantial reversible 350 mAh/g capacity. Additionally, it exhibits a plateau capacity of 250 mAh/g, indicating its possible suitability as a material for positrodes. The material has remarkable cycling stability, retaining 94% of its initial capacity after surviving 450 cycles at a current density of 100 mA/g. The EIS analysis showed that LS1400 has a lower charge transfer resistance and improved Na<sup>+</sup> diffusion kinetics compared to LS1200 and LS1600. The sodium storage

method entails the adsorption of  $\text{Na}^+$  ions in regions with imperfections, the insertion of  $\text{Na}^+$  ions between graphite layers, and the deposition of Na metal in confined pores [163]. The LS1400 version exhibits a significant proportion of closed pores, considerably enhancing its plateau capacity. This study highlights the ability of hard carbons derived from lotus stems to serve as high-performance positrode materials for nonaqueous NIHSCs. Several alternative carbon compounds from biomass have been used as electrodes in NIHSCs, showcasing their capability in advanced energy storage technologies [164–168]. These materials, obtained from natural sources including lotus stems, marine biomass, and other plant-based precursors, display various shapes, layered porosity, and doping characteristics that enhance their exceptional electrochemical capabilities. The progress in SIHSCs has received significant attention in recent years due to their promise as affordable and environmentally friendly energy storage options [78,79,169–172]. As a result of this interest, several studies have been conducted on utilizing BDC materials obtained from various biomasses. These studies aim to exploit these materials' renewable, environmentally benign, and economically advantageous properties. These materials have demonstrated considerable potential in enhancing the electrochemical efficiency of SIHSCs by optimizing variables such as the specific surface area, porosity, and electrical conductivity [173,174]. Several types of biomasses, including carrageenan [175], jute [176], cork [177], sodium lauryl sulfate/PANI [178], peanut shell [179], MOFs [180], sucrose [181], spring onion [182], rice husk [183], wheat bran [184], and recycled olive pits [185], have been documented as suitable sources for synthesizing BDCs for SIHSCs. The wide variety of carbon compounds obtained from biomass and their specific structural and electrochemical properties have played a crucial role in the progress in SIHSCs. Their utilization has resulted in significant enhancements in performance indicators, including the specific capacitance, energy density, power density, and cycling stability, consequently reinforcing their position in the future of sustainable energy storage solutions. Their performance, including important factors such as capacitance, cycle stability, and energy and power density, is outlined in Table 2.

#### 4.3. AIHSCs

BDC materials have proven to be a capable solution to boost the AIHSCs' performance. These materials, which are well known for their sustainability and low cost, have remarkably supported the efficiency of AIHSCs. The unique characteristics of BDC, including hierarchical porous structures, nitrogen doping, and high SSAs, facilitate excellent charge storage and improved electrochemical performance of AIHSCs [186]. The materials used in BDC have shown exceptional energy density, power density, and cycling stability. This makes them very appropriate for commercial application in aluminium-ion batteries for AIHSCs [187]. The application of BDC materials in AIHSCs is commercially applicable due to their structural flexibility and excellent electrochemical characteristics. The technology, therefore, comes with customization design and performance qualities required for high-performance supercapacitors. BDC materials help to improve the overall performance and efficiency of AIHSCs, making them commercially viable in the aluminium-ion battery industry. The materials' contributions are based on their renewable, abundant, and non-toxic nature and adjustable features. These qualities make them highly suitable for sustainable energy storage solutions in the aluminium-ion battery industry [187]. The existing research and applications regarding BDC for aluminium-ion energy storage solutions can potentially drive real-world applications and innovation in high-performance energy systems.

Feng et al. [86] reported an AIHSC composed of a PCS negatrode, an aluminium positrode, and an ionic liquid electrolyte called EMIMAlCl<sub>4</sub>. The AIHSC device and its accompanying electrochemical performances are depicted Figure 10a–h. The PCS negatrode, utilizing a double-layer capacitive process, demonstrates a consistent and reliable charge storage mechanism. It has a specific capacity of around 200 milliampere-hours per gram at a current density of 100 milliamperes per gram. The device's electrochemical performance is characterized by quasi-rectangular cyclic voltammetry profiles, which indicate its capacitive nature. The PCS negatrode exhibits remarkable rate capabilities, maintaining

approximately 80% capacity retention even at a current density of 2500 mA/g. Extended cycling investigations have demonstrated that the material's capacity reaches 150 mAh/g after undergoing 1500 cycles at a current density of 2000 mA/g. At a temperature of 50 °C, the supercapacitor achieves an energy density of 220 Wh/kg and a power density of 9 kW/kg, outperforming other aluminium-based energy storage devices in terms of both energy and power capabilities. Additionally, it has a lifespan of over 1000 cycles.

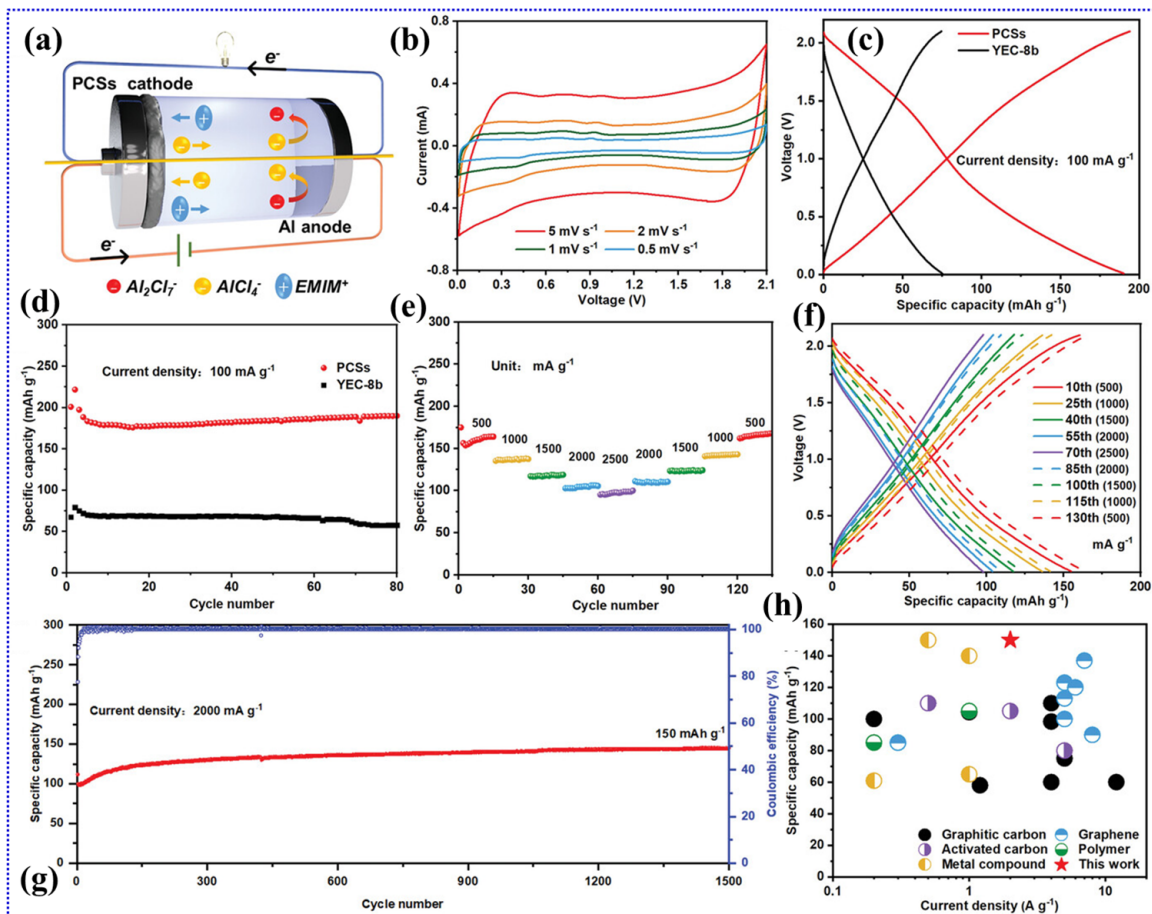


**Figure 10.** Electrochemical performance evaluation of AIHSC based on PCSs at 25 °C. (a) Schematic depiction of the rechargeable AIHSC working mechanism, (b) CV profiles observed at diverse scan rates, (c) GCD curves for PCSs and YEC-8b at 100 mA/g, (d) cycling stability comparison between PCSs and YEC-8b at 100 mA/g, (e) rate performance analysis and (f) corresponding GCD curves for PCSs at numerous current densities, (g) long-term cycling stability and Coulombic efficiency observed at 2000 mA/g, and (h) specific capacity comparison of Al-based AIHSCs with a cycle life exceeding 1000 cycles. Reproduced with permission from Ref. [86]. Copyright 2023, Wiley.

Soen et al. [87] demonstrated an AIHSC that has favourable electrochemical characteristics. The AIHSC produced using electrodeposition has a specific capacitance of 211 F/g, surpassing the electropolished counterpart by 20%. The ASC also exhibits an energy density of 151 Wh/kg at a power density of 3390 W/kg and maintains 70% of its capacitance even at a current density of 20 A/g, demonstrating exceptional rate capability. The device retains 87% of its capacity after completing 5000 cycles. The extraordinary performance may be attributed to the reduced resistance to charge transfer, the irregular and branching structure, and areas with elevated surface energy. This study demonstrates that using a surface treatment for aluminium electrodes can significantly enhance the performance of AIHSCs, rendering them a viable option for advanced energy storage devices in the future. Lie et al. [88] reported an HSC composed of an aluminium positrode, a graphene negatrode,

and an ionic liquid electrolyte. It has a specific discharge capacitance of 240 F/g at a current density of 0.1 A/g and a Coulombic efficiency of 90%. After undergoing 1000 cycles at a current density of 0.3 A/g, the device exhibits a capacitance of 254 F/g. Furthermore, after 2000 cycles at a current density of 2.0 A/g, the capacitance decreases to 130 F/g. These results indicate that the device has excellent cyclic stability and achieves almost 100% Coulombic efficiency. The electrochemical impedance spectrum indicates a charge transfer resistance of  $13.15\ \Omega$ , a series resistance of  $3.82\ \Omega$ , and a dispersed resistance of  $6.36\ \Omega$ . The primary energy storage mechanism in this case comprises the combination of electric double-layer capacitance resulting from the adsorption and desorption of  $\text{AlCl}_4^-$  ions, as well as weak intercalation and deintercalation in nitrogen-doped graphene. This makes it a desirable option for high-performance supercapacitors. Sun et al. [89] developed an AIHSC composed of a positrode made of aluminium foil, a negatrode made of NCS, and an electrolyte made of 1-ethyl-3-methylimidazolium chloride ( $[\text{EMIm}]^+\text{Cl}^-$ ) and  $\text{AlCl}_3$ . The device demonstrates non-ideal rectangular CV curves and achieves a high specific discharge capacitance of 224 mAh/g at a current density of 0.300 A/g, while maintaining a Coulombic efficiency of 98%. The NCS negatrode exhibits outstanding cycling performance, with a 114 mAh/g capacity at 10 A/g even after undergoing 35,000 cycles. Electrochemical impedance spectroscopy revealed a progressive reduction in charge transfer resistance throughout cycling, resulting in consistent and reliable performance. The Al-HSC exhibits a blend of battery-like and capacitor-like properties, making it a very promising energy storage device. It provides fast charge–discharge cycles and maintains long-term stability.

Using the most suitable carbon materials obtained from biomass can significantly improve the efficiency of AIHSCs, enhancing their electrochemical performance. BDC materials, such as corn wastes, corn cob, jute sticks, corn silk, sulfur-doped carbon, nitrogen-doped carbon, and porous carbon sheets, possess distinctive characteristics such as a high SSA, hierarchical porous structures, and diverse elemental distributions [188–192]. These characteristics render them very well suited for utilization as electrode materials. The materials exhibit outstanding electrochemical performance, characterized by a high specific capacitance, enhanced energy densities, and excellent cycling stability. The qualities listed in Table 2 are essential for improving the overall efficiency of supercapacitors. By carefully selecting and optimising carbon materials derived from biomass, it is possible to tailor the electrochemical properties of AIHSCs, leading to improved performance and long-lasting durability for energy storage.

#### 4.4. KIHSCs

BDC materials significantly improve the efficiency of KIHSCs. Biomass-derived materials have advantages such as hierarchical porous structures with nitrogen doping and high SSA. Rich nitrogen doping and defects with BDC gain due to these parameters exhibit high SSA and other features favourable to electrochemical energy storage. This means that a KIHSC has a larger charge storage capability [193]. According to the mentioned benefits, BDC materials can significantly enhance the energy and power density and the cyclic stability of KIHSCs. They possess great commercial potential in the potassium-ion battery field. BDC materials' structural and electrochemical properties prove their high commercial acumen. Strong structural characteristics and additional electrochemical properties are available. Two advantages are critical to the success of supercapacitors with high performance: they are highly effective and environmentally friendly. Unique materials are appreciated because of their design characteristics and possibilities for developing high-performance supercapacitors [94], a good choice for scaling KIHSCs for commercial application in the potassium-ion battery market.

The unique structural characteristics and cost-effectiveness of porous carbons derived from biomass make them promising electrode materials for KIHSCs. BDCs possess many advantageous properties that make them suitable for KIHSC applications. A substantial SSA and an intricate pore structure comprising micropores, mesopores, and macropores facilitate the efficient migration of ions and provide abundant active sites for storing

potassium ions. Heteroatom doping involves the introduction of heteroatoms, such as nitrogen, oxygen, and sulfur, into carbon materials derived from biomass [194]. This process can improve the capacity of the carbons to be wetted and conduct electricity, resulting in enhanced electrochemical performance. Tuneable surface chemistry refers to the ability to modify the chemical properties of BDCs by choosing specific biomass precursors and activation procedures. This allows for the enhancement of the potassium-ion storage capacity. KIHSCs, utilizing porous carbon electrodes generated from biomass, have exhibited encouraging electrochemical characteristics [99]. The high specific capacitance values, often exceeding 300 F/g, are attributed to the hierarchical pore structure and the incorporation of heteroatom doping. The exceptional rate capacity of the material is attributed to its linked pore network and strong electrical conductivity, which enable fast ion transport and consequently lead to outstanding rate capability and high power density. The robust carbon structure and uniform surface chemistry of carbons derived from biomass ensure exceptional stability after several charge–discharge cycles [195]. Although biomass-derived porous carbons have demonstrated encouraging outcomes in KIHSCs, some obstacles still need to be addressed. Additional investigation is required to enhance the pores' configuration and the surface's chemical composition to achieve the highest possible efficiency in storing and transporting potassium ions. To improve the energy density of KIHSCs, one can utilize strategies like incorporating battery-type materials or integrating pseudocapacitive materials. In order to make biomass-derived porous carbons commercially feasible, it is crucial to develop synthesis methods that are both scalable and cost-effective. Porous carbons generated from biomass provide a sustainable and cost-effective alternative for KIHSCs. There is potential for enhancing their performance by optimizing material design and synthesis.

Using AS-HC as the negatrode and AS-AC as the positrode in a potassium-based electrolyte, a KIHSC was created, as shown in Figure 11a [98]. The device has a remarkable electrochemical performance, as demonstrated in Figure 11b–d, with a specific energy of 105 Wh/kg and no capacitance degradation after 10,000 cycles, indicating exceptional cycling stability. The AC electrode exhibits a dual electrical layer capacitance characteristic and supplementary pseudocapacitive peaks, which augment the device's overall performance. The specific discharge capacity of the AS-HC electrode reaches a stable state after a few cycles, suggesting that potassium storage is reversible and plays a role in the device's high Coulombic efficiency and structural stability.

Chen et al. [99] constructed a KIHSC using plains–hills carbon as the positrode and negatrode. The device exhibits a reversible capacity of 147.2 mAh/g at a current density of 10 A/g after undergoing 5000 cycles, indicating excellent stability. CV and GCD experiments were used to evaluate the electrode's performance, demonstrating an energy density of 178.4 Wh/kg at a power density of 1115 W/kg. The KIHSC exhibits remarkable cycling performance, maintaining 75.2% of its capacity after 10,000 cycles. Its ideal blend of conductivity and pseudocapacitance accounts for the device's outstanding performance, making it an extremely advanced electrode material for potassium ion storage. A KIHSC device was constructed using the NOHC as the positrode and AC as the negatrode [100]. The device exhibits an initial reversible capacity of 186.3 mAh/g and maintains 93.5% of its capacity after undergoing 500 cycles at a current density of 0.1 A/g, thus displaying exceptional cycle stability. Furthermore, the device demonstrates an energy density of 68 Wh/kg at a power density of 2000 W/kh and sustains an 80% capacity retention after 1000 cycles at a current of 1 ampere per gram. The NOHC's structure and the development of a stable SEI layer during cycling enable a combination of K-ion intercalation and capacitive processes that contribute to the system's performance. Ultimately, while improving the synthesis methods, it is equally important to conduct electrochemical analysis on biomass-generated carbon to achieve optimal performance in KIHSCs. Electrochemical characterization techniques are crucial for comprehending the carbon material's charge storage mechanisms, kinetics, and overall electrochemical behaviour when exposed to potassium ions.

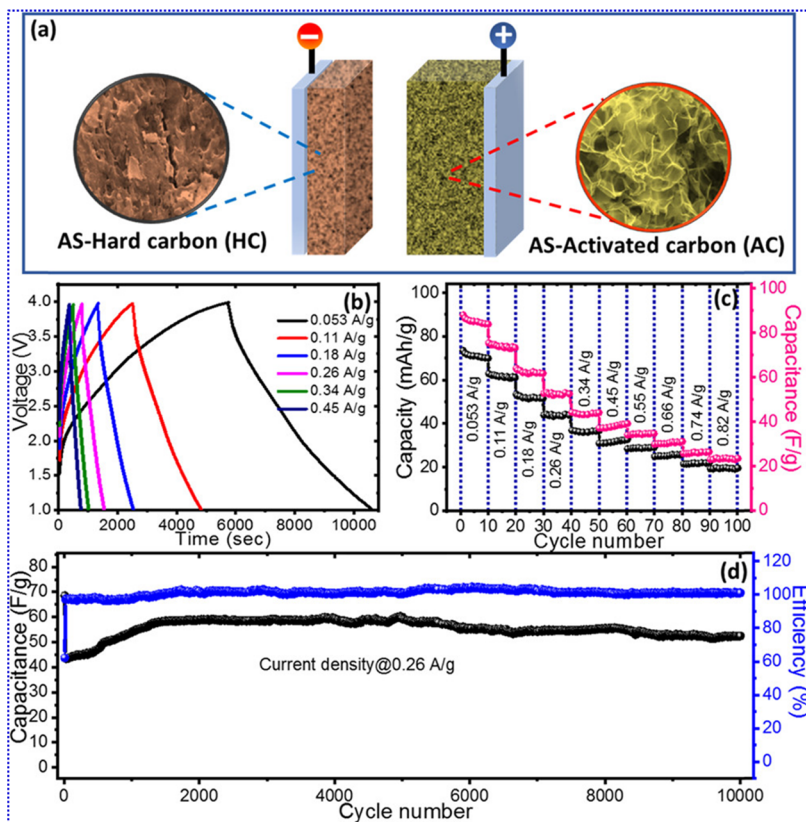


**Figure 11.** The complete cell KIHSC electrochemical performances of the HC-1000/AC-800: (a) a schematic representation of the KIHSC complete cell, (b) GCD profiles recorded at various current densities, (c) specific capacity and specific capacitance variation with several cycles at various current densities, and (d) cyclic stability of the full cell with corresponding Coulombic efficiency over 10,000 cycles. Reproduced with permission from Ref. [98]. Copyright 2020, American Chemical Society.

The field of energy storage has seen significant progress in the development of KIHSCs in recent years. The increasing interest in BDC compounds has led to several studies exploring their use, taking advantage of their sustainable, cost-effective, and environmentally beneficial properties. These materials have shown significant promise in improving the electrochemical performance of KIHSCs by optimizing variables such as specific surface area, porosity, and electrical conductivity [196–200]. Multiple prominent research studies have shown the utilization of different carbon materials derived from agaric [201], ganoderma lucidum [202], coffee grounds [203], rapeseed meal [204], lignin [205], and 2D tremella [206] for KIHSCs. The wide variety of carbon compounds obtained from biomass, each with its unique structure and electrochemical properties, has significantly contributed to the progress in potassium-ion hybrid supercapacitors (KIHSCs). Their utilization has resulted in significant enhancements in performance measures, including the specific capacitance, energy density, power density, and cycling stability, consequently confirming their position in the future of sustainable energy storage technologies. Table 2 presents a concise overview of the different electrochemical parameters required to evaluate the effectiveness of BDC in KIHSCs. Specific capacitance, rate capability, cycling stability, charge transfer resistance, and diffusion coefficients are crucial in optimizing electrochemical characterization techniques. The optimization of electrochemical characterization processes involves the utilization of many methods, including CV, GCD experiments, and EIS. Surface characterization techniques offer additional information about electrochemical behaviour, particularly in situ approaches. This information allows researchers to discover limitations and optimize the carbon material. Through meticulous analysis of the electrochemical data, researchers can gain insights into the ion transport pathways, kinetics of charge storage,

and the impact of functional surface groups on the electrochemical performance. This comprehension can improve the synthesis processes, electrode manufacturing procedures, and electrolyte compositions, boosting the energy storage capacity and lifespan of KIHSCs. Optimizing electrochemical characterization techniques is crucial for establishing correlations between structure and properties and constructing prediction models for carbon derived from biomass. Predictive models can direct and expedite the logical creation of carbon materials for certain uses, advancing high-efficiency and financially feasible energy storage technologies.

### 5. Various Factors Affecting the Electrochemical Behaviour of BDC-Based MIHSCs

BDC electrodes possess numerous advantages compared to alternative carbon-based electrodes for MIHSCs. The advantages encompass heightened electrical conductivity, enhanced surface wettability, the induction of pseudocapacitance, expedited charge transfer, and facilitated reactions at the electrode/electrolyte interface [207]. BDC materials provide both sustainability and cost-effectiveness, rendering them a compelling choice for supercapacitor electrodes. They have a structure that allows for the passage of substances through small holes, a high ability to store electrical charge per unit mass, and the ability to remain stable over time. These properties make them better than many other carbon-based materials used in MIHSCs [208]. Lignin/cellulose nanofibers from biomass exhibit potential as electrode materials because of their exceptional durability, favourable electronic conductivity, and porous structure [209]. Moreover, carbon compounds obtained from biomass, which are renewable, have shown considerable promise in improving the performance of electrodes for MIHSCs [84]. Porous BDCs, which can be tailored to have specific nano/microstructures, are attracting interest due to their high effectiveness and cost-effectiveness as materials for supercapacitor electrodes [210]. The use of biomass-generated carbon can result in various electrochemical characteristics, including specific capacitance and surface area, due to its varied internal structure [211]. BDC materials have distinctive characteristics, such as a highly developed porous structure, a substantial specific surface area, and excellent electrical conductivity. These attributes render them highly favourable as electrode materials for supercapacitors with exceptional performance capabilities [212]. Electrodes made from BDCs provide a sustainable, economically viable, and highly effective alternative for supercapacitors. Their distinctive qualities and benefits have led to their growing popularity in energy storage.

Several vital parameters that control the electrochemical behaviour of BDC-based MIHSCs for energy storage are tabulated in Table 3. Electrolyte choice, OPW range, and electrode material qualities are essential. Supercapacitors' ion transport efficiency depends on electrolyte choice. The electrolyte must promote fast ion movement and chemical stability within the device's working voltage range. BDCs, which frequently incorporate inherent functional groups derived from natural doping elements such as nitrogen, sulfur, and phosphorus, exhibit distinct interactions with electrolyte ions, influencing charge storage. Given the complex surface chemistry of BDCs, electrolyte stability and conductivity are crucial. These electrodes could use electrolytes with higher ionic conductivity to maximize their porous structure. The OPW determines the voltage range, which affects supercapacitor energy and power density. BDCs can withstand higher voltages due to their surface chemistries and structural stability. This trait may improve energy storage. However, deviating from the constant voltage range may cause rapid material degradation. Biomass carbons may have inherent heteroatoms that affect voltage range stability, supercapacitor lifetime, and efficiency. This depends on how heteroatoms interact with the electrolyte. BDC electrodes have many advantages over carbon-based electrodes. BDC electrodes are more sustainable since they use renewable resources. This reduces the environmental effect of electrode material manufacture and promotes sustainability. Bio-wastes minimize material costs compared to conventional electrodes that use expensive processed carbons or synthetic precursors. High porosity in BDCs helps MIHSCs store more ions. This structural benefit is achieved without activation or templating, which traditional carbon composites

require. BDCs store energy using pseudocapacitance mechanisms due to their heteroatoms. This increases energy storage capacities beyond double-layer capacitance. Supercapacitors can be customized and function better by changing electrode properties like conductivity and wettability using physical or chemical approaches. A number of biomass types can be used to make carbons with customized supercapacitor characteristics. Customization is harder with standard carbon sources. In addition, BDCs are thermally stable, ensuring constant performance across all operational temperatures. This is essential for energy storage applications that need durability. Carbon electrodes made from biomass are a sustainable energy storage solution. They have enhanced performance and are cost-effective and adaptable for supercapacitor applications. These advantages make them attractive alternatives to carbon-based electrodes, which are often limited by their environmental impact, high cost, and inflexibility.

**Table 3.** Merits of BDC electrodes compared with other types of carbon-based electrodes used in MIHSCs.

Feature	BDC Electrodes	Traditional Carbon-Based Electrodes
Sustainability	Produced from renewable materials, rendering them ecologically sound and enduring.	Frequently obtained from finite resources or artificial methods, which might result in a greater ecological footprint.
Cost	The cost is typically cheaper because waste or natural by-products are utilized, decreasing material prices.	Usually, the higher cost is a result of utilizing new or artificial materials.
Porous structure	The material has inherent high porosity, which results in a diverse range of pore diameters. This characteristic significantly improves its ability to store ions.	Porosity must be deliberately designed and controlled, often necessitating the use of supplementary processing procedures.
Natural doping	Includes inherent heteroatoms like nitrogen, sulfur, and phosphorus, improving electrochemical performance by increasing pseudocapacitance.	Doping necessitates the use of further chemical processing to insert heteroatoms, hence augmenting the intricacy and expense.
Modification flexibility	Can be readily adjusted through physical or chemical activation to customize characteristics such as surface area and conductivity.	Modifying synthetic or processed carbon materials is feasible, but their inherent qualities frequently limit flexibility.
Unique chemistries	The electrode characteristics can be modified to suit individual applications, as they vary greatly depending on the type of biomass used.	Typically uniform, with minimal variation in electrochemical characteristics until intentionally modified.
Thermal stability	Excellent thermal stability is advantageous for preserving performance over various temperature conditions.	The thermal stability of a material can vary and is influenced by the precursor and the procedure used to create it. Achieving consistent thermal stability may necessitate strict management.
Renewable production	The production cycle can be included in a sustainable bio-waste usage loop, fostering a circular economy.	Typically, it depends on industrial operations not included in a renewable cycle, with a greater emphasis on extracting resources.

### 5.1. Effect of Electrolytes on the Electrochemical Behaviour of BDC Electrodes

Electrolytes have a crucial role in determining the electrochemical characteristics of BDCs in MIHSCs. The selection of electrolytes substantially influences the performance of the supercapacitor system. Yoo et al. [126] showed that newly created nonaqueous electrolytes containing bis(trifluoromethylsulfonyl)imide salts allowed reversible deposition on metal positrodes and reversible adsorption on an AC negatroe. This led to the development of MIHSCs. Momodu et al. [213] highlighted the significance of electrolytes by demonstrating that gel-based electrolytes had exceptional stability and distinctive recuperative properties. This suggests that gel electrolytes formed from plant biomass can be

effectively utilized in supercapacitor devices. In their study, Zhu et al. [214] emphasized that carbon-based supercapacitors demonstrated significant gravimetric capacitance and energy density while using organic and ionic liquid electrolytes. This highlights the importance of choosing the proper electrolyte to improve the electrochemical performance of carbon electrodes generated from biomass. In addition, Li et al. [215] examined progress in electrode materials and electrolyte innovation for lithium-ion capacitors, highlighting the pivotal significance of electrolytes in energy storage devices. In addition, Biswal et al. [216] reported that carbon electrodes displayed almost perfect capacitive behaviour with minimal ionic resistance, highlighting the significance of the rapid diffusion of electrolyte ions into the porous network for effective supercapacitor functioning. Figure 12a depicts the intricate ecology of electrode materials and electrolytes in MIHSCs, highlighting the importance of selecting the proper electrolyte to enhance performance. These findings emphasize the crucial importance of electrolytes in controlling the electrochemical properties of BDCs for MIHSCs.

Han et al. [217] showed that water-in-salt electrolytes based on acetate successfully enhanced the performance of ZIHSCs. These electrolytes exhibited excellent reversibility and stability during zinc plating and stripping. Choosing the appropriate electrolyte composition is crucial for maintaining the durability and effectiveness of the supercapacitor device. In addition, Zhang et al. [217] emphasized the significance of the electrolyte mixture in improving the electrochemical efficiency of ZIHSCs. The study demonstrated that using a particular electrolyte mixture enhanced electrochemical performance by substituting the bound water within the solvation structure. This substitution led to an improvement in the solvation structure, ultimately resulting in superior overall performance. This highlights the electrolyte composition's significance in enhancing the supercapacitor device's electrochemical performance. In addition, Eskusson et al. [218] examined the electrochemical characteristics of different aqueous electrolytes in ZIHSCs. The study compared several electrolytes and their effects on the electrochemical properties of the supercapacitor device. A comprehensive understanding of the interactions between electrolytes and electrodes is essential for optimal performance and durability in ZIHSCs. Ultimately, selecting electrolytes plays a crucial role in influencing the electrochemical characteristics and overall efficiency of BDC electrodes in ZIHSCs. Optimizing the electrolyte composition can improve the supercapacitor system's efficiency, stability, and durability, enhancing energy storage capacity.

Shao et al. [219] highlighted the significance of asymmetric supercapacitors in extending the voltage range beyond the point when electrolytes break down due to thermodynamic factors. This offers a solution to the energy storage constraints faced by symmetric supercapacitors. This emphasizes the importance of considering the compatibility of electrolytes and electrode materials to improve the overall performance of supercapacitors. Moreover, Simon and Gogotsi [220] emphasized that combining appropriate electrode materials with the proper electrolyte can augment the supercapacitor system's energy storage capacity and power. It is crucial to recognize that there is no flawless active substance, and the choice of electrolyte should align with specific performance goals. Comprehending the interplay between electrode materials and electrolytes is essential for attaining optimal electrochemical performance in NIHSCs. In addition, Maurya et al. [221] examined the configuration of NIHSCs, highlighting the importance of the three constituents, i.e., positrode, negatrode, and electrolyte, which resemble those found in batteries. This highlights the need for electrolytes that can fulfil the specific demands of NIHSCs. By carefully choosing and designing electrolytes, it is possible to improve the electrochemical efficiency and longevity of carbon electrodes generated from biomass in NIHSCs. Ultimately, the selection of electrolyte composition has a substantial impact on the electrochemical characteristics and overall efficacy of BDC electrodes in NIHSCs. By integrating findings from studies on asymmetric supercapacitors, electrode–electrolyte compatibility, and NIHSCs design, it is possible to enhance the efficiency and performance of supercapacitor systems for energy

storage purposes. MIHSC applications make use of different types of aqueous electrolytes, including acidic, basic, and neutral solutions, as shown in Figure 12b.

The electrolyte's composition is vital for maximizing the performance and efficiency of the supercapacitor system. Dubal et al. [222] stressed the significance of creating a streamlined pathway for electron transport and ensuring optimal electrolyte access to the electrochemically active materials in carbon fibres. They underscored the importance of electrolyte permeability and connectivity within the electrode structure. In addition, Tomboc et al. [223] examined the energy storage mechanisms in supercapacitors, specifically emphasizing ion adsorption at the interface between the electrode and electrolyte (electric double-layer capacitance) and faradaic processes that involve electron transfer through oxidation/reduction reactions (pseudocapacitance). Comprehending these principles is essential for choosing electrolytes that can efficiently facilitate both forms of energy storage processes in AIHSCs. In addition, Kim et al. [224] showed that electric double-layer capacitors store charges by physically adsorbing electrolyte ions onto porous carbon electrodes, highlighting the significance of the electrode–electrolyte interface in the performance of supercapacitors. This emphasizes the need to ensure that the electrolyte is compatible with the electrode material in order to achieve efficient charge storage and transfer in AIHSCs. Ultimately, the choice of the correct electrolyte composition is crucial for controlling the electrochemical characteristics and overall efficiency of BDC electrodes in AIHSCs. By incorporating findings from studies on electron transport pathways, energy storage processes, and electrode–electrolyte interactions, it is feasible to improve the efficiency and functionality of supercapacitor devices used for energy storage purposes.

Dubal et al. [222] stressed the significance of creating a streamlined pathway for electron transport and ensuring that the electrolyte can effectively reach the electrochemically active materials in carbon fibres. They highlighted the importance of having good electrolyte permeability and connectivity within the electrode structure to improve the overall electrochemical performance. In addition, Kim et al. [224] explained how electric double-layer capacitors store charges utilizing the physisorption of electrolyte ions onto BDC electrodes. This highlights the importance of the interface between the electrode and electrolyte in determining the performance of supercapacitors. It emphasizes the need to use electrolytes compatible with the electrode material to achieve efficient storage and charge transfer in KIHSCs. Figure 12c illustrates the many energy storage technologies, including MIHSCs, and emphasizes the strategic integration of specific electrolytes to enhance performance. Stressing the importance of electrolyte selection [225], this study demonstrates how particular electrolytes utilized in BDC electrodes directly influence the efficiency and efficacy of MIHSCs in different applications. Choosing electrolyte composition is crucial for controlling BDC electrodes' electrochemical characteristics and overall efficiency in KIHSCs. By incorporating findings from studies on electron transport pathways, energy storage processes, and electrode–electrolyte interactions, it is feasible to enhance the efficiency and usefulness of supercapacitor systems for energy storage purposes.

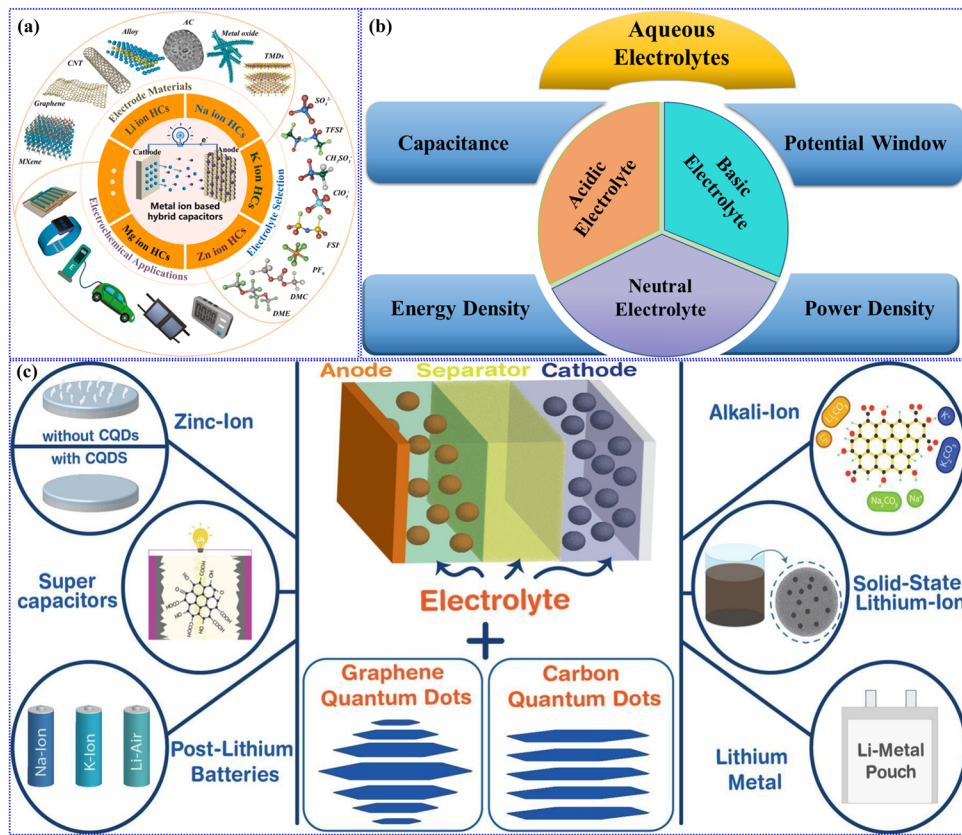


**Figure 12.** (a) Exploration of materials and electrolytes for MIHSCs. Reproduced with permission from Ref. [226]. Copyright 2021, Elsevier. (b) The impact of aqueous electrolytes on the efficiency of MIHSCs. Reproduced with permission from Ref. [227]. Copyright 2020, Elsevier. (c) Schematic representation of the effect of electrolytes on carbon-based electrodes in MIHSCs. Reproduced with permission from Ref. [225]. Reproduced under the term CC BY 4.0. Copyright 2024, Shaker et al., Elsevier.

### 5.2. Advancements in High-OPW MIHSCs

The energy density and overall performance of MIHSCs are greatly affected by a high OPW, making it a crucial aspect of these energy storage devices. Maximizing the OPW in such systems is essential for augmenting their capabilities. A practical approach to increase the OPWs in MIHSCs is utilizing electrode materials that can function efficiently at higher potentials. For instance, using materials such as BDCs and  $\text{MoO}_2$  with a more significant work function can aid in advancing high-voltage supercapacitors [228]. By incorporating materials like silicene into MIHSCs, it is possible to create devices with a broad range of OPWs, reaching up to 3 V [229]. This allows for higher energy and power densities in the MIHSCs. Moreover, the configuration of asymmetrical MIHSCs using BDCs can also enhance the OPWs. By manipulating electrode work functions and utilising specific electrode combinations, it is possible to fabricate high-voltage asymmetric MIHSCs that exhibit improved performance [228]. Furthermore, sophisticated electrode materials such as highly porous BDCs and metallic nanosheets can provide exceptional energy storage capabilities at increased OPWs, highlighting the need to select appropriate materials to achieve high supercapacitor OPWs [230]. Ultimately, high OPWs in MIHSCs are of utmost importance, as they are directly correlated with these devices' energy density and overall efficiency. Employing suitable electrode materials, implementing asymmetric configurations, and integrating novel substances such as silicene and metallic nanosheets makes it feasible to enhance the voltage in MIHSCs, thus unleashing their complete energy storage capacity.

High-voltage aqueous ZIHSCs are a noteworthy advancement in energy storage. They offer improved safety features and higher energy densities compared to conventional systems. The ability to attain elevated operational voltages is dependent on the inventive restructuring of the hydrogen bond network in the electrolyte, which is assisted by the use of co-solvents such as polyethylene glycol and N, N-dimethylformamide [231]. These co-solvents alter the structure of the hydrogen bonds, which decreases the movement and reactivity of water molecules. As a result, the electrolyte can withstand greater OPWs up to 4.27 V without breaking down. This method avoids the usual problems with water-based systems and takes advantage of the natural safety and environmental advantages of electrolytes based on water. This opens up the possibility of developing ZIHSCs in the future which have far better energy storage capacity. The advancement of high-voltage KIHSCs represents a crucial breakthrough in energy storage technology, providing a combination of high power and energy density essential for various applications [232]. These KIHSCs achieve high OPWs by exploiting the distinctive characteristics of potassium ions, such as their larger size and lower solvation energy than lithium and sodium. This enables easier removal of solvent molecules and faster movement of ions during ion insertion and removal processes. The lower typical electrode potential of potassium in electrolytes such as propylene carbonate is also a contributing factor to the high voltage capability of these devices. The reduced potential and the creation of robust electrochemical interfaces enable potassium-ion supercapacitors to function effectively at higher voltages. This maximizes energy density and improves the overall performance and efficiency of the MIHSCs.

### 5.3. Theoretical Calculations: Insights into Energy Storage Mechanisms in MIHSCs

Theoretical calculations are crucial for comprehending the energy storage mechanisms of MIHSCs. By employing density functional theory (DFT) calculations, researchers can obtain valuable information regarding charge separation mechanisms and the efficient confinement of precursors inside these systems [233,234]. The characteristics of metal-based hydroxides have been investigated using DFT calculations. These calculations have also been used to examine how the incorporation of transition metal ions and lattice defects affects the electronic properties of these hydroxides [235]. In addition, DFT has played a crucial role in comparing the characteristics of several polypyridyl dyes based on metal ions for dye-sensitized solar cells [236]. MIHSCs are a form of energy storage device that combines battery-like electrodes with capacitive electrodes. They have shown great potential in high energy and remarkable power densities [16]. Hybrid supercapacitors exhibit superior energy density compared to conventional electric double-layer capacitors and effectively surpass the power density constraints of batteries [52,237,238]. MIHSCs, specifically ZIHSCs, are recognized for their exceptional safety, impressive energy and power outputs, long-lasting performance, and cost-efficiency [106]. These devices combine the benefits of zinc-ion batteries, which have high energy density, with supercapacitors, which have excellent power density and cycle stability [14]. Zinc metal positrodes have generated considerable interest in energy storage systems due to their inherent advantages, leading to the development of aqueous ZIHSCs [38]. DFT simulations provide valuable insights into the energy storage mechanisms in MIHSCs, which contribute to developing high-performance energy storage devices with improved energy and power densities.

Recent advancements in DFT calculations have shed light on the energy barriers involved in the adsorption and desorption of  $Zn^{2+}$  ions on doped carbon electrodes, which is crucial for optimizing the chemisorption kinetics in ZIHSCs [239]. The addition of nitrogen and sulfur heteroatoms to the carbon structure considerably impacts the energy barriers, leading to improved electrochemical performance. DFT investigations reveal that the adsorption of  $Zn^{2+}$  ions commences by their contact with the oxygen sites of hydroxyl groups. This interaction leads to the breaking of O-H bonds and the subsequent creation of C-O-Zn bonds, accompanied by the release of  $H^+$  ions. The significance of this sequence is in its ability to determine the chemisorption kinetics, which directly impact the performance of ZIHSCs. The computational analysis in Figure 13a,b reveals that the

energy barrier for this process is significantly reduced when N/S co-doping is present, measuring at 1.17 eV, in contrast to 1.91 eV for N-doped alone and 3.21 eV for undoped electrodes. Incorporating N/S co-doping decreases the energy barriers, resulting in faster adsorption and improved ion exchange reversibility and efficiency at the electrode interface during charge–discharge cycles. The findings have significant ramifications, indicating that by strategically adding N and S heteroatoms to the electrode material of ZIHSCs, these capacitors' energy storage capacity and cycling stability can be significantly improved. Reducing energy barriers enables faster and more effective ion adsorption and desorption, which is crucial for high-performance supercapacitors that achieve rapid energy delivery and high power densities. Therefore, combining N/S co-doping is essential to improve future supercapacitors' design and functional capabilities, making them more efficient and long-lasting.

DFT computations are essential in studying and improving ion diffusion pathways within positrode materials in NIHSCs. These calculations play a crucial role in determining the energy barriers related to the movement of sodium ions. These barriers are essential factors that affect the electrochemical performance of supercapacitors. DFT is used to analyse and understand how changes in the structure and composition of the positrode might improve ion transport and increase the device's overall efficiency [240]. This is conducted by comparing the diffusion barriers in different materials or modified structures. A detailed analysis of the obstacles that hinder the movement of sodium ions in two different situations involving electrodes made of manganese oxide ( $\text{MnO}$ ) is depicted in Figure 13c–g. The initial scenario investigates the diffusion of sodium ions across the main body of cubic  $\text{MnO}$ . In this process, ions move by directly jumping between interstitial sites. This process does not entail the displacement of lattice atoms, but it does exhibit a relatively high energy barrier, which suggests that ion transport occurs at a slower rate. The second scenario examines the diffusion of sodium ions at the interface between Mn and  $\text{Na}_2\text{O}$ , a crucial region for enhancing ion transport. The interface reduces the energy needed for Na ions to move, making them more mobile than their movement through the more significant  $\text{MnO}$  material. The decrease in energy barriers at the interface can be ascribed to the distinctive structural and electrical interactions that occur, facilitating the migration of Na ions across the electrode. The insights obtained from DFT calculations are crucial and show that by strategically manipulating the interfaces in positrode materials, we may significantly influence the performance of NIHSCs. Reducing the obstacles to the movement of ions at essential points, like the interface between manganese and sodium oxide, makes it feasible to raise the speed at which ions are transported. This, in turn, can lead to improved performance regarding the rate at which the supercapacitor can charge and discharge and its overall efficiency. This research enhances our comprehension of material behaviours at the atomic scale and guides the future development and creation of advanced electrode materials for improved energy storage technologies.

DFT simulations have played a crucial role in understanding the adsorption process on heteroatom-doped carbon negatodes in AIHSCs [241]. These theoretical insights are essential for developing negatodes with the most efficient energy storage capacities. The DFT simulations were used to study the interaction between the  $[\text{AlCl}_4]^-$  moieties and the nitrogen and sulfur co-doped carbon negatode (N,S-C). The DFT analysis demonstrates that adding nitrogen and sulfur to the carbon structure dramatically improves the adsorption potency of  $[\text{AlCl}_4]^-$  ions. The improvement is due to the distinctive electronic characteristics provided by the N and S dopants, which alter the electronic surroundings of the carbon structure, thereby enabling more robust and more enduring interactions with the  $[\text{AlCl}_4]^-$  ions. Specifically, graphitic and pyridinic nitrogen sites were discovered to enhance adsorption energies, suggesting a more advantageous adsorption situation than carbon that is not doped. The computational findings provide a crucial explanation for the experimental data on the enhanced capacitance and cycling stability of the N,S-doped carbon negatodes in AIHSCs. DFT's predictive and explanatory power concerning the impact of heteroatom doping on adsorption characteristics highlights its usefulness in advancing

energy storage materials. The combination of theoretical predictions and experimental advancements offers a strong foundation for improving the efficiency of aluminium-ion batteries and supercapacitors.

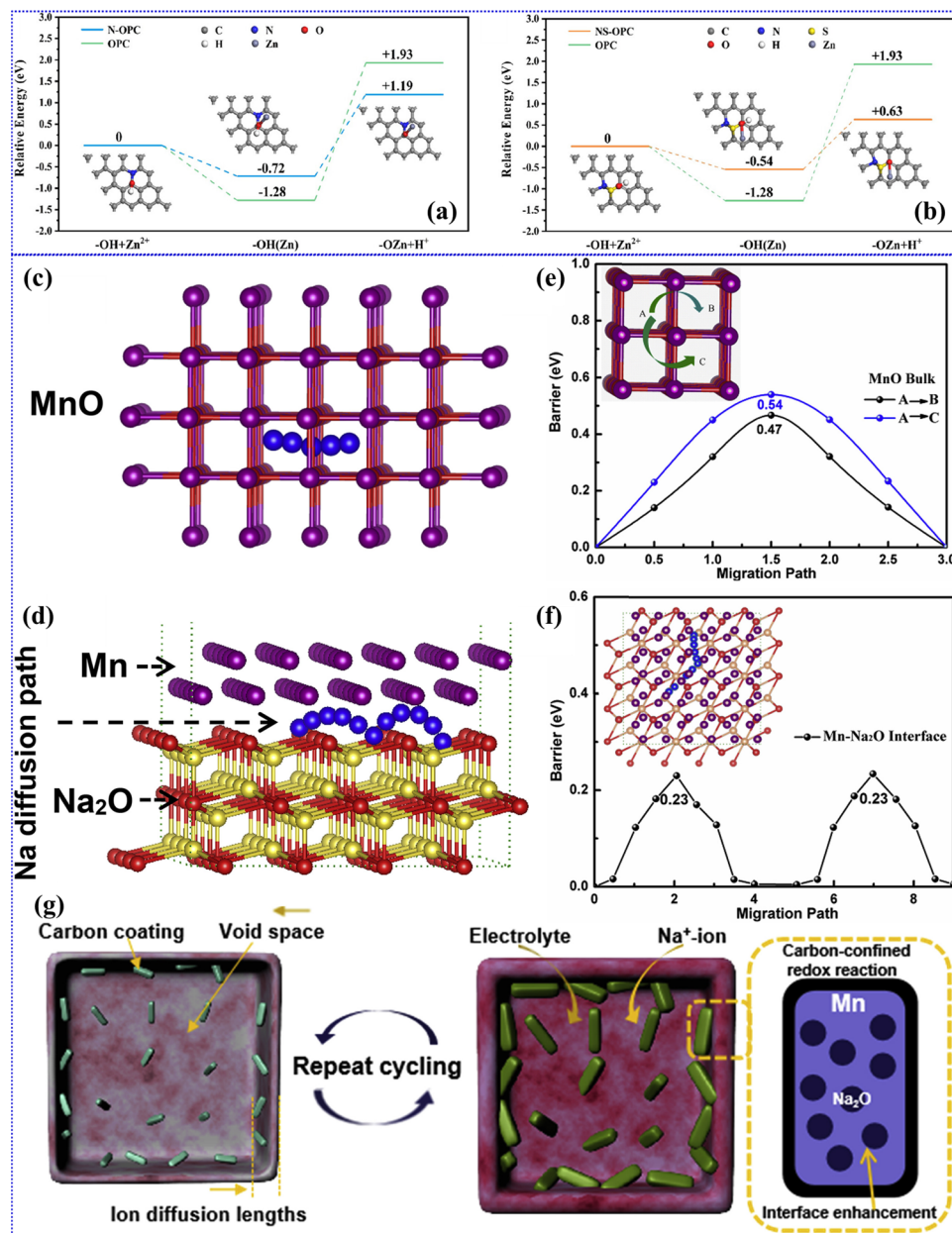


**Figure 13.** (a,b) Variations in the relative energy levels during the chemisorption process for ZIHSCs. Reproduced with permission from Ref. [239]. Copyright 2023, American Chemical Society. Atomic structures of various models and distinct Na diffusion pathways in (c) MnO and (d) Mn/Na<sub>2</sub>O interface. Diffusion energy barriers for Na atoms are shown for (e) MnO bulk and (f) Mn/Na<sub>2</sub>O interface. (g) Diagram illustrating the energy storage mechanisms for the MnO@HCNb electrode. Reproduced with permission from Ref. [240]. Copyright 2020, Elsevier.

DFT calculations provide valuable insights into the interactions at the interface and the mechanisms of charge transport in the electrode materials of KIHSCs [242]. These calculations have a substantial impact on the electrochemical performance of the supercapacitors. More precisely, bonding polyaniline (PANI) with molybdenum disulfide (MoS<sub>2</sub>) promotes improved reaction speed, essential for adequate energy storage. DFT investigations demonstrate that incorporating PANI into the MoS<sub>2</sub> layers substantially reduces the

barrier for  $K^+$  diffusion. This indicates that the molecular-level hybridization reinforces the material's structural integrity and improves its electrical conductivity. This alteration leads to an electronic structure that is easier to access and facilitates faster and more efficient ion transport. The formation of covalent connections between PANI and  $MoS_2$  establishes novel routes for electron transmission, reducing the energy obstacles linked to the insertion and removal of potassium ions in the charge–discharge procedures. Theoretical findings highlight the potential of employing organic–inorganic hybrid materials in supercapacitors to overcome the constraints imposed by conventional electrode materials. These hybrids can lower energy barriers and improve the movement of ions. As a result, they can attain a high capacitance and maintain excellent cycling stability. This makes them well suited for energy storage applications that require high performance. The findings obtained from DFT calculations play a vital role in directing the manufacture and enhancement of electrode materials to use these favourable characteristics fully.

## 6. Challenges and Future Research Perspectives

BDC materials are promising for high-performance MIHSCs, primarily due to their sustainable nature, widespread availability, and affordability. These materials exhibit significant attributes, including structural diversity, porosity, and heteroatom doping, greatly enhancing their electrochemical performance. This review thoroughly examines these characteristics and the obstacles that must be overcome for practical supercapacitor use. A major challenge lies in synthesizing BDC compounds with consistent and optimal structures for energy storage. The intricate chemical composition of biomasses hinders the continuous production of carbon nanotube fibres. Additionally, generating high-performance shape-memory carbon aerogels from biomass is a difficult task. To tackle these problems, several techniques have been suggested, such as altering the distance between layers in carbon materials, which can improve ion movement and storage. Incorporating nitrogen, phosphorus, and sulfur directly into the carbon structure enhances conductivity and electrochemical activity. Introducing multiple heteroatoms simultaneously generates a synergistic effect, improving overall supercapacitor performance.

BDC compounds also show promise as raw materials for metal-ion batteries, contributing to developing materials for such batteries. However, obstacles such as insufficient electrochemical storage capacity render BDCs unsuitable for battery applications. Efforts to enhance specific capacity and lifespan are necessary to make them viable for battery use. The complex structure of biomass precursors also hinders the continuous production of carbon nanotube fibres and shape-memory carbon aerogels, which are essential for battery applications. Several methodologies have been proposed to address these issues, such as biomass-derived nitrogen-doped porous carbons, which can replace noble metal catalysts in metal-ion batteries, improving battery performance. Improving electrode design, refining electrolyte composition, and innovating new energy storage mechanisms are crucial for progressing BDCs in MIHSCs. A deeper understanding of the correlation between the composition and characteristics of carbon compounds obtained from biomass will guide research focused on specific synthesis techniques, such as interlayer modulation and self-doping, to produce tailor-made materials with improved performance.

Advances in BDC materials for high-performance MIHSCs include electrode materials with high energy densities and mechanical stability, which are crucial for large-scale production. Surface engineering is vital for enhancing charge–discharge capabilities and maintaining consistent performance across multiple cycles, which is essential for industrial-scale applications. Encasing metal nanoparticles with metal oxides within zeolitic imidazolate frameworks can improve the performance of carbon materials for energy storage. Further enhancing capacitance is possible by using high-mass-loading biomass-based porous carbon electrodes.

BDCs have garnered considerable interest in advanced MIHSCs because of their notable characteristics, such as large surface area, conductivity, and cost-effectiveness [243]. Recent studies have investigated different types of carbon materials, such as nanoporous

carbon, graphene, carbon nanosheets, and carbon aerogels obtained from sustainable sources like bagasse. These studies have shown that these materials can be inexpensive and effective electrode materials for supercapacitors [244,245]. Moreover, combining MOFs and conductive materials such as polypyrrole has been recognized as a method to improve the capacitance properties of supercapacitors, effectively resolving concerns regarding inadequate electrical conductivity [246–248]. In addition, the progress in creating all-carbon hybrids, specifically rGO/CNF nanostructures, has demonstrated encouraging outcomes in attaining superior charging and discharging abilities for supercapacitor electrodes [249]. Researchers have explored using carbon materials and transition metal compounds to improve electrode materials for KIHSCs to achieve higher power and energy density in advanced metal-ion hybrid supercapacitors [12]. In addition, the use of yolk-shell-structured nickel cobalt sulfide and CNT composites has demonstrated excellent performance in hybrid supercapacitors, emphasizing the significance of carbon materials as key electrode components [250]. The development of MIHSCs has enabled the creation of energy storage devices that combine the advantages of batteries and supercapacitors. These devices offer large energy storage capacity, fast charge–discharge rates, and an extended cycle life [18,41]. These advancements highlight the potential of carbon materials sourced from biomass to influence the future of MIHSCs. They offer a sustainable and efficient alternative for energy storage applications.

The ongoing exploration of BDC compounds for energy storage indicates a promising future. Techniques such as co-incorporating phosphorus and boron can significantly prolong supercapacitors' lifespan, making them more suitable for practical applications. These materials can become ideal for commercial use by creating scalable and economical synthesis methods and advancing material design and performance. The challenges and outlook for using BDC materials in high-performance MIHSCs must address structural, functional, and material difficulties. Advanced synthesis methods, innovative design strategies, and a thorough study of structure–property relationships are essential for the progress of these materials in energy storage. Tackling these challenges will allow BDC materials to substantially contribute to advancing sustainable and high-performance energy storage systems.

## 7. Conclusions

This review study thoroughly examines the crucial significance of BDC materials in advancing the exceptional performance of MIHSCs. This paper concentrates explicitly on systems based on sodium, potassium, and zinc ions. These materials are highlighted for their plentiful supply, capacity to be renewed, and remarkable physical and chemical qualities, making them ideal for energy storage applications. This review extensively examines the process of creating, modifying, and structurally enhancing carbon materials obtained from biomass. It highlights the significance of their large SSA, adjustable porosity, and introduction of heteroatoms in enhancing their electrochemical capabilities. This study explores many methods of creating carbon materials from biomass, such as pyrolysis, hydrothermal carbonization, and activation procedures. These processes make materials with various structural properties and regulated shapes. These techniques facilitate the production of carbon materials with hierarchical porous architectures and tailored surface chemistry, rendering them appropriate for MIHSCs. This review analyses the electrochemical characteristics of carbon materials obtained from biomass in various MIHSCs. It showcases their capacity to attain high capacitance, energy density, and cycling stability. This research emphasizes the suitability of BDCs with metal-ion electrolytes, their function in aiding ion transport, and the mechanisms underlying their ability to store charges. This study discusses the practical uses of BDC materials in sodium, potassium, aluminium, and ZIHSCs. It highlights how these materials can improve the performance of these systems. The analysis of several metal-ion systems demonstrates the benefits of BDCs' structural characteristics for each form of supercapacitor. This review examines the present obstacles

in developing carbon materials produced from biomass for supercapacitors, encompassing scalability, cost-effectiveness, and performance consistency.

Additionally, it provides valuable insights for future studies, including enhancing the synthesis procedures, optimizing the structural configuration, and investigating novel energy storage mechanisms. This research highlights the significant impact of BDC materials in MIHSCs, which can lead to the development of environmentally friendly and efficient energy storage systems. This review is unusual because it comprehensively compares carbon compounds obtained from biomass in various metal-ion systems. It uncovers the distinct contributions of these materials to different types of supercapacitors. This comparison offers vital insights into the structural characteristics that improve electrochemical performance, influencing the advancement of sustainable energy storage solutions. This paper incorporates the latest developments in the field, emphasizing the breakthroughs in creating carbon materials from biomass and their usage in MIHSCs. The statement underscores the importance of ongoing innovation and interdisciplinary cooperation in investigating these sustainable materials better. This will help advance green energy technologies and harmoniously balance environmental sustainability and technical advancement. Overall, this review paper offers an in-depth examination of carbon materials produced from biomass in MIHSCs with exceptional performance. This study emphasizes the capacity of these materials to bring about significant changes, tackles existing obstacles, and provides insights for future investigations, thereby promoting the progress of sustainable energy storage technologies.

**Funding:** This work is supported by the Japan Society for the Promotion of Science (JSPS) through KAKENHI Grant Number 22F22336.

**Institutional Review Board Statement:** Not applicable.

**Informed Consent Statement:** Not applicable.

**Data Availability Statement:** Data are contained within this article.

**Acknowledgments:** The author acknowledges the support of the Japan Society for the Promotion of Science (JSPS) for the postdoctoral fellowship.

**Conflicts of Interest:** The author declares no conflicts of interest.

## References

- Guo, H.; Qiao, M.; Yan, J.; Jiang, L.; Yu, J.; Li, J.; Deng, S.; Qu, L. Fabrication of Hybrid Supercapacitor by  $\text{MoCl}_5$  Precursor-Assisted Carbonization with Ultrafast Laser for Improved Capacitance Performance. *Adv. Funct. Mater.* **2023**, *33*, 2213514. [[CrossRef](#)]
- Han, X.; Wang, B.; Yang, C.; Meng, G.; Zhao, R.; Hu, Q.; Triana, O.; Iqbal, M.; Li, Y.; Han, A.; et al. Inductive Effect in Mn-Doped NiO Nanosheet Arrays for Enhanced Capacitive and Highly Stable Hybrid Supercapacitor. *ACS Appl. Energy Mater.* **2019**, *2*, 2072–2079. [[CrossRef](#)]
- Lee, S.-H.; Kim, J.H.; Yoon, J.-R. Laser Scribed Graphene Cathode for Next Generation of High Performance Hybrid Supercapacitors. *Sci. Rep.* **2018**, *8*, 8179. [[CrossRef](#)]
- Larcher, D.; Tarascon, J.-M. Towards Greener and More Sustainable Batteries for Electrical Energy Storage. *Nat. Chem.* **2015**, *7*, 19–29. [[CrossRef](#)]
- Zhai, Y.; Dou, Y.; Zhao, D.; Fulvio, P.F.; Mayes, R.T.; Dai, S. Carbon Materials for Chemical Capacitive Energy Storage. *Adv. Mater.* **2011**, *23*, 4828–4850. [[CrossRef](#)] [[PubMed](#)]
- Zhang, X.; Hou, L.; Ciesielski, A.; Samorì, P. 2D Materials Beyond Graphene for High-Performance Energy Storage Applications. *Adv. Energy Mater.* **2016**, *6*, 1600671. [[CrossRef](#)]
- Mondal, M.; Goswami, D.K.; Bhattacharyya, T.K. High-Performing Asymmetric 2 V Supercapacitor Assembled with Leucine-Capped RGO- $\alpha$ -Fe<sub>2</sub>O<sub>3</sub> as Anode and PANI Decorated MWCNT-V<sub>2</sub>O<sub>5</sub> as Cathode. *J. Electrochem. Soc.* **2023**, *170*, 110521. [[CrossRef](#)]
- Li, J.; Zhu, J.; Dong, Z.; Wu, Q. Nanomaterials Derived from a Template Method for Supercapacitor Applications. *ChemistrySelect* **2023**, *8*, e202204487. [[CrossRef](#)]
- Genc, R.; Alas, M.O.; Harputlu, E.; Repp, S.; Kremer, N.; Castellano, M.; Colak, S.G.; Ocakoglu, K.; Erdem, E. High-Capacitance Hybrid Supercapacitor Based on Multi-Colored Fluorescent Carbon-Dots. *Sci. Rep.* **2017**, *7*, 11222. [[CrossRef](#)]

10. Li, S.; Chen, W.; Huang, X.; Ding, L.; Ren, Y.; Xu, M.; Zhu, J.; Miao, Z.; Liu, H. Enabling Wasted A4 Papers as a Promising Carbon Source to Construct Partially Graphitic Hierarchical Porous Carbon for High-Performance Aqueous Zn-Ion Storage. *ACS Appl. Mater. Interfaces* **2024**, *16*, 10126–10137. [[CrossRef](#)]
11. Díez, N.; Sevilla, M. Hybrid Metal-Ion Capacitors Based on Carbon Nanospheres. *ChemElectroChem* **2024**, *11*, e202300475. [[CrossRef](#)]
12. Wang, Z.; Hong, P.; Zhao, H.; Lei, Y. Recent Developments and Future Prospects of Transition Metal Compounds as Electrode Materials for Potassium-Ion Hybrid Capacitors. *Adv. Mater. Technol.* **2023**, *8*, 2200515. [[CrossRef](#)]
13. Gao, Q.; Li, P.; Ding, S.; He, H.; Cai, M.; Ning, X.; Cai, Y.; Zhang, M. Cu<sub>2</sub>Se-ZnSe Heterojunction Encapsulated in Carbon Fibers for High-Capacity Anodes of Sodium-Ion Batteries. *Ionics* **2020**, *26*, 5525–5533. [[CrossRef](#)]
14. Tang, H.; Yao, J.; Zhu, Y. Recent Developments and Future Prospects for Zinc-Ion Hybrid Capacitors: A Review. *Adv. Energy Mater.* **2021**, *11*, 2003994. [[CrossRef](#)]
15. Zeng, F.; Gong, X.; Xu, Z.; Du, Z.; Xu, J.; Deng, T.; Wang, D.; Zeng, Y.; Yu, S.; Meng, Z.; et al. A New Selection Criterion for Voltage Windows of Aqueous Zinc Ion Hybrid Capacitors: Achieving a Balance between Energy Density and Cycle Stability. *J. Mater. Chem. A* **2023**, *11*, 26698–26706. [[CrossRef](#)]
16. Shang, K.; Liu, Y.; Cai, P.; Li, K.; Wen, Z. N. P, and S Co-Doped 3D Porous Carbon-Architected Cathode for High-Performance Zn-Ion Hybrid Capacitors. *J. Mater. Chem. A* **2022**, *10*, 6489–6498. [[CrossRef](#)]
17. Zheng, H.; Zhou, H.; Zheng, B.; Wei, C.; Ma, A.; Jin, X.; Chen, W.; Liu, H. Stable Flexible Electronic Devices under Harsh Conditions Enabled by Double-Network Hydrogels Containing Binary Cations. *ACS Appl. Mater. Interfaces* **2024**, *16*, 7768–7779. [[CrossRef](#)]
18. Shaikh, N.S.; Lokhande, V.C.; Praserthdam, S.; Lokhande, C.D.; Ezema, F.I.; Salunkhe, D.J.; Shaikh, J.S.; Kanjanaboops, P. Recent Advancements in Energy Storage Based on Sodium Ion and Zinc Ion Hybrid Supercapacitors. *Energy Fuels* **2021**, *35*, 14241–14264. [[CrossRef](#)]
19. Dong, S.; Li, Z.; Xing, Z.; Wu, X.; Ji, X.; Zhang, X. Novel Potassium-Ion Hybrid Capacitor Based on an Anode of K<sub>2</sub>Ti<sub>6</sub>O<sub>13</sub> Microscaffolds. *ACS Appl. Mater. Interfaces* **2018**, *10*, 15542–15547. [[CrossRef](#)]
20. Qiu, D.; Guan, J.; Li, M.; Kang, C.; Wei, J.; Li, Y.; Xie, Z.; Wang, F.; Yang, R. Kinetics Enhanced Nitrogen-Doped Hierarchical Porous Hollow Carbon Spheres Boosting Advanced Potassium-Ion Hybrid Capacitors. *Adv. Funct. Mater.* **2019**, *29*, 1903496. [[CrossRef](#)]
21. Ruan, J.; Mo, F.; Chen, Z.; Liu, M.; Zheng, S.; Wu, R.; Fang, F.; Song, Y.; Sun, D. Rational Construction of Nitrogen-Doped Hierarchical Dual-Carbon for Advanced Potassium-Ion Hybrid Capacitors. *Adv. Energy Mater.* **2020**, *10*, 1904045. [[CrossRef](#)]
22. Buliyaminu, I.A.; Aziz, M.A.; Shah, S.S.; Mohamedkhair, A.K.; Yamani, Z.H. Preparation of Nano-Co<sub>3</sub>O<sub>4</sub>-Coated Albizia Procera-Derived Carbon by Direct Thermal Decomposition Method for Electrochemical Water Oxidation. *Arab. J. Chem.* **2020**, *13*, 4785–4796. [[CrossRef](#)]
23. Natarajan, S.; Lee, Y.; Aravindan, V. Biomass-Derived Carbon Materials as Prospective Electrodes for High-Energy Lithium- and Sodium-Ion Capacitors. *Chem. Asian J.* **2019**, *14*, 936–951. [[CrossRef](#)] [[PubMed](#)]
24. Shah, S.S.; Qasem, M.A.A.; Berni, R.; Del Casino, C.; Cai, G.; Contal, S.; Ahmad, I.; Siddiqui, K.S.; Gatti, E.; Predieri, S.; et al. Physico-Chemical Properties and Toxicological Effects on Plant and Algal Models of Carbon Nanosheets from a Nettle Fibre Clone. *Sci. Rep.* **2021**, *11*, 6945. [[CrossRef](#)] [[PubMed](#)]
25. Lai, F.; Miao, Y.-E.; Zuo, L.; Lu, H.; Huang, Y.; Liu, T. Biomass-Derived Nitrogen-Doped Carbon Nanofiber Network: A Facile Template for Decoration of Ultrathin Nickel-Cobalt Layered Double Hydroxide Nanosheets as High-Performance Asymmetric Supercapacitor Electrode. *Small* **2016**, *12*, 3235–3244. [[CrossRef](#)] [[PubMed](#)]
26. Wang, Q.; Qin, B.; Qu, C.; Wang, B.; Duan, H.; Cao, Q.; Li, H.; Qi, J. Synthesis of Hierarchical Porous Carbon from Bio-Oil for Supercapacitor Application. *Energy Fuels* **2023**, *37*, 16970–16978. [[CrossRef](#)]
27. Wang, T.; Hu, S.; Yu, W.; Hu, Y.; Yan, S.; Wang, M.; Zhao, W.; Xu, J.; Zhang, J. Biologically Inspired Small Herbal Biomolecules and Biomass Carbon for High-Performance Supercapacitors. *ACS Appl. Energy Mater.* **2023**, *6*, 2347–2357. [[CrossRef](#)]
28. Zhou, Y.; Parker, C.B.; Joshi, P.; Naskar, A.K.; Glass, J.T.; Cao, C. 4D Printing of Stretchable Supercapacitors via Hybrid Composite Materials. *Adv. Mater. Technol.* **2021**, *6*, 2001055. [[CrossRef](#)]
29. Liu, H.; Yao, M.; Yao, X. Improving Energy Density of Crystalline–Amorphous Multilayer Films Deposited on Ti Foils by Structural Modulation. *J. Am. Ceram. Soc.* **2021**, *104*, 1379–1390. [[CrossRef](#)]
30. Choi, N.; Chen, Z.; Freunberger, S.A.; Ji, X.; Sun, Y.; Amine, K.; Yushin, G.; Nazar, L.F.; Cho, J.; Bruce, P.G. Challenges Facing Lithium Batteries and Electrical Double-Layer Capacitors. *Angew. Chem. Int. Ed.* **2012**, *51*, 9994–10024. [[CrossRef](#)]
31. He, M.; Fic, K.; Frąckowiak, E.; Novák, P.; Berg, E.J. Towards More Durable Electrochemical Capacitors by Elucidating the Ageing Mechanisms under Different Testing Procedures. *ChemElectroChem* **2019**, *6*, 566–573. [[CrossRef](#)]
32. Wu, Z.; Parvez, K.; Feng, X.; Müllen, K. Graphene-Based in-Plane Micro-Supercapacitors with High Power and Energy Densities. *Nat. Commun.* **2013**, *4*, 2487. [[CrossRef](#)]
33. Kandambeth, S.; Jia, J.; Wu, H.; Kale, V.S.; Parvatkar, P.T.; Czaban-Józwiak, J.; Zhou, S.; Xu, X.; Ameur, Z.O.; Abou-Hamad, E.; et al. Covalent Organic Frameworks as Negative Electrodes for High-Performance Asymmetric Supercapacitors. *Adv. Energy Mater.* **2020**, *10*, 2001673. [[CrossRef](#)]
34. Nguyen, T.; Montemor, M.d.F. Metal Oxide and Hydroxide-Based Aqueous Supercapacitors: From Charge Storage Mechanisms and Functional Electrode Engineering to Need-Tailored Devices. *Adv. Sci.* **2019**, *6*, 1801797. [[CrossRef](#)] [[PubMed](#)]

35. Naoi, K.; Ishimoto, S.; Miyamoto, J.; Naoi, W. Second Generation ‘Nanohybrid Supercapacitor’: Evolution of Capacitive Energy Storage Devices. *Energy Environ. Sci.* **2012**, *5*, 9363–9373. [[CrossRef](#)]
36. Guo, Q.; Liu, J.; Bai, C.; Chen, N.; Qu, L. 2D Silicene Nanosheets for High-Performance Zinc-Ion Hybrid Capacitor Application. *ACS Nano* **2021**, *15*, 16533–16541. [[CrossRef](#)]
37. Xia, L.; Tang, B.; Wei, J.; Zhou, Z. Recent Advances in Alkali Metal-Ion Hybrid Supercapacitors. *Batter. Supercaps* **2021**, *4*, 1108–1121. [[CrossRef](#)]
38. Wang, Q.; Wang, S.; Li, J.; Ruan, L.; Wei, N.; Huang, L.; Dong, Z.; Cheng, Q.; Xiong, Y.; Zeng, W. A Novel Aqueous Zinc-Ion Hybrid Supercapacitor Based on TiS<sub>2</sub> (De)Intercalation Battery-Type Anode. *Adv. Electron. Mater.* **2020**, *6*, 2000388. [[CrossRef](#)]
39. Liu, Y.; Zhang, Y.; Sun, Z.; Cheng, S.; Cui, P.; Wu, Y.; Zhang, J.; Fu, J.; Xie, E. New Insight into the Mechanism of Multivalent Ion Hybrid Supercapacitor: From the Effect of Potential Window Viewpoint. *Small* **2020**, *16*, 2003403. [[CrossRef](#)] [[PubMed](#)]
40. Wang, H.; Zhu, C.; Chao, D.; Yan, Q.; Fan, H.J. Nonaqueous Hybrid Lithium-Ion and Sodium-Ion Capacitors. *Adv. Mater.* **2017**, *29*, 1702093. [[CrossRef](#)]
41. Ma, Y.; Chang, H.; Zhang, M.; Chen, Y. Graphene-Based Materials for Lithium-Ion Hybrid Supercapacitors. *Adv. Mater.* **2015**, *27*, 5296–5308. [[CrossRef](#)]
42. Zuo, W.; Li, R.; Zhou, C.; Li, Y.; Xia, J.; Liu, J. Battery-Supercapacitor Hybrid Devices: Recent Progress and Future Prospects. *Adv. Sci.* **2017**, *4*, 1600539. [[CrossRef](#)] [[PubMed](#)]
43. Peng, L.; Peng, X.; Liu, B.; Wu, C.; Xie, Y.; Yu, G. Ultrathin Two-Dimensional MnO<sub>2</sub>/Graphene Hybrid Nanostructures for High-Performance, Flexible Planar Supercapacitors. *Nano Lett.* **2013**, *13*, 2151–2157. [[CrossRef](#)]
44. Karri, S.N.; Ega, S.P.; Perupogu, V.; Srinivasan, P. Enhancing the Electrochemical Performance of Polyaniline Using Fly Ash of Coal Waste for Supercapacitor Application. *ChemistrySelect* **2021**, *6*, 2576–2589. [[CrossRef](#)]
45. Unnikrishnan, B.; Wu, C.-W.; Chen, I.-W.P.; Chang, H.-T.; Lin, C.-H.; Huang, C.-C. Carbon Dot-Mediated Synthesis of Manganese Oxide Decorated Graphene Nanosheets for Supercapacitor Application. *ACS Sustain. Chem. Eng.* **2016**, *4*, 3008–3016. [[CrossRef](#)]
46. Fan, W.; Wang, F.; Xiong, X.; Song, B.; Wang, T.; Cheng, X.; Zhu, Z.; He, J.; Liu, Y.; Wu, Y. Recent Advances in Functional Materials and Devices for Zn-Ion Hybrid Supercapacitors. *NPG Asia Mater.* **2024**, *16*, 18. [[CrossRef](#)]
47. Huang, C.; Zhao, X.; Xu, Y.; Zhang, Y.; Yang, Y.; Hu, A.; Tang, Q.; Song, X.; Jiang, C.; Chen, X. Sewable and Cuttable Flexible Zinc-Ion Hybrid Supercapacitor Using a Polydopamine/Carbon Cloth-Based Cathode. *ACS Sustain. Chem. Eng.* **2020**, *8*, 16028–16036. [[CrossRef](#)]
48. Zhang, H.; Liu, Q.; Fang, Y.; Teng, C.; Liu, X.; Fang, P.; Tong, Y.; Lu, X. Boosting Zn-Ion Energy Storage Capability of Hierarchically Porous Carbon by Promoting Chemical Adsorption. *Adv. Mater.* **2019**, *31*, 1904948. [[CrossRef](#)] [[PubMed](#)]
49. Zheng, Y.; Zhao, W.; Jia, D.; Liu, Y.; Cui, L.; Wei, D.; Zheng, R.; Liu, J. Porous Carbon Prepared via Combustion and Acid Treatment as Flexible Zinc-Ion Capacitor Electrode Material. *Chem. Eng. J.* **2020**, *387*, 124161. [[CrossRef](#)]
50. Li, Z.; Chen, D.; An, Y.; Chen, C.; Wu, L.; Chen, Z.; Sun, Y.; Zhang, X. Flexible and Anti-Freezing Quasi-Solid-State Zinc Ion Hybrid Supercapacitors Based on Pencil Shavings Derived Porous Carbon. *Energy Storage Mater.* **2020**, *28*, 307–314. [[CrossRef](#)]
51. Yin, J.; Zhang, W.; Wang, W.; Alhebshi, N.A.; Salah, N.; Alshareef, H.N. Electrochemical Zinc Ion Capacitors Enhanced by Redox Reactions of Porous Carbon Cathodes. *Adv. Energy Mater.* **2020**, *10*, 2001705. [[CrossRef](#)]
52. Shah, S.S.; Aziz, M.A.; Ali, M.; Hakeem, A.S.; Yamani, Z.H. Advanced High-Energy All-Solid-State Hybrid Supercapacitor with Nickel-Cobalt-Layered Double Hydroxide Nanoflowers Supported on Jute Stick-Derived Activated Carbon Nanosheets. *Small* **2023**, *23*, 2306665. [[CrossRef](#)]
53. Wang, R.; Han, M.; Zhao, Q.; Ren, Z.; Guo, X.; Xu, C.; Hu, N.; Lu, L. Hydrothermal Synthesis of Nanostructured Graphene/Polyaniline Composites as High-Capacitance Electrode Materials for Supercapacitors. *Sci. Rep.* **2017**, *7*, 44562. [[CrossRef](#)]
54. Young, C.; Park, T.; Yi, J.W.; Kim, J.; Hossain, M.S.A.; Kaneti, Y.V.; Yamauchi, Y. Advanced Functional Carbons and Their Hybrid Nanoarchitectures towards Supercapacitor Applications. *ChemSusChem* **2018**, *11*, 3546–3558. [[CrossRef](#)]
55. Abouelamaiem, D.I.; He, G.; Parkin, I.; Neville, T.P.; Jorge, A.B.; Ji, S.; Wang, R.; Titirici, M.-M.; Shearing, P.R.; Brett, D.J.L. Synergistic Relationship between the Three-Dimensional Nanostructure and Electrochemical Performance in Biocarbon Supercapacitor Electrode Materials. *Sustain. Energy Fuels* **2018**, *2*, 772–785. [[CrossRef](#)]
56. Wang, K.; Zhang, Z.; Sun, Q.; Wang, P.; Li, Y. Durian Shell-Derived N, O, P-Doped Activated Porous Carbon Materials and Their Electrochemical Performance in Supercapacitor. *J. Mater. Sci.* **2020**, *55*, 10142–10154. [[CrossRef](#)]
57. Liu, B.; Zhang, X.; Tian, D.; Li, Q.; Zhong, M.; Chen, S.; Hu, C.; Ji, H. In Situ Growth of Oriented Polyaniline Nanorod Arrays on the Graphite Flake for High-Performance Supercapacitors. *ACS Omega* **2020**, *5*, 32395–32402. [[CrossRef](#)]
58. Mehandoust, M.; Li, G.; Erk, N. Biomass-Derived Carbon Materials as an Emerging Platform for Advanced Electrochemical Sensors: Recent Advances and Future Perspectives. *Ind. Eng. Chem. Res.* **2023**, *62*, 4628–4635. [[CrossRef](#)]
59. Galek, P.; Mackowiak, A.; Bujewska, P.; Fic, K. Three-Dimensional Architectures in Electrochemical Capacitor Applications—Insights, Opinions, and Perspectives. *Front. Energy Res.* **2020**, *8*, 139. [[CrossRef](#)]
60. Olabi, A.G.; Abbas, Q.; Abdelkareem, M.A.; Alami, A.H.; Mirzaeian, M.; Sayed, E.T. Carbon-Based Materials for Supercapacitors: Recent Progress, Challenges and Barriers. *Batteries* **2022**, *9*, 19. [[CrossRef](#)]
61. Jiang, L.; Sheng, L.; Fan, Z. Biomass-Derived Carbon Materials with Structural Diversities and Their Applications in Energy Storage. *Sci. China Mater.* **2018**, *61*, 133–158. [[CrossRef](#)]

62. Falco, C.; Marco-Lozar, J.P.; Salinas-Torres, D.; Morallón, E.; Cazorla-Amorós, D.; Titirici, M.M.; Lozano-Castelló, D. Tailoring the Porosity of Chemically Activated Hydrothermal Carbons: Influence of the Precursor and Hydrothermal Carbonization Temperature. *Carbon* **2013**, *62*, 346–355. [[CrossRef](#)]
63. Chen, D.; Yang, L.; Li, J.; Wu, Q. Effect of Self-Doped Heteroatoms in Biomass-Derived Activated Carbon for Supercapacitor Applications. *ChemistrySelect* **2019**, *4*, 1586–1595. [[CrossRef](#)]
64. Guo, D.; Li, Z.; Wang, D.; Sun, M.; Wang, H. Design and Synthesis of Zinc-Activated  $\text{Co}_x\text{Ni}_{2-x}\text{P}$ /Graphene Anode for High-Performance Zinc Ion Storage Device. *ChemSusChem* **2021**, *14*, 2205–2215. [[CrossRef](#)]
65. Yang, J.; Bissett, M.A.; Dryfe, R.A.W. Investigation of Voltage Range and Self-Discharge in Aqueous Zinc-Ion Hybrid Supercapacitors. *ChemSusChem* **2021**, *14*, 1700–1709. [[CrossRef](#)]
66. Lu, J.; Lin, X.; Wang, S.; Xu, X.; Zhou, Y.; Zhang, Y.; Li, Q.; Liu, H. High Ionic Conductivity and Toughness Hydrogel Electrolyte for High-Performance Flexible Solid-State Zinc-Ion Hybrid Supercapacitors Enabled by Cellulose-Bentonite Coordination Interactions. *Green Chem.* **2023**, *25*, 1635–1646. [[CrossRef](#)]
67. Chen, S.; Yang, G.; Zhao, X.; Wang, N.; Luo, T.; Chen, X.; Wu, T.; Jiang, S.; van Aken, P.A.; Qu, S.; et al. Hollow Mesoporous Carbon Spheres for High Performance Symmetrical and Aqueous Zinc-Ion Hybrid Supercapacitor. *Front. Chem.* **2020**, *8*, 663. [[CrossRef](#)]
68. Chang, H.; Khan, I.; Yuan, A.; Khan, S.; Sadiq, S.; Khan, A.; Shah, S.A.; Chen, L.; Humayun, M.; Usman, M. Polyarylimide-Based COF/MOF Nanoparticle Hybrids for  $\text{CO}_2$  Conversion, Hydrogen Generation, and Organic Pollutant Degradation. *ACS Appl. Nano Mater.* **2024**, *7*, 10451–10465. [[CrossRef](#)]
69. Shah, S.A.; Khan, I.; Yuan, A.  $\text{MoS}_2$  as a Co-Catalyst for Photocatalytic Hydrogen Production: A Mini Review. *Molecules* **2022**, *27*, 3289. [[CrossRef](#)]
70. Samage, A.; Halakarni, M.; Yoon, H.; Sanna Kotrappanavar, N. Sustainable Conversion of Agricultural Biomass Waste into Electrode Materials with Enhanced Energy Density for Aqueous Zinc-Ion Hybrid Capacitors. *Carbon* **2024**, *219*, 118774. [[CrossRef](#)]
71. Naik, P.B.; Yadav, P.; Nagaraj, R.; Puttaswamy, R.; Beere, H.K.; Maiti, U.N.; Mondal, C.; Sanna Kotrappanavar, N.; Ghosh, D. Developing High-Performance Flexible Zinc Ion Capacitors from Agricultural Waste-Derived Carbon Sheets. *ACS Sustain. Chem. Eng.* **2022**, *10*, 1471–1481. [[CrossRef](#)]
72. Li, S.; Luo, X.; Xiao, H.; Li, D.; Chen, Y. Nitrogen and Sulfur Codoped Hierarchical Porous Carbon Derived from Lignin for High-Performance Zinc Ion Capacitors. *ACS Appl. Energy Mater.* **2023**, *6*, 6700–6711. [[CrossRef](#)]
73. Zhao, X.; Hong, R.; Lu, R.; Chen, Y.; Yang, X. Sustainable Synthesis of Hierarchically Porous Hollow Carbon Spheres for Enhanced Zinc-Ion Hybrid Supercapacitors. *ACS Appl. Energy Mater.* **2024**, *7*, 931–940. [[CrossRef](#)]
74. Du, X.; Ma, Y.; Xie, X.; Jiang, H.; Sun, X.; Yang, X.; Zhang, Y.; Hou, C.; Du, W. Preparation of Two-Dimensional Porous Nitrogen-oxygen Co-Doped Recycled Yeast Cell Wall Derived-carbon Matrix for High-Performance Zinc Ion Supercapacitors. *J. Energy Storage* **2024**, *82*, 110428. [[CrossRef](#)]
75. Wang, J.; Nie, P.; Ding, B.; Dong, S.; Hao, X.; Dou, H.; Zhang, X. Biomass Derived Carbon for Energy Storage Devices. *J. Mater. Chem. A* **2017**, *5*, 2411–2428. [[CrossRef](#)]
76. Yan, M.; Qin, Y.; Wang, L.; Song, M.; Han, D.; Jin, Q.; Zhao, S.; Zhao, M.; Li, Z.; Wang, X.; et al. Recent Advances in Biomass-Derived Carbon Materials for Sodium-Ion Energy Storage Devices. *Nanomaterials* **2022**, *12*, 930. [[CrossRef](#)]
77. Cheng, P.; Gao, S.; Zang, P.; Yang, X.; Bai, Y.; Xu, H.; Liu, Z.; Lei, Z. Hierarchically Porous Carbon by Activation of Shiitake Mushroom for Capacitive Energy Storage. *Carbon* **2015**, *93*, 315–324. [[CrossRef](#)]
78. Liu, H.; Liu, H.; Di, S.; Zhai, B.; Li, L.; Wang, S. Advantageous Tubular Structure of Biomass-Derived Carbon for High-Performance Sodium Storage. *ACS Appl. Energy Mater.* **2021**, *4*, 4955–4965. [[CrossRef](#)]
79. Niu, J.; Guan, J.; Dou, M.; Zhang, Z.; Kong, J.; Wang, F. Sustainable Synthesis of Biomass-Derived Carbon Electrodes with Hybrid Energy-Storage Behaviors for Use in High-Performance Na-Ion Capacitors. *ACS Appl. Energy Mater.* **2020**, *3*, 2478–2489. [[CrossRef](#)]
80. Guo, Y.; Liu, W.; Wu, R.; Sun, L.; Zhang, Y.; Cui, Y.; Liu, S.; Wang, H.; Shan, B. Marine-Biomass-Derived Porous Carbon Sheets with a Tunable N-Doping Content for Superior Sodium-Ion Storage. *ACS Appl. Mater. Interfaces* **2018**, *10*, 38376–38386. [[CrossRef](#)]
81. Liu, H.; Liu, X.; Wang, H.; Zheng, Y.; Zhang, H.; Shi, J.; Liu, W.; Huang, M.; Kan, J.; Zhao, X.; et al. High-Performance Sodium-Ion Capacitor Constructed by Well-Matched Dual-Carbon Electrodes from a Single Biomass. *ACS Sustain. Chem. Eng.* **2019**, *7*, 12188–12199. [[CrossRef](#)]
82. Zhang, L.; Sun, J.; Zhao, H.; Sun, Y.; Dai, L.; Yao, F.; Fu, Y.; Zhu, J. Gas Expansion-Assisted Preparation of 3D Porous Carbon Nanosheet for High-Performance Sodium Ion Hybrid Capacitor. *J. Power Sources* **2020**, *475*, 228679. [[CrossRef](#)]
83. Zhang, N.; Liu, Q.; Chen, W.; Wan, M.; Li, X.; Wang, L.; Xue, L.; Zhang, W. High Capacity Hard Carbon Derived from Lotus Stem as Anode for Sodium Ion Batteries. *J. Power Sources* **2018**, *378*, 331–337. [[CrossRef](#)]
84. Gao, Z.; Zhang, Y.; Song, N.; Li, X. Biomass-Derived Renewable Carbon Materials for Electrochemical Energy Storage. *Mater. Res. Lett.* **2017**, *5*, 69–88. [[CrossRef](#)]
85. Jiang, B.; Cao, L.; Yuan, Q.; Ma, Z.; Huang, Z.; Lin, Z.; Zhang, P. Biomass Straw-Derived Porous Carbon Synthesized for Supercapacitor by Ball Milling. *Materials* **2022**, *15*, 924. [[CrossRef](#)] [[PubMed](#)]
86. Feng, S.; Xing, L.; Li, K.; Wang, H.; An, Q.; Zhou, L.; Mai, L. Solvent-Free Synthesis of Polymer Spheres and the Activation to Porous Carbon Spheres for Advanced Aluminum-Ion Hybrid Capacitors. *Small Methods* **2023**, *7*, 2300150. [[CrossRef](#)]

87. Seon, E.; Jang, S.; Raj, M.R.; Tak, Y.; Lee, G. Ultrahigh Energy Density and Long-Life Cyclic Stability of Surface-Treated Aluminum-Ion Supercapacitors. *ACS Appl. Mater. Interfaces* **2022**, *14*, 45059–45072. [[CrossRef](#)] [[PubMed](#)]
88. Lei, H.; Tu, J.; Tian, D.; Jiao, S. A Nitrogen-Doped Graphene Cathode for High-Capacitance Aluminum-Ion Hybrid Supercapacitors. *New J. Chem.* **2018**, *42*, 15684–15691. [[CrossRef](#)]
89. Sun, W.; Xing, L.; Zhang, B.; Shi, W.; Ren, J.; Zhang, X.; Xiong, F.; An, Q. Ultra-High-Performance Aluminum-Based Hybrid Supercapacitors Prepared for Nitrogen-Doped Micro-Mesoporous Carbon Sphere. *J. Power Sources* **2023**, *571*, 233052. [[CrossRef](#)]
90. Zhang, K.; Liu, M.; Si, M.; Wang, Z.; Zhuo, S.; Chai, L.; Shi, Y. Polyhydroxyalkanoate-Modified Bacterium Regulates Biomass Structure and Promotes Synthesis of Carbon Materials for High-Performance Supercapacitors. *ChemSusChem* **2019**, *12*, 1732–1742. [[CrossRef](#)]
91. Feng, T.; Wang, S.; Hua, Y.; Zhou, P.; Liu, G.; Ji, K.; Lin, Z.; Shi, S.; Jiang, X.; Zhang, R. Synthesis of Biomass-Derived N,O-Codoped Hierarchical Porous Carbon with Large Surface Area for High-Performance Supercapacitor. *J. Energy Storage* **2021**, *44*, 103286. [[CrossRef](#)]
92. Shah, S.S.; Aziz, M.A.; Yamani, Z.H. Recent Progress in Carbonaceous and Redox-Active Nanoarchitectures for Hybrid Supercapacitors: Performance Evaluation, Challenges, and Future Prospects. *Chem. Rec.* **2022**, *22*, e202200018. [[CrossRef](#)] [[PubMed](#)]
93. Sudhan, N.; Subramani, K.; Karnan, M.; Ilayaraja, N.; Sathish, M. Biomass-Derived Activated Porous Carbon from Rice Straw for a High-Energy Symmetric Supercapacitor in Aqueous and Non-Aqueous Electrolytes. *Energy Fuels* **2017**, *31*, 977–985. [[CrossRef](#)]
94. Yin, Y.; Liu, Q.; Zhao, Y.; Chen, T.; Wang, J.; Gui, L.; Lu, C. Recent Progress and Future Directions of Biomass-Derived Hierarchical Porous Carbon: Designing, Preparation, and Supercapacitor Applications. *Energy Fuels* **2023**, *37*, 3523–3554. [[CrossRef](#)]
95. Zhang, W.; Yin, J.; Wang, C.; Zhao, L.; Jian, W.; Lu, K.; Lin, H.; Qiu, X.; Alshareef, H.N. Lignin Derived Porous Carbons: Synthesis Methods and Supercapacitor Applications. *Small Methods* **2021**, *5*, 2100896. [[CrossRef](#)]
96. Cui, Y.; Liu, W.; Feng, W.; Zhang, Y.; Du, Y.; Liu, S.; Wang, H.; Chen, M.; Zhou, J. Controlled Design of Well-Dispersed Ultrathin MoS<sub>2</sub> Nanosheets inside Hollow Carbon Skeleton: Toward Fast Potassium Storage by Constructing Spacious “Houses” for K Ions. *Adv. Funct. Mater.* **2020**, *30*, 1908755. [[CrossRef](#)]
97. Baskar, A.V.; Singh, G.; Ruban, A.M.; Davidraj, J.M.; Bahadur, R.; Sooriyakumar, P.; Kumar, P.; Karakoti, A.; Yi, J.; Vinu, A. Recent Progress in Synthesis and Application of Biomass-Based Hybrid Electrodes for Rechargeable Batteries. *Adv. Funct. Mater.* **2023**, *33*, 2208349. [[CrossRef](#)]
98. Pham, H.D.; Mahale, K.; Hoang, T.M.L.; Mundree, S.G.; Gomez-Romero, P.; Dubal, D.P. Dual Carbon Potassium-Ion Capacitors: Biomass-Derived Graphene-like Carbon Nanosheet Cathodes. *ACS Appl. Mater. Interfaces* **2020**, *12*, 48518–48525. [[CrossRef](#)]
99. Chen, M.; Liu, W.; Du, Y.; Cui, Y.; Feng, W.; Zhou, J.; Gao, X.; Wang, T.; Liu, S.; Jin, Y. “Plains–Hills”: A New Model to Design Biomass-Derived Carbon Electrode Materials for High-Performance Potassium Ion Hybrid Supercapacitors. *ACS Sustain. Chem. Eng.* **2021**, *9*, 3931–3941. [[CrossRef](#)]
100. Huang, F.; Liu, W.; Wang, Q.; Wang, F.; Yao, Q.; Yan, D.; Xu, H.; Xia, B.Y.; Deng, J. Natural N/O-Doped Hard Carbon for High Performance K-Ion Hybrid Capacitors. *Electrochim. Acta* **2020**, *354*, 136701. [[CrossRef](#)]
101. Rajkumar, P.; Thirumal, V.; Radhika, G.; Gnanamuthu, R.M.; Subadevi, R.; Sivakumar, M.; Yoo, K.; Kim, J. Eco-Friendly Production of Carbon Electrode from Biomass for High Performance Lithium and Zinc Ion Capacitors with Hybrid Energy Storage Characteristics. *Mater. Lett.* **2024**, *354*, 135320. [[CrossRef](#)]
102. Tian, Z.; Yang, C.; Zhang, C.; Han, X.; Han, J.; Liu, K.; He, S.; Duan, G.; Jian, S.; Hu, J.; et al. In-Situ Activation of Resorcinol-Furfural Resin Derived Hierarchical Porous Carbon for Supercapacitors and Zinc-Ion Hybrid Capacitors. *J. Energy Storage* **2024**, *85*, 111130. [[CrossRef](#)]
103. Chen, G.; Hu, Z.; Pan, Z.; Wang, D. Design of Honeycomb-like Hierarchically Porous Carbons with Engineered Mesoporosity for Aqueous Zinc-Ion Hybrid Supercapacitors Applications. *J. Energy Storage* **2021**, *38*, 102534. [[CrossRef](#)]
104. Zhao, L.; Jian, W.; Zhang, X.; Wen, F.; Zhu, J.; Huang, S.; Yin, J.; Lu, K.; Zhou, M.; Zhang, W.; et al. Multi-Scale Self-Templating Synthesis Strategy of Lignin-Derived Hierarchical Porous Carbons toward High-Performance Zinc Ion Hybrid Supercapacitors. *J. Energy Storage* **2022**, *53*, 105095. [[CrossRef](#)]
105. Yu, H.; Chen, X.; Zhou, J.; Wang, H. Tannin-Derived Ordered Mesoporous Carbon Cathode for Zn-Ion Hybrid Supercapacitor with Remarkable Energy Density. *Ind. Eng. Chem. Res.* **2023**, *62*, 62–71. [[CrossRef](#)]
106. Zheng, J.; Song, Q.; Qi, Y.; Leng, H.; Zhou, W.; Li, S.; Qiu, J. N, O Co-Doped Porous Carbon Derived from Pine Needles for Zinc-Ion Hybrid Supercapacitors. *New J. Chem.* **2023**, *47*, 9692–9700. [[CrossRef](#)]
107. Gupta, H.; Dahiya, Y.; Rathore, H.K.; Awasthi, K.; Kumar, M.; Sarkar, D. Energy-Dense Zinc Ion Hybrid Supercapacitors with S, N Dual-Doped Porous Carbon Nanocube Based Cathodes. *ACS Appl. Mater. Interfaces* **2023**, *15*, 42685–42696. [[CrossRef](#)] [[PubMed](#)]
108. Sielicki, K.; Maślana, K.; Mijowska, E. Fallen Autumn Leaves—The Source of Highly Porous Carbon for Zn-Ion Hybrid Supercapacitors. *Diam. Relat. Mater.* **2024**, *144*, 111021. [[CrossRef](#)]
109. Wei, F.; Wei, Y.; Wang, J.; Han, M.; Lv, Y. N, P Dual Doped Foamy-like Carbons with Abundant Defect Sites for Zinc Ion Hybrid Capacitors. *Chem. Eng. J.* **2022**, *450*, 137919. [[CrossRef](#)]
110. Wang, H.; Chen, X.; Zhang, J.; Yuan, Z.; Ye, P.; Shen, J.; Zhong, Y.; Hu, Y. Unveiling the Cooperative Roles of Pyrrolic-N and Carboxyl Groups in Biomass-Derived Hierarchical Porous Carbon Nanosheets for High Energy-Power Zn-Ion Hybrid Supercapacitors. *Appl. Surf. Sci.* **2022**, *598*, 153819. [[CrossRef](#)]
111. Zhu, Y.; Chen, M.; Li, Q.; Yuan, C.; Wang, C. A Porous Biomass-Derived Anode for High-Performance Sodium-Ion Batteries. *Carbon* **2018**, *129*, 695–701. [[CrossRef](#)]

112. Muruganantham, R.; Wang, F.-M.; Liu, W.-R. A Green Route N, S-Doped Hard Carbon Derived from Fruit-Peel Biomass Waste as an Anode Material for Rechargeable Sodium-Ion Storage Applications. *Electrochim. Acta* **2022**, *424*, 140573. [[CrossRef](#)]
113. Chen, J.; Zhou, X.; Mei, C.; Xu, J.; Zhou, S.; Wong, C.-P. Evaluating Biomass-Derived Hierarchically Porous Carbon as the Positive Electrode Material for Hybrid Na-Ion Capacitors. *J. Power Sources* **2017**, *342*, 48–55. [[CrossRef](#)]
114. Ragul, S.; Sujithkrishnan, E.; Elumalai, P. Inherent Heteroatom-Enriched Amorphous Carbon as High-Performance Electrode for Sodium-Ion Battery and Sodium-Ion Ultracapacitor. *Energy Fuels* **2022**, *36*, 15221–15233. [[CrossRef](#)]
115. Vadivazhagan, M.; Parameswaran, P.; Mani, U.; Nallathamby, K. Waste-Driven Bio-Carbon Electrode Material for Na-Ion Storage Applications. *ACS Sustain. Chem. Eng.* **2018**, *6*, 13915–13923. [[CrossRef](#)]
116. Zou, X.; Dong, C.; Jin, Y.; Wang, D.; Li, L.; Wu, S.; Xu, Z.; Chen, Y.; Li, Z.; Yang, H. Engineering of N, P Co-Doped Hierarchical Porous Carbon from Sugarcane Bagasse for High-Performance Supercapacitors and Sodium Ion Batteries. *Colloids Surf. A Physicochem. Eng. Asp.* **2023**, *672*, 131715. [[CrossRef](#)]
117. Wu, C.; Xu, Q.; Ning, H.; Zhao, Y.; Guo, S.; Sun, X.; Wang, Y.; Hu, H.; Wu, M. Petroleum Pitch Derived Carbon as Both Cathode and Anode Materials for Advanced Potassium-Ion Hybrid Capacitors. *Carbon* **2022**, *196*, 727–735. [[CrossRef](#)]
118. Yang, M.; Kong, Q.; Feng, W.; Yao, W. N/O Double-Doped Biomass Hard Carbon Material Realizes Fast and Stable Potassium Ion Storage. *Carbon* **2021**, *176*, 71–82. [[CrossRef](#)]
119. Cao, W.; Zhang, E.; Wang, J.; Liu, Z.; Ge, J.; Yu, X.; Yang, H.; Lu, B. Potato Derived Biomass Porous Carbon as Anode for Potassium Ion Batteries. *Electrochim. Acta* **2019**, *293*, 364–370. [[CrossRef](#)]
120. Wang, P.; Gong, Z.; Ye, K.; Gao, Y.; Zhu, K.; Yan, J.; Wang, G.; Cao, D. N-Rich Biomass Carbon Derived from Hemp as a Full Carbon-Based Potassium Ion Hybrid Capacitor Anode. *Appl. Surf. Sci.* **2021**, *553*, 149569. [[CrossRef](#)]
121. Gao, C.; Wang, Q.; Luo, S.; Wang, Z.; Zhang, Y.; Liu, Y.; Hao, A.; Guo, R. High Performance Potassium-Ion Battery Anode Based on Biomorphic N-Doped Carbon Derived from Walnut Septum. *J. Power Sources* **2019**, *415*, 165–171. [[CrossRef](#)]
122. Gong, Y.; Fu, D.; Fan, M.; Zheng, S.; Xue, Y. Multilayer Core–Sheath Wires with Radially Aligned N-Doped Carbon Nanohole Arrays for Boosting Energy Storage in Zinc-Ion Hybrid Supercapacitors. *ACS Appl. Mater. Interfaces* **2024**, *16*, 4793–4802. [[CrossRef](#)] [[PubMed](#)]
123. Sun, Z.; Jiao, X.; Chu, S.; Li, Z. Low-cost Porous Carbon Materials Prepared from Peanut Red Peels for Novel Zinc-ion Hybrid Capacitors. *ChemistrySelect* **2023**, *8*, e202304071. [[CrossRef](#)]
124. Chen, J.; Yang, B.; Liu, B.; Lang, J.; Yan, X. Recent Advances in Anode Materials for Sodium- and Potassium-Ion Hybrid Capacitors. *Curr. Opin. Electrochem.* **2019**, *18*, 1–8. [[CrossRef](#)]
125. Zeng, Z.; Mao, Y.; Hu, Z.; Chen, K.; Huang, Q.; Song, Y.; Wu, Z.; Zhang, P.; Chen, T.; Guo, X. Research Progress and Commercialization of Biologically Derived Hard Carbon Anode Materials for Sodium-Ion Batteries. *Ind. Eng. Chem. Res.* **2023**, *62*, 15343–15359. [[CrossRef](#)]
126. Yoo, H.D.; Han, S.-D.; Bayliss, R.D.; Gewirth, A.A.; Genorio, B.; Rajput, N.N.; Persson, K.A.; Burrell, A.K.; Cabana, J. “Rocking-Chair”-Type Metal Hybrid Supercapacitors. *ACS Appl. Mater. Interfaces* **2016**, *8*, 30853–30862. [[CrossRef](#)]
127. Han, J.; Mariani, A.; Zarrabeitia, M.; Jusys, Z.; Behm, R.J.; Varzi, A.; Passerini, S. Zinc-Ion Hybrid Supercapacitors Employing Acetate-Based Water-in-Salt Electrolytes. *Small* **2022**, *18*, 2201563. [[CrossRef](#)]
128. Varanasi, S.R.; Bhatia, S.K. Optimal Electrode Mass Ratio in Nanoporous Carbon Electrochemical Supercapacitors. *J. Phys. Chem. C* **2016**, *120*, 27925–27933. [[CrossRef](#)]
129. Cho, S.; Lim, J.; Seo, Y. Flexible Solid Supercapacitors of Novel Nanostructured Electrodes Outperform Most Supercapacitors. *ACS Omega* **2022**, *7*, 37825–37833. [[CrossRef](#)]
130. Cherusseri, J.; Sambath Kumar, K.; Choudhary, N.; Nagaiah, N.; Jung, Y.; Roy, T.; Thomas, J. Novel Mesoporous Electrode Materials for Symmetric, Asymmetric and Hybrid Supercapacitors. *Nanotechnology* **2019**, *30*, 202001. [[CrossRef](#)]
131. Wang, J.; Kaskel, S. KOH Activation of Carbon-Based Materials for Energy Storage. *J. Mater. Chem.* **2012**, *22*, 23710–23725. [[CrossRef](#)]
132. Ahmad, S.; Hussain, A.; Mian, S.A.; Rahman, G.; Ali, S.; Jang, J. Sensing and Conversion of Carbon Dioxide to Methanol Using Ag-Decorated Zinc Oxide Nanocatalyst. *Mater. Adv.* **2024**, *5*, 1119–1129. [[CrossRef](#)]
133. Wang, Z.; Zhang, M.; Ma, W.; Zhu, J.; Song, W. Application of Carbon Materials in Aqueous Zinc Ion Energy Storage Devices. *Small* **2021**, *17*, 2100219. [[CrossRef](#)]
134. Javed, M.S.; Asim, S.; Najam, T.; Khalid, M.; Hussain, I.; Ahmad, A.; Assiri, M.A.; Han, W. Recent Progress in Flexible Zn-ion Hybrid Supercapacitors: Fundamentals, Fabrication Designs, and Applications. *Carbon Energy* **2023**, *5*, e271. [[CrossRef](#)]
135. Yu, J.; Wang, L.; Peng, J.; Jia, X.; Zhou, L.; Yang, N.; Li, L. O-Doped Porous Carbon Derived from Biomass Waste for High-Performance Zinc-Ion Hybrid Supercapacitors. *Ionics (Kiel)* **2021**, *27*, 4495–4505. [[CrossRef](#)]
136. Amiri, A.; Swart, E.N.; Polycarpou, A.A. Recent Advances in Electrochemically-Efficient Materials for Zinc-Ion Hybrid Supercapacitors. *Renew. Sustain. Energy Rev.* **2021**, *148*, 111288. [[CrossRef](#)]
137. Hou, X.; Ren, P.; Tian, W.; Xue, R.; Fan, B.; Ren, F.; Jin, Y. High-Performance Zn-Ion Hybrid Supercapacitors Based on Biomass-Derived Hierarchical Porous Carbon through Template-Activated Bifunctional Induced and Ice-Crystal Assisted Strategy. *J. Power Sources* **2024**, *603*, 234408. [[CrossRef](#)]
138. Zhou, S.; Li, C.; Gao, G.; Fan, H.; Hu, X. Bio-Based Resins with Tannin and Hydroxymethylfurfural Derived High-Yield Carbon for Zn-Ion Hybrid Supercapacitors. *J. Clean. Prod.* **2023**, *389*, 136067. [[CrossRef](#)]

139. Zhang, W.; Yin, J.; Jian, W.; Wu, Y.; Chen, L.; Sun, M.; Schwingenschlögl, U.; Qiu, X.; Alshareef, H.N. Supermolecule-Mediated Defect Engineering of Porous Carbons for Zinc-Ion Hybrid Capacitors. *Nano Energy* **2022**, *103*, 107827. [[CrossRef](#)]
140. Ma, Y.; Hou, C.; Kimura, H.; Xie, X.; Jiang, H.; Sun, X.; Yang, X.; Zhang, Y.; Du, W. Recent Advances in the Application of Carbon-Based Electrode Materials for High-Performance Zinc Ion Capacitors: A Mini Review. *Adv. Compos. Hybrid Mater.* **2023**, *6*, 59. [[CrossRef](#)]
141. Li, Y.; Zhang, X.; Lu, T.; Zhang, Y.; Li, X.; Yu, D.; Zhao, G. Boosting the Capacitance of Aqueous Zinc-Ion Hybrid Capacitors by Engineering Hierarchical Porous Carbon Architecture. *Batteries* **2023**, *9*, 429. [[CrossRef](#)]
142. Tekin, B.; Topcu, Y. Novel Hemp Biomass-Derived Activated Carbon as Cathode Material for Aqueous Zinc-Ion Hybrid Supercapacitors: Synthesis, Characterization, and Electrochemical Performance. *J. Energy Storage* **2024**, *77*, 109879. [[CrossRef](#)]
143. Yao, L.; Jiang, J.; Peng, H.; Yang, H.; Liu, S.; Wen, X.; Cai, P.; Zou, Y.; Zhang, H.; Xu, F.; et al. Glutinous Rice-Derived Carbon Material for High-Performance Zinc-Ion Hybrid Supercapacitors. *J. Energy Storage* **2023**, *58*, 106378. [[CrossRef](#)]
144. Yuksel, R.; Karakehya, N. High Energy Density Biomass-Derived Activated Carbon Materials for Sustainable Energy Storage. *Carbon* **2024**, *221*, 118934. [[CrossRef](#)]
145. Jiang, G.; Chen, M.; Sun, Y.; Pan, J. Dual N-Doped Porous Carbon Derived from Pyrolytic Carbon Black and Critical PANIs Constructing High-Performance Zn Ion Hybrid Supercapacitor. *J. Energy Storage* **2023**, *63*, 106955. [[CrossRef](#)]
146. Wang, D.; Li, Z.; Guo, D.; Sun, M. Metal-Organic Framework Derived Zinc and Nitrogen Co-Doped Porous Carbon Materials for High Performance Zinc-Ion Hybrid Supercapacitors. *Electrochim. Acta* **2022**, *427*, 140854. [[CrossRef](#)]
147. Jia, D.; Shen, Z.; Zhou, W.; Li, Y.; He, J.; Jiang, L.; Wei, Y.; He, X. Ultrahigh N-Doped Carbon with Hierarchical Porous Structure Derived from Metal-Organic Framework for High-Performance Zinc Ion Hybrid Capacitors. *Chem. Eng. J.* **2024**, *485*, 149820. [[CrossRef](#)]
148. Liu, H.; Chen, W.; Peng, H.; Huang, X.; Li, S.; Jiang, L.; Zheng, M.; Xu, M.; Zhu, J. Bioinspired Design of Graphene-Based N/O Self-Doped Nanoporous Carbon from Carp Scales for Advanced Zn-Ion Hybrid Supercapacitors. *Electrochim. Acta* **2022**, *434*, 141312. [[CrossRef](#)]
149. Zhang, X.; Tian, X.; Song, Y.; Wu, J.; Yang, T.; Liu, Z. High-Performance Activated Carbon Cathodes from Green Cokes for Zn-Ion Hybrid Supercapacitors. *Fuel* **2022**, *310*, 122485. [[CrossRef](#)]
150. Wang, J.; Huang, Y.; Han, X.; Li, Z.; Zhang, S.; Zong, M. A Flexible Zinc-Ion Hybrid Supercapacitor Constructed by Porous Carbon with Controllable Structure. *Appl. Surf. Sci.* **2022**, *579*, 152247. [[CrossRef](#)]
151. Zhang, X.; Zhang, Y.; Zhang, H.; Zhang, Y.; Ma, Z.; Sun, L. Zinc-ion Hybrid Capacitor with High Energy Density Constructed by Bamboo Shavings Derived Spongy-like Porous Carbon. *ChemistrySelect* **2021**, *6*, 6937–6943. [[CrossRef](#)]
152. Liu, Y.; Tan, H.; Tan, Z.; Cheng, X. Rice Husk-Derived Carbon Materials for Aqueous Zn-Ion Hybrid Supercapacitors. *Appl. Surf. Sci.* **2023**, *608*, 155215. [[CrossRef](#)]
153. Fan, H.; Zhou, S.; Li, Q.; Gao, G.; Wang, Y.; He, F.; Hu, G.; Hu, X. Hydrogen-Bonded Frameworks Crystals-Assisted Synthesis of Flower-like Carbon Materials with Penetrable Meso/Macropores from Heavy Fraction of Bio-Oil for Zn-Ion Hybrid Supercapacitors. *J. Colloid Interface Sci.* **2021**, *600*, 681–690. [[CrossRef](#)] [[PubMed](#)]
154. Dang, Z.; Li, X.; Li, Y.; Dong, L. Heteroatom-Rich Carbon Cathodes toward High-Performance Flexible Zinc-Ion Hybrid Supercapacitors. *J. Colloid Interface Sci.* **2023**, *644*, 221–229. [[CrossRef](#)] [[PubMed](#)]
155. Song, B.; Liu, Q.; Shi, F.; Xue, T.; Yang, C.; Zang, L. Porous Carbon Derived from a By-Product of Traditional Chinese Medicine for High-Performance Aqueous Zinc-Ion Hybrid Supercapacitors. *Diam. Relat. Mater.* **2024**, *142*, 110785. [[CrossRef](#)]
156. Lou, G.; Pei, G.; Wu, Y.; Lu, Y.; Wu, Y.; Zhu, X.; Pang, Y.; Shen, Z.; Wu, Q.; Fu, S.; et al. Combustion Conversion of Wood to N, O Co-Doped 2D Carbon Nanosheets for Zinc-Ion Hybrid Supercapacitors. *Chem. Eng. J.* **2021**, *413*, 127502. [[CrossRef](#)]
157. Liu, H.; Chen, H.; Shi, K.; Zhang, F.; Xiao, S.; Huang, L.; Zhu, H. Lignin-Derived Porous Carbon for Zinc-Ion Hybrid Capacitor. *Ind. Crops Prod.* **2022**, *187*, 115519. [[CrossRef](#)]
158. Xue, B.; Liu, C.; Wang, X.; Feng, Y.; Xu, J.; Gong, F.; Xiao, R. Urea-Boosted Gas-Exfoliation Synthesis of Lignin-Derived Porous Carbon for Zinc Ion Hybrid Supercapacitors. *Chem. Eng. J.* **2024**, *480*, 147994. [[CrossRef](#)]
159. Yang, S.; Cui, Y.; Yang, G.; Zhao, S.; Wang, J.; Zhao, D.; Yang, C.; Wang, X.; Cao, B. ZnCl<sub>2</sub> Induced Hierarchical Porous Carbon for Zinc-Ion Hybrid Supercapacitors. *J. Power Sources* **2023**, *554*, 232347. [[CrossRef](#)]
160. Xue, B.; Xu, J.; Xiao, R. Ice Template-Assisting Activation Strategy to Prepare Biomass-Derived Porous Carbon Cages for High-Performance Zn-Ion Hybrid Supercapacitors. *Chem. Eng. J.* **2023**, *454*, 140192. [[CrossRef](#)]
161. Liu, H.; Li, S.; Huang, X.; Chen, W.; Xu, M.; Ren, Y.; Zhang, R.; Miao, Z.; Zhu, J. High Energy-Power Zinc-Ion Hybrid Supercapacitors Achieved by 3D Channels Enriched Biomass-Derived N/O Co-Doped 2D Arcuate Carbon Nanosheets. *Mater. Today Chem.* **2023**, *29*, 101476. [[CrossRef](#)]
162. Muruganantham, R.; Wang, F.-M.; Yuwono, R.A.; Sabugaa, M.; Liu, W.-R. Biomass Feedstock of Waste Mango-Peel-Derived Porous Hard Carbon for Sustainable High-Performance Lithium-Ion Energy Storage Devices. *Energy Fuels* **2021**, *35*, 10878–10889. [[CrossRef](#)]
163. Ding, J.; Li, Z.; Cui, K.; Boyer, S.; Karpuzov, D.; Mitlin, D. Heteroatom Enhanced Sodium Ion Capacity and Rate Capability in a Hydrogel Derived Carbon Give Record Performance in a Hybrid Ion Capacitor. *Nano Energy* **2016**, *23*, 129–137. [[CrossRef](#)]
164. Liao, K.; Wang, H.; Wang, L.; Xu, D.; Wu, M.; Wang, R.; He, B.; Gong, Y.; Hu, X. A High-Energy Sodium-Ion Capacitor Enabled by a Nitrogen/Sulfur Co-Doped Hollow Carbon Nanofiber Anode and an Activated Carbon Cathode. *Nanoscale Adv.* **2019**, *1*, 746–756. [[CrossRef](#)]

165. Hong, K.; Qie, L.; Zeng, R.; Yi, Z.; Zhang, W.; Wang, D.; Yin, W.; Wu, C.; Fan, Q.; Zhang, W.; et al. Biomass Derived Hard Carbon Used as a High Performance Anode Material for Sodium Ion Batteries. *J. Mater. Chem. A* **2014**, *2*, 12733–12738. [[CrossRef](#)]
166. Liu, L.; Sun, X.; Dong, Y.; Wang, D.; Wang, Z.; Jiang, Z.; Li, A.; Chen, X.; Song, H. N-Doped Hierarchical Porous Hollow Carbon Spheres with Multi-Cavities for High Performance Na-Ion Storage. *J. Power Sources* **2021**, *506*, 230170. [[CrossRef](#)]
167. Han, P.; Han, X.; Yao, J.; Zhang, L.; Cao, X.; Huang, C.; Cui, G. High Energy Density Sodium-Ion Capacitors through Co-Intercalation Mechanism in Diglyme-Based Electrolyte System. *J. Power Sources* **2015**, *297*, 457–463. [[CrossRef](#)]
168. Ghanem, A.S.; Ba-Shammakh, M.; Usman, M.; Khan, M.F.; Dafallah, H.; Habib, M.A.M.; Al-Maythalony, B.A. High Gas Permselectivity in ZIF-302/Polyimide Self-consistent Mixed-matrix Membrane. *J. Appl. Polym. Sci.* **2020**, *137*, 48513. [[CrossRef](#)]
169. Xiang, A.; Shi, D.; Chen, P.; Li, Z.; Tu, Q.; Liu, D.; Zhang, X.; Lu, J.; Jiang, Y.; Yang, Z.; et al.  $\text{Na}_4\text{Fe}_3(\text{PO}_4)_2(\text{P}_2\text{O}_7)@\text{C}/\text{Ti}_3\text{C}_2\text{T}_x$  Hybrid Cathode Materials with Enhanced Performances for Sodium-Ion Batteries. *Batteries* **2024**, *10*, 121. [[CrossRef](#)]
170. Thirumal, V.; Sreekanth, T.V.M.; Yoo, K.; Kim, J. Biomass-Derived Hard Carbon and Nitrogen-Sulfur Co-Doped Graphene for High-Performance Symmetric Sodium Ion Capacitor Devices. *Energies* **2023**, *16*, 802. [[CrossRef](#)]
171. Zhu, J.; Roscow, J.; Chandrasekaran, S.; Deng, L.; Zhang, P.; He, T.; Wang, K.; Huang, L. Biomass-Derived Carbons for Sodium-Ion Batteries and Sodium-Ion Capacitors. *ChemSusChem* **2020**, *13*, 1275–1295. [[CrossRef](#)]
172. Thangavel, R.; Kannan, A.G.; Ponraj, R.; Yoon, G.; Aravindan, V.; Kim, D.-W.; Kang, K.; Yoon, W.-S.; Lee, Y.-S. Surface Enriched Graphene Hollow Spheres towards Building Ultra-High Power Sodium-Ion Capacitor with Long Durability. *Energy Storage Mater.* **2020**, *25*, 702–713. [[CrossRef](#)]
173. Panda, M.R.; Kathribail, A.R.; Modak, B.; Sau, S.; Dutta, D.P.; Mitra, S. Electrochemical Properties of Biomass-Derived Carbon and Its Composite along with  $\text{Na}_2\text{Ti}_3\text{O}_7$  as Potential High-Performance Anodes for Na-Ion and Li-Ion Batteries. *Electrochim. Acta* **2021**, *392*, 139026. [[CrossRef](#)]
174. Wang, H.; Yu, W.; Shi, J.; Mao, N.; Chen, S.; Liu, W. Biomass Derived Hierarchical Porous Carbons as High-Performance Anodes for Sodium-Ion Batteries. *Electrochim. Acta* **2016**, *188*, 103–110. [[CrossRef](#)]
175. Dong, G.; Wang, H.; Liu, W.; Shi, J.; Sun, S.; Li, D.; Zhang, H.; Yang, Y.; Cui, Y. Nitrate Salt Assisted Fabrication of Highly N-Doped Carbons for High-Performance Sodium Ion Capacitors. *ACS Appl. Energy Mater.* **2018**, *1*, 5636–5645. [[CrossRef](#)]
176. Nagmani; Satpathy, B.K.; Singh, A.K.; Pradhan, D.; Puravankara, S. Utilization of Single Biomass-Derived Micro-Mesoporous Carbon for Dual-Carbon Symmetric and Hybrid Sodium-Ion Capacitors. *New J. Chem.* **2023**, *47*, 12658–12669. [[CrossRef](#)]
177. Casal, M.D.; Díez, N.; Payá, S.; Sevilla, M. Cork-Derived Carbon Sheets for High-Performance Na-Ion Capacitors. *ACS Appl. Energy Mater.* **2023**, *6*, 8120–8131. [[CrossRef](#)]
178. Liu, H.; Jia, M.; Sun, N.; Cao, B.; Chen, R.; Zhu, Q.; Wu, F.; Qiao, N.; Xu, B. Nitrogen-Rich Mesoporous Carbon as Anode Material for High-Performance Sodium-Ion Batteries. *ACS Appl. Mater. Interfaces* **2015**, *7*, 27124–27130. [[CrossRef](#)]
179. Ding, J.; Wang, H.; Li, Z.; Cui, K.; Karpuzov, D.; Tan, X.; Kohandehghan, A.; Mitlin, D. Peanut Shell Hybrid Sodium Ion Capacitor with Extreme Energy-Power Rivals Lithium Ion Capacitors. *Energy Environ. Sci.* **2015**, *8*, 941–955. [[CrossRef](#)]
180. Shi, X.; Yu, J.; Liu, Q.; Shao, L.; Cai, J.; Sun, Z. Metal-Organic-Framework-Derived Multi-Heteroatom Doped Cu<sub>1.8</sub>Se/C Composites for High-Performance Na-Ion Hybrid Capacitor. *Sustain. Mater. Technol.* **2021**, *28*, e00275. [[CrossRef](#)]
181. Yan, R.; Leus, K.; Hofmann, J.P.; Antonietti, M.; Oschatz, M. Porous Nitrogen-Doped Carbon/Carbon Nanocomposite Electrodes Enable Sodium Ion Capacitors with High Capacity and Rate Capability. *Nano Energy* **2020**, *67*, 104240. [[CrossRef](#)]
182. Zhao, G.; Yu, D.; Zhang, H.; Sun, F.; Li, J.; Zhu, L.; Sun, L.; Yu, M.; Besenbacher, F.; Sun, Y. Sulphur-Doped Carbon Nanosheets Derived from Biomass as High-Performance Anode Materials for Sodium-Ion Batteries. *Nano Energy* **2020**, *67*, 104219. [[CrossRef](#)]
183. Li, L.; Sun, M.; Xu, Z.; Wang, Z.; Liu, K.; Chen, Y.; Wang, Z.; Chen, H.; Yang, H. Hierarchical Porous Hard Carbon Derived from Rice Husks for High-Performance Sodium Ion Storage. *Colloids Surf. A Physicochem. Eng. Asp.* **2023**, *661*, 130927. [[CrossRef](#)]
184. Zhang, L.; Wang, Y.; Yang, S.; Zhao, G.; Han, L.; Li, Y.; Zhu, G. Biomass-Derived S, P, Cl Tri-Doped Porous Carbon for High-Performance Supercapacitor. *Diam. Relat. Mater.* **2022**, *126*, 109061. [[CrossRef](#)]
185. Ajuria, J.; Redondo, E.; Arnaiz, M.; Mysyk, R.; Rojo, T.; Goikolea, E. Lithium and Sodium Ion Capacitors with High Energy and Power Densities Based on Carbons from Recycled Olive Pits. *J. Power Sources* **2017**, *359*, 17–26. [[CrossRef](#)]
186. Dos Reis, G.S.; Petnikota, S.; Subramaniyam, C.M.; de Oliveira, H.P.; Larsson, S.; Thyrel, M.; Lassi, U.; García Alvarado, F. Sustainable Biomass-Derived Carbon Electrodes for Potassium and Aluminum Batteries: Conceptualizing the Key Parameters for Improved Performance. *Nanomaterials* **2023**, *13*, 765. [[CrossRef](#)]
187. Li, B.; Dai, F.; Xiao, Q.; Yang, L.; Shen, J.; Zhang, C.; Cai, M. Activated Carbon from Biomass Transfer for High-Energy Density Lithium-Ion Supercapacitors. *Adv. Energy Mater.* **2016**, *6*, 1600802. [[CrossRef](#)]
188. Xie, K.; Zhang, W.; Ren, K.; Zhu, E.; Lu, J.; Chen, J.; Yin, P.; Yang, L.; Guan, X.; Wang, G. Electrochemical Performance of Corn Waste Derived Carbon Electrodes Based on the Intrinsic Biomass Properties. *Materials* **2023**, *16*, 5022. [[CrossRef](#)]
189. Nayem, S.M.A.; Islam, S.; Shah, S.S.; Sultana, N.; Mahfoz, W.; Ahammad, A.J.S.; Aziz, A. Biomass Based S-doped Carbon for Supercapacitor Application. In *Biomass-Based Supercapacitors*; Wiley: Hoboken, NJ, USA, 2023; pp. 315–327.
190. Wei, X.; Qiu, B.; Xu, L.; Qin, Q.; Zhang, W.; Liu, Z.; Wei, F.; Lv, Y. High Performance Hierarchical Porous Carbon Derived from Waste Shrimp Shell for Supercapacitor Electrodes. *J. Energy Storage* **2023**, *62*, 106900. [[CrossRef](#)]
191. Zeng, Y.; Zhao, W.; Li, X.; Chen, X.; Song, J.; Wu, X.; Huang, Z. Biomass Waste Derived Heteroatom Doping Porous Carbon Sheets for High Performance Supercapacitor. *Mater. Today Commun.* **2023**, *36*, 106623. [[CrossRef](#)]
192. Wahed, F.; Shah, S.S.; Hayat, K.; Shah, S.K.; Aziz, M.A. Conduction Mechanisms and Thermoelectric Applications of La<sub>1-X</sub> Sr<sub>x</sub> CoO<sub>3</sub> Nanofibers. *J. Mater. Sci.* **2022**, *57*, 8828–8844. [[CrossRef](#)]

193. Hou, J.; Cao, C.; Idrees, F.; Ma, X. Hierarchical Porous Nitrogen-Doped Carbon Nanosheets Derived from Silk for Ultrahigh-Capacity Battery Anodes and Supercapacitors. *ACS Nano* **2015**, *9*, 2556–2564. [[CrossRef](#)]
194. Shen, Y.; Zhu, Y. One-Pot Synthesis of Biomass-Derived Porous Carbons for Multipurpose Energy Applications. *J. Mater. Chem. A* **2024**, *12*, 6211–6242. [[CrossRef](#)]
195. Li, Z.; Guo, D.; Liu, Y.; Wang, H.; Wang, L. Recent Advances and Challenges in Biomass-Derived Porous Carbon Nanomaterials for Supercapacitors. *Chem. Eng. J.* **2020**, *397*, 125418. [[CrossRef](#)]
196. Qian, Y.; Wu, B.; Li, Y.; Pan, Z.; Tian, J.; Lin, N.; Qian, Y. Pressure-Dependent Self-Template Pyrolysis Modulates the Porosity and Surface Chemical Configuration of Carbon for Potassium Ion Hybrid Capacitors. *Chem. Eng. J.* **2023**, *451*, 138579. [[CrossRef](#)]
197. Zhao, L.; Sun, S.; Lin, J.; Zhong, L.; Chen, L.; Guo, J.; Yin, J.; Alshareef, H.N.; Qiu, X.; Zhang, W. Defect Engineering of Disordered Carbon Anodes with Ultra-High Heteroatom Doping Through a Supermolecule-Mediated Strategy for Potassium-Ion Hybrid Capacitors. *Nano-Micro Lett.* **2023**, *15*, 41. [[CrossRef](#)]
198. Pan, Z.; Qian, Y.; Li, Y.; Xie, X.; Lin, N.; Qian, Y. Novel Bilayer-Shelled N, O-Doped Hollow Porous Carbon Microspheres as High Performance Anode for Potassium-Ion Hybrid Capacitors. *Nano-Micro Lett.* **2023**, *15*, 151. [[CrossRef](#)]
199. Gao, Q.; Li, T.; Liu, C.; Sun, J.; Liu, Y.; Hou, L.; Yuan, C. Hierarchically Porous N-Doped Carbon Framework with Enlarged Interlayer Spacing as Dual-Carbon Electrodes for Potassium Ion Hybrid Capacitors. *Carbon Neutrality* **2023**, *2*, 18. [[CrossRef](#)]
200. Yvenat, M.-E.; Chavillon, B.; Mayousse, E.; Perdu, F.; Azaïs, P. Development of an Adequate Formation Protocol for a Non-Aqueous Potassium-Ion Hybrid Supercapacitor (KIC) through the Study of the Cell Swelling Phenomenon. *Batteries* **2022**, *8*, 135. [[CrossRef](#)]
201. Zhu, L.; Zhang, Z.; Luo, J.; Zhang, H.; Qu, Y.; Yang, Z. Self-Templated Synthesis of Hollow Hierarchical Porous Olive-like Carbon toward Universal High-Performance Alkali (Li, Na, K)-Ion Storage. *Carbon* **2021**, *174*, 317–324. [[CrossRef](#)]
202. Yang, M.; Dai, J.; He, M.; Duan, T.; Yao, W. Biomass-Derived Carbon from Ganoderma Lucidum Spore as a Promising Anode Material for Rapid Potassium-Ion Storage. *J. Colloid Interface Sci.* **2020**, *567*, 256–263. [[CrossRef](#)] [[PubMed](#)]
203. Cao, B.; Gao, S.; Ma, Y.; Zhang, D.; Guo, Z.; Du, M.; Xin, Z.; Zhou, C.; Liu, H. Biomass-Derived Carbon-Sulfur Hybrids Boosting Electrochemical Kinetics to Achieve High Potassium Storage Performance. *J. Colloid Interface Sci.* **2024**, *661*, 598–605. [[CrossRef](#)] [[PubMed](#)]
204. Lu, S.; Xiao, Q.; Yang, W.; Wang, X.; Guo, T.; Xie, Q.; Ruan, Y. Multi-Heteroatom-Doped Porous Carbon with High Surface Adsorption Energy of Potassium Derived from Biomass Waste for High-Performance Supercapacitors. *Int. J. Biol. Macromol.* **2024**, *258*, 128794. [[CrossRef](#)] [[PubMed](#)]
205. Zhong, L.; Qiu, X.; Yang, S.; Sun, S.; Chen, L.; Zhang, W. Supermolecule-Regulated Synthesis Strategy of General Biomass-Derived Highly Nitrogen-Doped Carbons toward Potassium-Ion Hybrid Capacitors with Enhanced Performances. *Energy Storage Mater.* **2023**, *61*, 102887. [[CrossRef](#)]
206. Zhu, L.; Zhang, Z.; Zhang, H.; Wang, Y.; Luo, J.; Yu, J.; Qu, Y.; Yang, Z. Tunable 2D Tremella-Derived Carbon Nanosheets with Enhanced Pseudocapacitance Behavior for Ultrafast Potassium-Ion Storage. *Sci. China Technol. Sci.* **2021**, *64*, 2047–2056. [[CrossRef](#)]
207. Hu, W.; Xiang, R.; Lin, J.; Cheng, Y.; Lu, C. Lignocellulosic Biomass-Derived Carbon Electrodes for Flexible Supercapacitors: An Overview. *Materials* **2021**, *14*, 4571. [[CrossRef](#)]
208. Xie, K.; Qin, X.; Wang, X.; Wang, Y.; Tao, H.; Wu, Q.; Yang, L.; Hu, Z. Carbon Nanocages as Supercapacitor Electrode Materials. *Adv. Mater.* **2012**, *24*, 347–352. [[CrossRef](#)]
209. Adam, A.A.; Ojur Dennis, J.; Al-Hadeethi, Y.; Mkawi, E.M.; Abubakar Abdulkadir, B.; Usman, F.; Mudassir Hassan, Y.; Wadi, I.A.; Sani, M. State of the Art and New Directions on Electrospun Lignin/Cellulose Nanofibers for Supercapacitor Application: A Systematic Literature Review. *Polymers* **2020**, *12*, 2884. [[CrossRef](#)]
210. Yang, X.; Lv, T.; Qiu, J. High Mass-Loading Biomass-Based Porous Carbon Electrodes for Supercapacitors: Review and Perspectives. *Small* **2023**, *19*, 2300336. [[CrossRef](#)]
211. Zhang, M.; Peng, L. Research Progress of Biomass-Derived Carbon for the Supercapacitors. *Mater. Res. Express* **2024**, *11*, 012004. [[CrossRef](#)]
212. Lu, Q.; Zhou, S.; Zhang, Y.; Chen, M.; Li, B.; Wei, H.; Zhang, D.; Zhang, J.; Liu, Q. Nanoporous Carbon Derived from Green Material by an Ordered Activation Method and Its High Capacitance for Energy Storage. *Nanomaterials* **2020**, *10*, 1058. [[CrossRef](#)] [[PubMed](#)]
213. Momodu, D.; Bello, A.; Oyedotun, K.; Ochai-Ejeh, F.; Dangbegnon, J.; Madito, M.; Manyala, N. Enhanced Electrochemical Response of Activated Carbon Nanostructures from Tree-Bark Biomass Waste in Polymer-Gel Active Electrolytes. *RSC Adv.* **2017**, *7*, 37286–37295. [[CrossRef](#)]
214. Zhu, Y.; Murali, S.; Stoller, M.D.; Ganesh, K.J.; Cai, W.; Ferreira, P.J.; Pirkle, A.; Wallace, R.M.; Cybosz, K.A.; Thommes, M.; et al. Carbon-Based Supercapacitors Produced by Activation of Graphene. *Science* **2011**, *332*, 1537–1541. [[CrossRef](#)] [[PubMed](#)]
215. Li, B.; Zheng, J.; Zhang, H.; Jin, L.; Yang, D.; Lv, H.; Shen, C.; Shellikeri, A.; Zheng, Y.; Gong, R.; et al. Electrode Materials, Electrolytes, and Challenges in Nonaqueous Lithium-Ion Capacitors. *Adv. Mater.* **2018**, *30*, 1705670. [[CrossRef](#)]
216. Biswal, M.; Banerjee, A.; Deo, M.; Ogale, S. From Dead Leaves to High Energy Density Supercapacitors. *Energy Environ. Sci.* **2013**, *6*, 1249–1259. [[CrossRef](#)]
217. Zhang, Q.; Yuan, M.; Liu, L.; Li, S.; Chen, X.; Liu, J.; Pang, X.; Wang, X. Study of Zinc Diffusion Based on S, N-Codoped Honeycomb Carbon Cathodes for High-Performance Zinc-Ion Capacitors. *Langmuir* **2024**, *40*, 5326–5337. [[CrossRef](#)] [[PubMed](#)]

218. Eskusson, J.; Thomberg, T.; Lust, E.; Jänes, A. Electrochemical Characteristics of Zn-Ion Hybrid Supercapacitors Based on Aqueous Solution of Different Electrolytes. *J. Electrochem. Soc.* **2022**, *169*, 020512. [[CrossRef](#)]
219. Shao, Y.; El-Kady, M.F.; Sun, J.; Li, Y.; Zhang, Q.; Zhu, M.; Wang, H.; Dunn, B.; Kaner, R.B. Design and Mechanisms of Asymmetric Supercapacitors. *Chem. Rev.* **2018**, *118*, 9233–9280. [[CrossRef](#)]
220. Simon, P.; Gogotsi, Y. Capacitive Energy Storage in Nanostructured Carbon-Electrolyte Systems. *Acc. Chem. Res.* **2013**, *46*, 1094–1103. [[CrossRef](#)]
221. Maurya, D.K.; Murugadoss, V.; Guo, Z.; Angaiah, S. Designing  $\text{Na}_2\text{Zn}_2\text{TeO}_6$ -Embedded 3D-Nanofibrous Poly(Vinylidenefluoride)-Co-Hexafluoropropylene-Based Nanohybrid Electrolyte via Electrospinning for Durable Sodium-Ion Capacitors. *ACS Appl. Energy Mater.* **2021**, *4*, 8475–8487. [[CrossRef](#)]
222. Dubal, D.P.; Ayyad, O.; Ruiz, V.; Gómez-Romero, P. Hybrid Energy Storage: The Merging of Battery and Supercapacitor Chemistries. *Chem. Soc. Rev.* **2015**, *44*, 1777–1790. [[CrossRef](#)] [[PubMed](#)]
223. Tomboc, G.M.; Tesfaye Gadisa, B.; Jun, M.; Chaudhari, N.K.; Kim, H.; Lee, K. Carbon Transition-metal Oxide Electrodes: Understanding the Role of Surface Engineering for High Energy Density Supercapacitors. *Chem.—Asian J.* **2020**, *15*, 1628–1647. [[CrossRef](#)] [[PubMed](#)]
224. Kim, T.; Jung, G.; Yoo, S.; Suh, K.S.; Ruoff, R.S. Activated Graphene-Based Carbons as Supercapacitor Electrodes with Macro- and Mesopores. *ACS Nano* **2013**, *7*, 6899–6905. [[CrossRef](#)] [[PubMed](#)]
225. Shaker, M.; Ng, S.; Sadeghi Ghazvini, A.A.; Javanmardi, S.; Gaho, M.A.; Jin, Z.; Ge, Q. Carbon/Graphene Quantum Dots as Electrolyte Additives for Batteries and Supercapacitors: A Review. *J. Energy Storage* **2024**, *85*, 111040. [[CrossRef](#)]
226. Liu, X.; Sun, Y.; Tong, Y.; Wang, X.; Zheng, J.; Wu, Y.; Li, H.; Niu, L.; Hou, Y. Exploration in Materials, Electrolytes and Performance towards Metal Ion (Li, Na, K, Zn and Mg)-Based Hybrid Capacitors: A Review. *Nano Energy* **2021**, *86*, 106070. [[CrossRef](#)]
227. Iqbal, M.Z.; Zakar, S.; Haider, S.S. Role of Aqueous Electrolytes on the Performance of Electrochemical Energy Storage Device. *J. Electroanal. Chem.* **2020**, *858*, 113793. [[CrossRef](#)]
228. Kumar, K.S.; Pandey, D.; Thomas, J. High Voltage Asymmetric Supercapacitors Developed by Engineering Electrode Work Functions. *ACS Energy Lett.* **2021**, *6*, 3590–3599. [[CrossRef](#)]
229. Guo, Q.; Bai, C.; Gao, C.; Chen, N.; Qu, L. Two Dimensional Silicene Nanosheets: A New Choice of Electrode Material for High-Performance Supercapacitor. *ACS Appl. Mater. Interfaces* **2022**, *14*, 39014–39021. [[CrossRef](#)] [[PubMed](#)]
230. Wan, F.; Wang, X.; Tang, C.; Jiang, C.; Wang, W.; Li, B.; Zhang, Y.; Zhu, X. Metallic 1T-MoS<sub>2</sub> Coupled with MXene towards Ultra-High Rate-Capabilities for Supercapacitors. *J. Mater. Chem. A* **2022**, *10*, 12258–12268. [[CrossRef](#)]
231. Hu, Z.; Song, Z.; Huang, Z.; Tao, S.; Song, B.; Cao, Z.; Hu, X.; Wu, J.; Li, F.; Deng, W.; et al. Reconstructing Hydrogen Bond Network Enables High Voltage Aqueous Zinc-Ion Supercapacitors. *Angew. Chem.* **2023**, *135*, e202309601. [[CrossRef](#)]
232. Komaba, S.; Hasegawa, T.; Dahbi, M.; Kubota, K. Potassium Intercalation into Graphite to Realize High-Voltage/High-Power Potassium-Ion Batteries and Potassium-Ion Capacitors. *Electrochem. Commun.* **2015**, *60*, 172–175. [[CrossRef](#)]
233. Zhang, F.; Dong, H.; Li, Y.; Fu, D.; Yang, L.; Shang, Y.; Li, Q.; Shao, Y.; Gang, W.; Ding, T.; et al. In Situ Metal-Oxygen-Hydrogen Modified B-TiO<sub>2</sub>@Co<sub>2</sub> P-X S-Scheme Heterojunction Effectively Enhanced Charge Separation for Photo-assisted Uranium Reduction. *Adv. Sci.* **2024**, *11*, 2305439. [[CrossRef](#)] [[PubMed](#)]
234. Huang, Z.; Wang, T.; Song, H.; Li, X.; Liang, G.; Wang, D.; Yang, Q.; Chen, Z.; Ma, L.; Liu, Z.; et al. Effects of Anion Carriers on Capacitance and Self-Discharge Behaviors of Zinc Ion Capacitors. *Angew. Chem.* **2021**, *133*, 1024–1034. [[CrossRef](#)]
235. Li, X.; Chen, F.; Zhao, B.; Zhang, S.; Zheng, X.; Wang, Y.; Jin, X.; Dai, C.; Wang, J.; Xie, J.; et al. Ultrafast Synthesis of Metal-Layered Hydroxides in a Dozen Seconds for High-Performance Aqueous Zn (Micro-) Battery. *Nano-Micro Lett.* **2023**, *15*, 32. [[CrossRef](#)] [[PubMed](#)]
236. Sen, A.; Groß, A. Promising Sensitizers for Dye Sensitized Solar Cells: A Comparison of Ru(II) with Other Earth’s Scarce and Abundant Metal Polypyridine Complexes. *Int. J. Quantum Chem.* **2019**, *119*, e25963. [[CrossRef](#)]
237. dos Santos Junior, G.A.; Fortunato, V.D.S.; Bastos, G.A.A.; Silva, G.G.; Ortega, P.F.R.; Lavall, R.L. High-Performance Lithium-Ion Hybrid Supercapacitors Based on Lithium Salt/Imidazolium Ionic Liquid Electrolytes and Ni-Doped LiMn<sub>2</sub>O<sub>4</sub> Cathode Materials. *ACS Appl. Energy Mater.* **2020**, *3*, 9028–9039. [[CrossRef](#)]
238. Shah, S.S.; Aziz, M.A.; Cevik, E.; Ali, M.; Gunday, S.T.; Bozkurt, A.; Yamani, Z.H. Sulfur Nano-Confinement in Hierarchically Porous Jute Derived Activated Carbon towards High-Performance Supercapacitor: Experimental and Theoretical Insights. *J. Energy Storage* **2022**, *56*, 105944. [[CrossRef](#)]
239. Yu, J.; Jia, X.; Peng, J.; Meng, B.; Wei, Y.; Hou, X.; Zhao, J.; Yang, N.; Xie, K.; Chu, D.; et al. Synergistic Effect of Nitrogen–Sulfur Codoping on Honeycomb-like Carbon-Based High-Energy-Density Zinc-Ion Hybrid Supercapacitors. *ACS Appl. Energy Mater.* **2023**, *6*, 2728–2738. [[CrossRef](#)]
240. Qin, J.; Sari, H.M.K.; Wang, X.; Yang, H.; Zhang, J.; Li, X. Controlled Design of Metal Oxide-Based ( $\text{Mn}^{2+}/\text{Nb}^{5+}$ ) Anodes for Superior Sodium-Ion Hybrid Supercapacitors: Synergistic Mechanisms of Hybrid Ion Storage. *Nano Energy* **2020**, *71*, 104594. [[CrossRef](#)]
241. Li, J.; El-Demellawi, J.K.; Sheng, G.; Björk, J.; Zeng, F.; Zhou, J.; Liao, X.; Wu, J.; Rosen, J.; Liu, X.; et al. Pseudocapacitive Heteroatom-Doped Carbon Cathode for Aluminum-Ion Batteries with Ultrahigh Reversible Stability. *Energy Environ. Mater.* **2024**, *e12733*. [[CrossRef](#)]
242. Chen, J.; Liu, B.; Cai, H.; Liu, S.; Yamauchi, Y.; Jun, S.C. Covalently Interlayer-Confined Organic–Inorganic Heterostructures for Aqueous Potassium Ion Supercapacitors. *Small* **2023**, *19*, 2204275. [[CrossRef](#)] [[PubMed](#)]

243. Huang, J.; Sumpter, B.G.; Meunier, V. A Universal Model for Nanoporous Carbon Supercapacitors Applicable to Diverse Pore Regimes, Carbon Materials, and Electrolytes. *Chem.—Eur. J.* **2008**, *14*, 6614–6626. [[CrossRef](#)] [[PubMed](#)]
244. Han, C.; Wang, X.; Peng, J.; Xia, Q.; Chou, S.; Cheng, G.; Huang, Z.; Li, W. Recent Progress on Two-Dimensional Carbon Materials for Emerging Post-Lithium ( $\text{Na}^+$ ,  $\text{K}^+$ ,  $\text{Zn}^{2+}$ ) Hybrid Supercapacitors. *Polymers* **2021**, *13*, 2137. [[CrossRef](#)] [[PubMed](#)]
245. Hao, P.; Zhao, Z.; Tian, J.; Li, H.; Sang, Y.; Yu, G.; Cai, H.; Liu, H.; Wong, C.P.; Umar, A. Hierarchical Porous Carbon Aerogel Derived from Bagasse for High Performance Supercapacitor Electrode. *Nanoscale* **2014**, *6*, 12120–12129. [[CrossRef](#)] [[PubMed](#)]
246. Xu, X.; Tang, J.; Qian, H.; Hou, S.; Bando, Y.; Hossain, M.S.A.; Pan, L.; Yamauchi, Y. Three-Dimensional Networked Metal–Organic Frameworks with Conductive Polypyrrole Tubes for Flexible Supercapacitors. *ACS Appl. Mater. Interfaces* **2017**, *9*, 38737–38744. [[CrossRef](#)]
247. Khan, A.; Sadiq, S.; Khan, I.; Humayun, M.; Jiyuan, G.; Usman, M.; Khan, A.; Khan, S.; Alanazi, A.F.; Bououdina, M. Preparation of Visible-Light Active MOFs-Perovskites (ZIF-67/LaFeO<sub>3</sub>) Nanocatalysts for Exceptional CO<sub>2</sub> Conversion, Organic Pollutants and Antibiotics Degradation. *Heliyon* **2024**, *10*, e27378. [[CrossRef](#)] [[PubMed](#)]
248. Sadiq, S.; Khan, S.; Khan, I.; Khan, A.; Humayun, M.; Wu, P.; Usman, M.; Khan, A.; Alanazi, A.F.; Bououdina, M. A Critical Review on Metal-Organic Frameworks (MOFs) Based Nanomaterials for Biomedical Applications: Designing, Recent Trends, Challenges, and Prospects. *Heliyon* **2024**, *10*, e25521. [[CrossRef](#)] [[PubMed](#)]
249. Yuksel, R.; Yarar Kaplan, B.; Bicer, E.; Yurum, A.; Alkan Gursel, S.; Unalan, H.E. All-Carbon Hybrids for High Performance Supercapacitors. *Int. J. Energy Res.* **2018**, *42*, 3575–3587. [[CrossRef](#)]
250. Deng, Y.; Wang, X.; Wang, Z.; Wang, X.; Li, Z.; Wang, L.; Zhou, C.; Chen, D.; Luo, Y. Yolk–Shell Structured Nickel Cobalt Sulfide and Carbon Nanotube Composite for High-Performance Hybrid Supercapacitors. *Energy Fuels* **2021**, *35*, 5342–5351. [[CrossRef](#)]

**Disclaimer/Publisher’s Note:** The statements, opinions and data contained in all publications are solely those of the individual author(s) and contributor(s) and not of MDPI and/or the editor(s). MDPI and/or the editor(s) disclaim responsibility for any injury to people or property resulting from any ideas, methods, instructions or products referred to in the content.